

FTS THESIS
676.320287 EAG
30001004467074
Eagleton, Danny Geoffrey
Creep properties of
corrugated fibreboard
containers for produce in

**CREEP PROPERTIES OF CORRUGATED FIBREBOARD
CONTAINERS FOR PRODUCE IN
SIMULATED ROAD TRANSPORT ENVIRONMENT**



Submitted as a requirement for the degree of
Master of Engineering

by

Danny Geoffrey Eagleton

Supervisors:

Dr Michael Sek, Centre for Packaging, Transportation, and Storage

Mr Jim Selway, Amcor Research and Technology Centre

Department of Mechanical Engineering

Faculty of Engineering

Victoria University of Technology

Submitted:

August 1995

ABSTRACT

Standard methods for the performance testing of corrugated fibreboard boxes use some static or quasi-static characteristic of the box as the performance indicator. The aim of this project was to develop a performance-based test method for corrugated boxes for fresh horticultural produce, using a dynamic fatigue-type approach. It was hypothesised that a dynamic test is more appropriate for produce packaging due to the relatively dynamic nature of the produce distribution environment. Measurements were made of vibration, shock, temperature, relative humidity, and handling impacts in a typical produce distribution environment, and a dynamic performance test method was developed. It was concluded that this dynamic test method is more sensitive to performance differences between boxes than standard quasi-static methods. The dynamic tests, however, take considerably more time to conduct than standard quasi-static methods and are not suitable for automation. This dynamic test method may have uses in developing a database for the comparison of different box types, however for routine performance testing the quasi-static methods are more appropriate.

ACKNOWLEDGMENTS

I would like to thank the following people for their generous support and assistance during this project: *Centre for Packaging, Transportation, and Storage*: Dr Jorge Marcondes, Dr Michael Sek, Rob Richmond, Barbara Rubeli, Murray Hogg, Rodney Bartlett, Sandy Dong, Praba Naganathan. *Department of Mechanical Engineering*: Prof. Geoffrey Leonart, Assoc. Prof. Kevin Duke, Ben Smit, Vincent Rouillard, Denise Colledge, Marlene Schutt, Milan Mejak, Ray McIntosh, Harry Braley, Harry Friedrich, Greg Pearse. *Department of Civil and Building Engineering*: Ass. Prof. Graham Thorpe, Vinayaga Sarma. *Fellow VUT students*: Todd Perry, David Ip, Dino Dioguardi, Karen Lee, Soon Poh Tay, Arvinder Kaur, Mounzer El-Eter, Roy Choudhury, Suzana Klopovic, Ben Bruscella. *Amcor Research and Technology Centre*: Jim Selway, Peter Bennett, Jim Kirkpatrick, Janet McGahy, John Trewick, Nola Porteous, Chris Tseglakoff. *Amcor Fibre Packaging*: Barry Robinson, Rick Andre, Gabriel Forlani, Andrew Kerr, Glenn Davey, Carl Klingstrom. *Department of Agriculture, Victoria*: Dr Kevin Clayton-Greene, Dr Wendy Morgan, Brenden Stevenson. *CSIRO*: Dr Alister Sharp. *Linfox Transport*: Alan Pollock, Kevin Harper, Richard Vanden Driesen, Bruce Forsyth. *Costa's Distribution Centre*: Mark Leng. *EGVIB/Vegco*: Chris Egan.

CONTENTS

1. INTRODUCTION	1
2. LITERATURE REVIEW	3
2.1 FIBREBOARD PACKAGING FOR PHYSICAL DISTRIBUTION	3
2.1.1 Strength Requirements of Corrugated Boxes	4
2.1.2 Failure of Corrugated Boxes Under Compressive Loading.....	5
2.1.3 Fibreboard Treatments	7
2.1.4 Other Performance Requirements of Corrugated Fibreboard Boxes	9
2.2 PREDICTION OF CORRUGATED BOX PERFORMANCE	9
2.2.1 Effect of Moisture on Box Performance	13
2.2.2 Effect of Cyclic Humidity on Box Performance.....	15
2.2.3 Effect of Storage Time on Box Performance.....	19
2.2.4 Effect of Mechanical Inputs on Box Performance	20
2.2.5 Effect of Contents on Box Performance.....	21
2.2.6 Effect of Packaging on Horticultural Produce Quality.....	22
2.3 ENVIRONMENTAL HAZARDS IN PRODUCE DISTRIBUTION	23
2.3.1 Vibration Hazards	24
2.3.2 Shock Hazards	31
2.3.3 Handling Hazards	38
2.3.4 Temperature and Humidity Hazards	41
2.3.5 Compression Hazards.....	45
2.4 LABORATORY TESTING OF PACKAGING SYSTEMS	46
2.4.1 International Standard ISO 4180	48
2.4.2 Standard Practice ASTM D 4169	50
2.4.3 TAPPI Useful Method UM 800.....	53
2.4.4 Australian Standard AS 2584	54
2.5 SUMMARY	55
3. AIMS AND OBJECTIVES	57

4. FIELD EXPERIMENTS	59
4.1 SHOCK AND VIBRATION	59
4.1.1 Methodology.....	60
4.1.2 Results and Discussion	62
4.1.2.1 Vibration	63
4.1.2.2 Shock.....	68
4.2 TEMPERATURE AND RELATIVE HUMIDITY	88
4.2.1 Methodology.....	89
4.2.2 Results And Discussion	91
4.2.2.1 Temperature.....	91
4.2.2.2 Relative Humidity.....	94
4.3 MANUAL AND MECHANICAL HANDLING	97
4.3.1 Methodology.....	97
4.3.2 Results And Discussion	99
4.3.2.1 Peak Acceleration, Duration, and Velocity Change Distributions.....	99
4.3.2.2 Equivalent Drop Height and Direction Distributions	107
4.4 SUMMARY OF RESULTS	112
4.4.1 Vibration.....	112
4.4.2 Shock.....	113
4.4.3 Temperature.....	113
4.4.4 Relative Humidity.....	114
4.4.5 Handling	114
 5. LABORATORY EXPERIMENTS	 115
5.1 METHODOLOGY	115
5.2 RESULTS AND DISCUSSION	117
5.2.1 Quasi-Static Compression of Corrugated Fibreboard Boxes.....	117
5.2.2 Dynamic Creep Testing of Corrugated Fibreboard Boxes	120
5.2.2.1 Raw Survival Time Data.....	121
5.2.2.2 Regression Modelling of Survival Time Data	124
5.3 SUMMARY OF RESULTS	132

6. CONCLUSIONS..... 135

7. REFERENCES 138

APPENDICES

A. PACKAGING PERFORMANCE TEST STANDARDS

B. DESCRIPTION OF EXPERIMENTAL EQUIPMENT

C. SET-UP OF EXPERIMENTAL EQUIPMENT

LIST OF FIGURES

Figure 1: (a) Summary of commercial transport random vibration spectra; (b) Comparison of leaf spring truck vertical vibration for different roads.....	26
Figure 2: Probability curves for package drops during handling operations.	40
Figure 3: Power spectral density: Average of all journeys, trailer PT298 in Melbourne. ..	64
Figure 4: Power spectral density: Average of all journeys, trailer PT279 in Melbourne. ..	65
Figure 5: Power spectral density: Average of all journeys, trailer PT279 to Bairnsdale. ..	65
Figure 6: Power spectral density: Average of all trailer/location combinations (1 - 100 Hz).....	66
Figure 7: Power spectral density: Average of all trailer/location combinations (1 - 10 Hz).....	66
Figure 8: Environmental damage potential plot: Trailer PT298 in Melbourne.....	75
Figure 9: Environmental damage potential plot: Trailer PT279 in Melbourne.....	75
Figure 10: Environmental damage potential plot: Trailer PT279 to Bairnsdale.....	76
Figure 11: Modelling of shock event peak acceleration distribution: Trailer PT298 in Melbourne.	79
Figure 12: Modelling of shock event peak acceleration distribution: Trailer PT279 in Melbourne.	80
Figure 13: Modelling of shock event peak acceleration distribution: Trailer PT279 to Bairnsdale.....	80
Figure 14: Modelling of shock event velocity change distribution: Trailer PT298 in Melbourne.	81
Figure 15: Modelling of shock event velocity change distribution: Trailer PT279 in Melbourne.	82
Figure 16: Modelling of shock event velocity change distribution: Trailer PT279 to Bairnsdale.....	82
Figure 17: Modelling of shock event crest factor distribution: Trailer PT298 in Melbourne.	83
Figure 18: Modelling of shock event crest factor distribution: Trailer PT279 in Melbourne.	84

Figure 19: Modelling of shock event crest factor distribution: Trailer PT279 to Bairnsdale.	84
Figure 20: Mean and 95% confidence intervals for temperature by vertical and lateral position in trailer.	92
Figure 21: Mean and 95% confidence intervals for temperature by longitudinal position in trailer.	93
Figure 22: Mean and 95% confidence intervals for relative humidity by vertical and lateral position in trailer.	95
Figure 23: Mean and 95% confidence intervals for relative humidity by longitudinal position in trailer.	96
Figure 24: Shock event peak acceleration distributions.	101
Figure 25: Shock event duration distributions.	102
Figure 26: Shock event velocity change distributions: Unloading operations.	103
Figure 27: Shock event velocity change distributions: Loading operations.	104
Figure 28: Shock event velocity change distributions: Resultant of all directions.	105
Figure 29: Environmental damage potential plot: Unloading operations.	106
Figure 30: Environmental damage potential plot: Loading operations.	106
Figure 31: Shock event impact direction distribution: Face impacts.	108
Figure 32: Shock event impact direction distribution: Edge impacts.	109
Figure 33: Shock event impact direction distribution: Corner impacts.	109
Figure 34: Calculation of equivalent drop height for half-sine waveform: Unloading operations.	110
Figure 35: Calculation of equivalent drop height for half-sine waveform: Loading operations.	111
Figure 36: Shock event equivalent drop height distribution assuming half-sine waveforms.	112
Figure 37: Estimated box natural frequencies (mean and 95% confidence bounds for mean).	119
Figure 38: Box performance indices for raw survival time data.	124
Figure 39: Applied mass during vibration vs box survival time (all raw data).	125
Figure 40: Box survival time vs applied mass during vibration (mean, standard error of mean, standard deviation, and fitted exponential regression model).	126

Figure 41: Comparison of observed and predicted box survival times (140 kg).....	128
Figure 42: Comparison of observed and predicted box survival times (165 kg).....	128
Figure 43: Comparison of observed and predicted box survival times (190 kg).....	129
Figure 44: Comparison of observed and predicted box survival times (215 kg).....	129
Figure 45: Prediction of the maximum mass supported by a box for a specified duration of vibration (mean and 95% confidence bounds for mean).	131
Figure 46: Example of EDR event-triggered acceleration waveform recording in overwrite memory mode.	156
Figure 47: Verification of EDR test rig using ASTM D 4728 truck spectrum on vibration table.....	166
Figure 48: Typical package drop shock pulse (vertical axis).	170
Figure 49: Typical package drop shock pulse (triaxial resultant).....	171
Figure 50: Comparison of experimental and standard ASTM truck PSD profiles.	172

LIST OF TABLES

Table 1: Vibration frequencies and maximum acceleration levels encountered in distribution.....	29
Table 2: Severest probable handling environments.....	40
Table 3: ISO test methods and factors requiring quantification before testing.	49
Table 4: ASTM D 4169 distribution cycles and element test sequences.	52
Table 5: ASTM D 4169 hazard elements and ASTM test methods.	52
Table 6: AS test methods and factors requiring quantification.	55
Table 7: EDR files generated during transport shock and vibration recording.	62
Table 8: Number of journeys, events, and samples for each trailer/location combination.	63
Table 9: RMS acceleration levels for each journey.	67
Table 10: Average RMS acceleration levels for each trailer/location combination.	67
Table 11: Shock event peak acceleration distributions: Distribution for each journey.....	69
Table 12: Shock event velocity change distributions: Distribution for each journey.....	70
Table 13: Shock event peak acceleration distributions: Overall distribution for each trailer/location combination.	71
Table 14: Shock event velocity change distributions: Overall distribution for each trailer/location combination.	72
Table 15: Shock event crest factor distributions: Overall distribution for each trailer/location combination.	73
Table 16: Fitted model parameters: Shock event peak acceleration distributions.....	86
Table 17: Fitted model parameters: Shock event velocity change distributions.....	87
Table 18: Fitted model parameters: Shock event crest factor distributions.	88
Table 19: Shock event peak acceleration distributions.	100
Table 20: Shock event duration distributions.....	102
Table 21: Shock event velocity change distributions: Resultant of all directions.....	105
Table 22: Shock event impact direction distribution summary.....	108
Table 23: Calculated equivalent drop height distribution for handling operations.	111
Table 24: Description of corrugated fibreboard boxes used for testing.....	116
Table 25: Box quasi-static compression strengths.....	117

Table 26: Box quasi-static compression strength differences.....	118
Table 27: Stiffness of boxes during quasi-static compression.	118
Table 28: Estimated box mean natural frequencies during vibration assuming a simple spring-mass system.....	119
Table 29: General observations of box deformation and failure during dynamic testing.	121
Table 30: Observed box survival times.	122
Table 31: Summary of observed box survival times.	122
Table 32: Differences between mean box survival times.	123
Table 33: Box performance indices for raw survival time data.	124
Table 34: Regression parameters for non-censored data analysis.	127
Table 35: Regression parameters for censored data analysis.	127
Table 36: Prediction of the maximum mass supported by a box for a specified duration of vibration (mean and 95% confidence bounds for mean).	130
Table 37: Regression parameters for censored data analysis of physical structure of box.	132
Table 38: International (ISO) transport packaging test standards and test procedure equivalents.	150
Table 39: PCB ICP accelerometers for transport shock and vibration recording.	156
Table 40: EDR-3 internal accelerometers used for handling recording.	161
Table 41: Calibration of ultrasonic displacement transducers.	162
Table 42: EDR2S RCPs for EDR for transport shock and vibration recording.....	163
Table 43: EDR1S RCPs for EDR-3 for handling recording.	168
Table 44: Drop test verification of EDR-3 for handling study.	169
Table 45: Breakpoints used for programming the experimental PSD profile on the random vibration controller.....	172

SYMBOLS AND ABBREVIATIONS USED

SYMBOLS

a	Cumulative random variable; amplitude of acceleration peak.
a_0	Median acceleration peak height.
B	Band-pass filter bandwidth (Hz).
c	Damping coefficient (kg/s).
c_c	Critical damping coefficient (kg/s).
C_r	Creep rate ((m/m)/hr $\times 10^6$).
D_x	Bending stiffness; machine direction (Nm).
D_y	Bending stiffness; cross direction (Nm).
e	Coefficient of restitution.
f	Frequency (Hz).
f_n	Natural frequency (Hz).
$F(a)$	Cumulative probability distribution function of random variable a .
$f(x)$	Probability distribution function of random variable x .
g	Acceleration at Earth's surface due to gravity (9.81 m/s ²).
g -RMS	Root mean square acceleration.
G_m	Peak acceleration on recorded shock waveform (g).
h	Combined corrugated fibreboard thickness (m); Drop height (m).
h_{eq}	Equivalent drop height (m).
H_R	Relative humidity (%).
i	Variable integer.
k	General coefficient; stiffness (N/m).
m	Mass (kg).
M	Moisture content (g H ₂ O/100 g dry material).
M_0	Box moisture content compression strength correction factor.
N	The set of positive integers, including zero.
n	Variable integer.
P	Container compression strength (N).

P_0	Box pallet pattern compression strength correction factor.
P_m	Edgewise compression strength (N/m).
r	Correlation coefficient.
R	The set of real numbers, including zero.
s	Sample standard deviation.
s^2	Sample variance.
t	Time (s); Storage time (days).
t_s	Survival time (s).
T_0	Box storage time compression strength correction factor.
V_i	Impact velocity of dropped object.
V_r	Rebound velocity of dropped object.
x	Random variable; Independent variable.
\bar{x}	Sample mean.
$\overline{x^2}$	Mean square value.
z	Perimeter of corrugated fibreboard box (m).

GREEK LETTERS

ξ	Damping ratio.
Σ	Denotes 'the summation of'.
γ	Location parameter of Weibull probability distribution.
μ	Population mean.
σ	Population standard deviation.
δ	Scale parameter of Weibull probability distribution.
α	Shape parameter of gamma probability distribution.
β	Shape parameter of Weibull probability distribution; Scale parameter of gamma probability distribution; Regression parameter of exponential regression model.
τ	Time to box failure (hr); Duration of recorded shock waveform (s).
$\Gamma(x)$	Gamma function of independent variable x .

σ^2	Population variance.
Δf	Frequency interval (Hz).
ΔV	Velocity change.
ΔV_R	Resultant velocity change.

ABBREVIATIONS

ADC	Analogue-to-digital converter.
ANSI	American National Standards Institute.
APPITA	The Technical Association of the Australia and New Zealand Pulp and Paper Industry.
AQIS	Australian Quarantine and Inspection Service.
ASCII	American Standard Code for Information Interchange.
ASTM	American Society for Testing and Materials.
Ba	Back orientation of EDR.
Bo	Bottom orientation of EDR.
BPF	Band-pass filter.
BSF	Board strength factor.
CD	Cross direction.
CSIRO	Commonwealth Scientific and Industrial Research Organisation.
DBC	Damage boundary curve.
DBW	Digital bandwidth.
DC	Distribution cycle.
DPI&E	Department of Primary Industries and Energy.
DTP	Dead-time period.
EBI	Equivalent bruise index.
ECT	Edge crush test.
EDH	Equivalent drop height.
EDR	Environmental Data Recorder.
EGVIB	East Gippsland Vegetable Industry Board.
EVA	Ethylene-vinyl acetate copolymer.

FAC	Forced air cooling.
fcc	Face centred cubic.
FFT	Fast Fourier transform.
FL	Frame length.
Fr	Front orientation of EDR.
IBM	International Business Machines.
ICP	Integrated circuit piezoelectric.
IHD	Institute for Horticultural Development, Department of Agriculture, Victoria.
ISO	International Organisation for Standardisation.
IST	Instrumented Sensor Technology, Inc.
ISTA	International Safe Transit Association.
Le	Left orientation of EDR.
LPF	Low-pass filter.
MC	Moisture content.
PC	IBM-compatible personal computer.
PCB	PCB Piezotronics, Inc.
PE	Polyethylene.
PS	Power spectrum.
PSD	Power spectral density.
PT279 etc.	Trailer identification numbers.
RCP	Recording control parameter.
RCT	Ring crush test.
RH	Relative humidity.
Ri	Right orientation of EDR.
RMS	Root mean square.
RS-232 etc.	Standards for serial data transfer between computers and devices.
RSC	Regular slotted container (International Fibreboard Box Code 0201).
RV	Random vibration.
SAA	Standards Association of Australia.
SF	Sampling frequency.
SPI	The Society of Plastics Industry, Inc.
SSR	Sum of the squares of the residuals.

TAPPI Technical Association of Pulp and Paper Industries.
TDT Trigger duration threshold.
To Top orientation of EDR.

1. INTRODUCTION

Packaging of fresh horticultural produce performs several functions, with two major functions being the prevention of physiological deterioration and the prevention of mechanical damage during distribution. Physiological deterioration can be minimised through the control of the atmosphere, relative humidity, and temperature during distribution of the produce. Mechanical damage can be minimised by lowering the levels of mechanical inputs received by the produce. Although caused by different sources, physiological deterioration and mechanical damage are linked. Physiological deterioration will eventually increase the susceptibility of the product to mechanical damage, and mechanical damage will eventually contribute to increased physiological deterioration.

Horticultural produce has traditionally been packaged in corrugated fibreboard boxes, and physiological deterioration has been controlled using cool temperatures at some, or more rarely, all parts of the distribution system. Produce is also transported and stored at high humidities to prevent moisture loss. It is well known that the strength of corrugated fibreboard is affected by relative humidity. To prevent structural failure of the boxes, manufacturers have used a number of design techniques, including thicker board, wax coatings and laminates, and multilayer constructions. Although each of these techniques has the advantage of improving the strength of the fibreboard at high relative humidities, this has been at the expense of recyclability, cost, and increased use of packaging materials.

Additionally, unpredictable humidity levels, the little understood effects of cyclic humidity, environmental shock, vibration, and compression, and variations in transpiration rates between products, cultivars, and seasons, have all contributed to the overdesign of boxes to withstand any likely occurrence during distribution. In this respect, the design of transport packaging for horticultural produce has been based on considerable trial and error.

Considerable work has been performed in recent years on the effect of high or cyclic humidity on the performance of corrugated fibreboard boxes and their component materials. This work has generally used some static mechanical characteristic of the box as a performance indicator, such as long-term survival time, long-term creep rate, or quasi-static compression strength. These methods, while allowing for dynamic humidity and/or temperature conditions, do not allow for dynamic loading of the box over the test duration. In obtaining the properties of a fibreboard box relating to its stress-strain diagram (e.g. peak force and deflection, static creep, and energy adsorption), either a large load is applied gradually, or a small load is applied over a long time, allowing sufficient time for the strain to develop.

For many products, long-term storage under cycling humidity conditions is a realistic distribution condition, but this is not necessarily the case for fresh horticultural produce. A typical distribution system for fresh produce involves long transport distances, relatively short storage times, and reasonably constant (or involving few cycles) humidity conditions. For distribution systems where the storage times are greater than the transportation times, static or quasi-static mechanical properties may be an effective measure of the performance of produce packaging systems. In a fresh produce distribution system, however, where transportation times are about the same as storage times, and hence the transportation phase constitutes a larger proportion of the total distribution system, some form of dynamic measure may be more relevant.

The concept for this project arose from the changes currently taking place in the East Gippsland vegetable industry, with the introduction of several lines of products for domestic markets, and, ultimately, export to the Asia/Pacific region. The perishable nature of these products, the extended transport distances, and the need to ensure consistently high quality at a competitive price all advocate research into this particular area of horticultural packaging.

2. LITERATURE REVIEW

This section contains relevant background from the literature regarding fibreboard packaging for horticultural products. It is organised into four major sections as follows:

1. *Fibreboard packaging for physical distribution*, including an introduction to corrugated fibreboard boxes, and their strength requirements, performance, and failure modes with respect to horticultural products.
2. *Prediction of corrugated box performance*, including the effects of distribution hazards and contents on box performance, and the effects of packaging on produce quality.
3. *Environmental hazards in produce distribution*, including vibration, shock, handling operations, compression, temperature, and humidity hazards.
4. *Laboratory testing of packaging systems*, including an introduction to the most common packaging system performance test schedules used in Australia and the world.

2.1 FIBREBOARD PACKAGING FOR PHYSICAL DISTRIBUTION

The manufacture of corrugated fibreboard and boxes began near the end of the 19th century and grew rapidly early in the 20th century. This growth was due largely to US railways permitting fibreboard boxes to replace wood boxes for many commodities. Corrugated boxes are lightweight and inexpensive, can be mass produced in many sizes and weights, and take up little storage space before use (Swéc, 1986).

A corrugated box is made from two or more sheets of linerboard and one or more fluted sheets of corrugating medium. Most of the liner for corrugated board made today is unbleached kraft. Linerboard comes in a variety of weights, commonly ranging from about 100-300 g/m². The important characteristics of linerboard are its stiffness, bursting strength, uniform moisture content, and surface finish (Wright et al., 1992).

The most widely used grades of corrugating media range from about 120-180 g/m². Corrugated box stacking strength (vertical compression strength) is more sensitive to

medium weight than to liner weight. Recycled material is often used in corrugating media, either ex-factory clippings or good quality post-consumer waste. The important characteristics of corrugating media are its runnability on a corrugator and its resistance to flat crush (Wright et al., 1992).

The corrugations, or flutes, impressed in the medium give corrugated board its strength and cushioning qualities. In corrugated boxes, flutes are usually vertical to give maximum stacking strength. They come in four standard sizes, each with its own special qualities. Corrugating medium faced with linerboard is called corrugated fibreboard. If it is lined on one side only, it is called single-face board. If it is lined on both sides, it is called single-wall or double-face board. Additional media and liners yield double-wall and triple-wall board.

Single-face board is used primarily as a protective wrap and cushioning material, and is especially useful as an interior packing for fragile products such as glass. It represents less than 1% of the total corrugated box industry, but does not seem to be prevalent at all in horticultural packaging.

Single-wall board is the backbone of the corrugated box industry. About 90% of all corrugated boxes are made of single-wall. Corrugated boxes used in the horticultural industry seem to consist almost exclusively of this form of board. Single-wall board is also used to make partitions and other forms of interior packing for boxes.

Double-wall and triple-wall boards are used for packing large and heavy items, or when greater strength and rigidity are required. Their use represents about 9% of the corrugated box industry (Wright et al., 1992), but their use in horticultural packaging seems to be restricted to bulk bins.

2.1.1 Strength Requirements of Corrugated Boxes

Strength in a corrugated fibreboard box is required in two basic areas depending on the nature of the box contents: containability and stacking strength (Wright et al., 1992).

Containability is the major functional requirement for weight-bearing contents such as cans or bottles, where internal forces are generated by the contents as they tend to jostle loose and burst open the box. For non-weight-bearing contents, such as most horticultural products, the major functional requirement of the box is stacking strength, as the bottom box must withstand the weight imposed in a warehouse or transport stack.

The load carrying capability of a corrugated box is related to the strength of the vertical panels in compression. The box is weakest in the centre of the panels and strongest at the corners. The greatest stacking strength is obtained by arranging the stack so that the strongest areas match each other, so that the deflection along the horizontal edges of each panel is uniform. This relationship is achieved by column stacking the boxes directly above one another. In contrast, when interlock stacking is used the strong corners of one panel match the weaker areas in the adjoining layers, creating uneven deflection along the horizontal edge of the panel. This causes excessive panel bulge and consequent box failure at a lower load than for column stacking.

The strength of corrugated boxes is also affected by the moisture content (MC) of the component materials. This in turn is determined by the relative humidity (RH) of the distribution atmosphere. Equations relating the moisture content of a typical corrugated fibreboard material to the storage RH have been developed by Eagleton & Marcondes (1994). Packing of wet produce or storing boxes in a high humidity environment can significantly affect the stacking performance of the box due to migration of moisture into the board. These problems can be overcome by improved handling techniques, and where moisture cannot be avoided, by using specially treated boxes that give improved stacking strength but at a greater cost.

2.1.2 Failure of Corrugated Boxes Under Compressive Loading

Performance under vertical compressive load is the major functional requirement for corrugated fibreboard boxes containing horticultural products. Corrugated board is an efficient structural material in terms of strength to weight ratio, and has two separate but related requirements: stiffness, and failure strength. Burst strength has in the past also

been an important requirement, but with the recent moves away from regulatory to performance-based criteria, this is no longer the case.

Several researchers (notably Fox, 1978, and Fox et al., 1978) have modelled the response of corrugated boxes to various loadings. Peterson & Fox (1978) extended this previous work and developed a unified container performance and failure theory which accurately predicts box end-use performance. Their major results were:

1. Regardless of the end-use loading, the compressive strength of the liner is a key attribute to be maximised to improve corrugated box performance.
2. Corrugated boxes can be successfully modelled using conventional methods of engineering mechanics.
3. When loaded internally, corrugated boxes fail in compression, rather than in tension, in a manner morphologically similar to that experienced by boxes subjected to external loading.
4. Boxes loaded simultaneously with both internal and external loads also fail in compression.

Failure of corrugated fibreboard in compression is buckling dominated, with most obvious sign of the onset of box failure being bulging of the box panels. This bulge causes a redistribution of stresses within the panels from uniform vertical compression to a concentration of stress towards the vertical edges of the box, combined with a general redistribution of compressive stress toward the inside liner (assuming outward bulge).

Wright et al (1992) summarised the mechanisms of box compression and failure. In general, the predominant factor developing or causing the stresses is the bulge, or more precisely, the curvature of the panel. Whatever can be done to limit bulge and curvature will be beneficial to box performance. Bulge that occurs slowly (under sustained load and perhaps high or cyclic RH) will develop higher curvatures before failure than in standard laboratory testing which is relatively instantaneous. This is because individual fibres within the paper have time to accommodate the changes in geometry as they occur, without producing the high stresses that are typical of rapid testing.

The ultimate failure of a corrugated box depends on the mode of failure of the individual panels. This is due to the different strains and deflection patterns induced in the panel so as to be compatible with the strains and stresses of the adjacent panels, where the panels meet at the vertical creases. Two basic modes of failure are observed: (i) transverse shear failure at the vertical crease, and (ii) bending failure.

Transverse shear failure at the vertical crease is generally associated with a horizontal failure line, meeting at the vertical crease in a delta of tributary crease lines. The adjacent panel will fail in a similar mode but may be of the same or opposite curvature. Kutt & Mithel (1968) showed that the most serious loss of compression strength occurs when all corners fail by shear type failure, when adjacent panels have opposite curvature. Under these circumstances it is important for the box to have a strong medium and well-formed vertical creases to make it more difficult for shear failure and its associated vertical crease mobility to occur.

Bending failure is generally associated with a failure line running from the corner of the panel. A fully developed failure involves all four corners of each panel, but sometimes only part of the complete pattern may occur. The angle of the failure line to the horizontal crease at the corner of the box is around 30° (for an RSC). At times these two types of failure can be combined in the one panel. This can happen in the panels adjacent to the manufacturer's joint as the joint has the effect of reinforcing the panel against a transverse shear type of failure. It has also been observed that long shallow panels have a tendency to transverse shear failure rather than bending failure.

2.1.3 Fibreboard Treatments

Several papermaking machine treatments are available to improve the properties of linerboard. These include the addition of small amounts of a thermosetting resin to improve wet strength (e.g. for iced poultry, fish, and produce boxes), and colloidal silica to improve skid resistance (e.g. to improve running on some automatic packing lines and to improve the stability of some pallet loads) (Swec, 1986).

Other aqueous emulsion surface treatments have been developed to improve various properties while the linerboard is on the corrugator. These include specialised chemicals to enhance water repellence, skid resistance, scuff resistance, oil and grease resistance, and saleability and release properties. Wax impregnation may also take place while on the corrugator, and in this case paraffin wax is applied at weights of about 25-50 g/m². Wax impregnation helps to delay and minimise the absorption of water by the corrugated board, and is mainly used for iced poultry, fish, and fresh horticultural produce.

The most extensively used type of coating for finished corrugated board is curtain coating. Water-resistant board is obtained in this manner by coating the finished printed blank as the final step before the box is formed. The wax blends usually used for curtain coating may include paraffin wax, microcrystalline wax, ethylene-vinyl acetate (EVA) copolymer, and a petroleum resin. Usually about 25-50 g/m² of coating is sufficient to give a continuous waterproof layer that has enough flexibility to withstand folding at the scores. Curtain coated boxes are often used for frozen products such as fish, poultry, meat, and wet produce.

Corrugated boxes may also be coated by wax-dipping or cascading. In this process a finished box with a glued joint is completely saturated with paraffin wax, either by dipping or by cascading the molten wax through and around the board flutes. Considerably more wax (about 40-50% by weight of the board) is picked up in these processes compared with wax impregnation and curtain coating both sides. A dipped or cascaded box is relatively stiff because most of the crystalline wax is impregnated into the fibreboard. Such a box will withstand water spraying and excessive exposure to water for short periods of time. It is most often used for fresh vegetables that are hydrocooled, such as celery and broccoli.

Polyethylene coated linerboard is also a good moisture barrier for corrugated boxes, however this extrusion coated board is expensive and not used extensively. Polyethylene coated board is particularly useful where a good water vapour barrier is needed, or where the excellent release characteristics of PE are needed on the inside box surface. Extrusion coated board is also recyclable, whereas wax coated board is not usually recyclable.

2.1.4 Other Performance Requirements of Corrugated Fibreboard Boxes

In addition to providing compression strength in stacks and contents containability, corrugated fibreboard boxes often perform other functions.

One such function is the provision of cushioning protection to the contents. This is achieved both through the stiffness of the corrugating medium, and the presence of air between the corrugations (Marcondes, 1994). When a filled corrugated fibreboard box is dropped, the energy of the impact is dissipated into both the fibreboard and the contents. When strain energy is dissipated into horticultural produce, mechanical damage of one form or another is the likely result. Unlike many resilient foam cushioning materials, repeated impacts will eventually destroy the energy dissipating properties of corrugated fibreboard as each impact breaks more fibres and decreases its resilience.

Corrugated boxes can also contribute to the efficiency of produce cooling. During room cooling, a small amount of heat escapes from produce in boxes by conduction through the produce and the fibreboard walls. However more heat can escape through air movement within the box and through vents in the box walls. When rapid cooling is required, or when forced air cooling (FAC) is used, boxes should always be vented. Venting of 5% of the side area of a box is expected to reduce its stacking strength by only about 3% if the vents are positioned away from the corners, but the presence of vents may also make boxes more prone to bulge (Langbridge, 1983). It has been recommended that where any cooling is required, 5-7% of the box side area should be vented (Story, 1994).

2.2 PREDICTION OF CORRUGATED BOX PERFORMANCE

During distribution, the three major activities that present a potential for physiological and/or mechanical damage to products and packages are transportation, handling, and storage. The forces in the distribution environment which contribute to mechanical damage originate from impacts, vibration, and compression. Control of temperature,

humidity, and air flow is also essential for the prevention of physiological degeneration during any of these activities.

For the design of optimal packaging, three components should be known and clearly understood: the hazards present in the distribution environment, the properties of the packaging materials, and the susceptibility of the products to damage. The hazards in the distribution environment can be identified using measurement and analysis techniques, and the properties of the packaging materials can be determined using laboratory test procedures. There are standard procedures available for the quantification of these two components. For the third component, however, the determination of product damage susceptibility is often a complex task. The damage susceptibility of many mechanical products can be quantified using relatively simple mathematical models, and again there are standard procedures available for this purpose. Agricultural and horticultural products, however, cannot generally be modelled in such a straightforward manner, and effective techniques are not available for many classes of products (Marcondes, 1993).

Classification systems for corrugated boards used in boxes have traditionally been based on their burst strength and grammage. This practice stemmed from the United States' Uniform Freight Classification Rule 41, in which the responsibility for product damage during distribution is on the carrier rather than the owner of the product. A more detailed history of Rule 41 is given by Maltenfort (1988). The result of Rule 41 is that United States board grades are highly standardised, with great uniformity of both linerboard and media (Wright et al., 1992).

However in Australia, as in most other countries, there are no rules transferring financial responsibility from the owner to the carrier of the product. The result of this is that there are no 'standard' board grades, no uniformity of components, and a strong movement toward performance-based criteria for classification systems. The importance of performance-based criteria was finally recognised in the United States by the adoption of alternative carrier rules from early 1991.

The performance of a corrugated fibreboard box is generally defined in terms of its stacking strength (Langbridge, 1983), i.e. its resistance to vertical compression loading. The most common measure for the stacking strength potential of corrugated boards is the Edge Crush Test (ECT). However there are a number of limitations to the ECT (Wright et al., 1992):

1. There is still no international uniformity in test methods for ECT.
2. ECT must be combined with bending stiffness to give a measure of stacking strength.
3. ECT does not properly account for the effects of changing the balance or disposition of components in a particular application.
4. As a test it is more suited to process control than verification of grades, particularly when the steps between grades are small.
5. ECT is a failure test conducted at a fixed loading speed under specific test conditions. Stacking performance also involves elastic properties and is evaluated, in practice, with a sustained load in a variable environment of humidity and temperature.

McKee et al. (1961, 1962, 1963) developed several models for estimating the top-to-bottom compression strength of corrugated fibreboard boxes from tests of individual component materials and combined boards under fixed environmental conditions. The best known estimator of box compression strength is the McKee formula:

$$P = 2.028P_m^{0.746} (D_y D_x)^{0.127} z^{0.492} \quad (2.1)$$

or in its simplified form:

$$P = 5.87P_m \sqrt{hz} \quad (2.2)$$

where P is the estimated container compression strength (N), P_m is the ECT edgewise compression strength (N/m), D_y and D_x are the board bending stiffness (N/m) for the cross and machine directions respectively, h is the combined corrugated fibreboard thickness (m), and z is the box perimeter (m).

Johnson et al. (1979, 1984, 1989) took the prediction of corrugated behaviour one step further than McKee, and included the constitutive behaviour of the components. Their results agree well with McKee's work. Their model has more flexibility than McKee's formula, because it can be incorporated into finite element (FE) programs that allow the user to predict multi-wall corrugated behaviour. Urbanik (1981) used an early version of this model to successfully predict ECT values given the constitutive behaviour of the components.

Thorough work in FE modelling was performed by Luo et al. (1992). This work analysed the corrugated structure with the added simplicity of a commercial FE program. Similar work was conducted by Pommier et al. (1991); both works incorporated the behaviour of components in the prediction of the combined board behaviour.

In recent times, many board manufacturers have developed alternative performance specification systems for their boards. An example is the rating system developed by Amcor Fibre Packaging in which boards are rated in terms of both stacking performance and containment performance (Wright et al., 1992). Stacking performance is rated by means of a 'board strength factor' (BSF) which indicates the predicted top-to-bottom compression strength of a regular slotted container (RSC) of fixed dimensions. The BSF is calculated using minimum cross-direction ring crush test (CD RCT) and thickness properties of components obtained from papermill specifications and is corrected from the results of regular audits of made-up boxes. Containment performance is likewise rated by means of a containment index for each combination of components, as described by Stott (1991).

The McKee formula given in Equations (2.1) and (2.2) is only valid for constant ambient RH, temperature, storage time, and pallet stacking pattern. The performance of produce packaging is greatly affected by the physical conditions experienced during transport and distribution, including shock, vibration, compression, loading history, RH and cyclic humidity, and any combinations of these. Several researchers have developed empirical equations and correction factors to allow for the effects of these environmental variables if the compression strength of the box at some standard conditions is known.

2.2.1 Effect of Moisture on Box Performance

Humidity changes regularly occur in most distribution environments (Ievans, 1977), particularly in environments during the distribution of fresh horticultural products (Langbridge, 1983), and McKee's models (Equations 2.2.1 and 2.2.2) do not include the effects of moisture content (Kawanishi, 1989). Thus corrugated boxes are often evaluated for their performance at constant RH conditions without considering how different types of liners, mediums, or adhesives may be affected by the humidity profile of the true distribution environment (Laufenburg, 1991). It has been reported that in high humidity environments, corrugated containers typically have between 10% and 20% of their 50% RH compressive strength (Considine & Laufenburg, 1992).

Wink (1961) published a summary of the results to date on the understanding of paperboard behaviour in different static RH and temperature environments. He presented evidence showing that paper experiences irreversible property changes after excursions to any RH greater than 65%. Wink also showed that mechanical properties were more sensitive to RH than temperatures in traditional operating environments. Benson's (1971) work further demonstrated the irreversible changes experienced by paper during exposure to high RH environments. His work showed that (i) tensile properties could be related to moisture content of the paper, and (ii) the moisture isotherm of paper indicated that moisture content was a more reliable predictor of paper behaviour than RH.

De Ruvo et al. (1976) published a comprehensive study on the behaviour of paper and cellulose fibres in different temperature and RH environments. He made three main conclusions: (i) a direct relationship exists between the elastic properties and hygroexpansion of the sheet; (ii) sheet anisotropy changes with sheet moisture content; and (iii) cellulose behaves irregularly during moisture sorption, indicating that transient moisture sorption was evident.

Okushima & Robertson (1979) examined the MC sensitivity of the tensile behaviour of paper. Their experiments showed that during cyclic loading the modulus initially

increased. They theorised that as the load increased, more fibre-to-fibre bonds became available and improved the stress distribution within the sheet. De Ruvo et al. (1976) showed that the total water uptake for paper reached equilibrium after only 1 hr; however the water within the sheet continues to migrate for up to 85 hr. Apparently, the water uptake places the water molecules in unfavourable positions. The water molecules then slowly move to more favourable energy locations and, as a result, improves the stress distribution in the sheet.

Back (1985) compared moisture sensitivity as related to compressive strength and tensile strength. His work indicated that compressive strength is more adversely affected by moisture than is tensile strength. Back also concluded that for static RH conditions, compressive and tensile strengths are not a function of moisture history, but only of moisture content.

Gunderson et al. (1988) examined the compressive behaviour at different load rates and in different static RH environments and showed the nonlinear viscoelastic nature of both a neutral sulphite semichemical corrugating medium and a kraft linerboard. Both materials showed increased failure strain, reduced compressive strength, and reduced stiffness at lower load rates. The effects of load rate were more significant at 90% RH than at 50% RH.

Haslach et al. (1990) proposed a viscoelastic model to predict the effect of linearly varying moisture content on the tensile creep of paper. This model generalised previous constant moisture content models for creep and for uniaxial stress-strain tests. Results showed that both the creep and swelling strain magnitudes are dependent on the rate at which the RH varies.

Considine et al. (1994) studied the effect of cyclic humidity on the creep properties of containerboard components. They found that creep performance could not be predicted by compressive strength, failure strain, stiffness, or energy adsorption, but could be adequately predicted by hygroexpansive strain.

Kellicutt & Landt (1951) found that box compression strength and the fibreboard moisture content are linked by the following relationship:

$$\frac{P_2}{P_1} = \frac{10^{3.01M_1}}{10^{3.01M_2}} \quad (2.3)$$

where P_1 and P_2 are the ultimate compression strengths of boxes having moisture contents M_1 and M_2 respectively. The moisture content is expressed as a decimal determined by dividing the weight of water in the board by the dry-oven weight of fibreboard. Eagleton & Marcondes (1994) have described a model relating board moisture content to the RH of the storage environment.

The Society of Plastics Industry, Inc, have also suggested the use of the following correction factor for the strength of corrugated boxes stored at RHs above 50% (SPI, 1980):

$$M_0 = 1 - \frac{(H_R - 50)}{67} \quad (2.4)$$

where M_0 is the box moisture content compression strength correction factor, and H_R is the relative humidity (%) in which the box is stored.

Considine & Laufenburg (1992) report that typical compressive strength design factors for corrugated boxes range from 7 (for low RH conditions) to 20 (for high RH conditions).

2.2.2 Effect of Cyclic Humidity on Box Performance

The previously described studies have dealt primarily with paper and combined board behaviour in constant moisture environments. The work of some scientists investigating solid wood (Armstrong & Kingston, 1960; Armstrong & Christensen, 1961; Armstrong & Kingston, 1962) indicated that variable moisture environments, such as those experienced

during the use of paper and paperboard, should be investigated. In their work, they found that the bending of solid wood beams was greatly accelerated by cyclic humidity.

Many researchers have since studied the behaviour of converted and unconverted structural paper under dynamic environmental conditions. Results from these studies have shown that the compressive strength of paperboard and combined board is significantly reduced by fluctuating or cyclic RH conditions. The interaction between the load and the moisture sorption behaviour is defined as mechanosorption. This effect is found in all wood and wood products, and mechanosorptive behaviour is most frequently recognised by reduced duration of load in changing moisture environments. Mechanosorptive creep also exhibits frequency independence; the creep is independent of the frequency of moisture change and depends only on the number of moisture cycles, assuming all the moisture cycles were between the same RH levels (Gunderson & Tobey, 1990).

Byrd (1972a, 1972b) examined the tensile and compressive creep behaviour of paperboard in cyclic humidity environments and compared these results to creep tests in constant humidity environments. He showed that at equal creep loads, the specimens in cyclic humidity environments had higher creep rates and more frequent failures than those in constant humidity environments. Byrd also performed tensile creep tests on single fibres. Results showed that fibril angle decreased in constant RH environments, but increased in cyclic RH environments.

Later, Byrd & Koning (1978) examined the compressive creep behaviour of ECT specimens. In this work, they showed that recycled paperboards and high-yield paperboard (i.e. paperboard made from high-yield semichemical or mechanical pulping processes) had greater deformation than did virgin low-yield paperboard. The differences between these paperboards were not evident during creep at constant RH; only during cyclic RH.

Byrd (1984a, 1984b) examined the compressive creep behaviour of paperboard with a new device developed by Gunderson (1981). Byrd further validated previous results by showing that high-yield and recycled paperboard performed more poorly than did virgin,

low-yield paperboard. He also showed that the rate of creep was related to the moisture uptake of the paperboard. Furthermore, Byrd showed that the deformation of the components was not as large as that of the ECT specimens made with the same material. He proposed a mechanism of cyclic humidity creep based on his measurements of moisture content during creep tests. His experiments found that MC continually increases during creep tests.

Considine et al. (1989) measured the compressive creep behaviour of paperboard in a cyclic humidity environment. In that experiment, they observed a reduction of paperboard stiffness directly related to the amount of creep. They also measured compressive creep strains several times larger than those measured during short term compressive strength tests at constant RH.

Haslach et al. (1989, 1991) also examined the tensile creep of paperboard during cyclic humidity and found a dependence of deformation of the rate of humidity change. They are trying to reconcile their work with that of Gunderson. Other variables, such as load and RH magnitude, may play an important role.

Soremark & Fellers (1991) examined the bending behaviour of corrugated specimens in constant and cyclic humidity environments. They proposed an additional mechanism that contributes to the large deformations in cyclic humidity environments. Once deformation was accounted for, it was found that the amount of hygroexpansion depended on whether the specimen was loaded in compression or tension. They called this phenomena stress-induced hygroexpansion; compression increases hygroexpansion, and tension reduces hygroexpansion.

Byrd (1986) showed that the creep deformation of the adhesive joint in corrugated specimens could be greater than that of either component. Whitsitt & McKee (1975) showed the importance of a water-resistant adhesive in constant high-humidity environments. Leake & Wojcik (1988) showed that water-resistant adhesives could significantly improve box behaviour in uncontrolled RH environments.

Leake (1988) examined the behaviour of boxes loaded in top-to-bottom compression and subjected to constant and cyclic humidity environments. He found that ECT results at 50% and 90% RH could not predict the box behaviour in cyclic RH environments. This study also demonstrated the important contribution of the corrugating medium in box behaviour. Similar work in this area was also done by Boonyasarn et al. (1992) and Leake & Wojcik (1993).

Marcondes (1993) also noted that although the compressive strength of corrugated fibreboard boxes always decreases as RH increases, the shock absorbing characteristics may or may not improve, depending on the energy involved in the impact (i.e. the drop height and the coefficient of restitution) and on the static load. These results are particularly important when packaging fresh horticultural produce as it is necessary to provide both compression resistance and energy dissipation characteristics (Marcondes, 1992a).

Recent measurements published by Laufenburg (1991) demonstrated the difficulty of relating the cyclic creep behaviour of paperboard, combined board, and containers from experimental data. Several researchers have tried to determine the mechanisms of accelerated creep of paperboard in cyclic humidity environments. Back et al. (1983, 1985) measured the transient mechanical behaviour of paperboard during tension while sorbing moisture. They compared their results with researchers working on wool and other natural fibres. It was concluded that the amount of transient behaviour is governed by the rate of moisture sorption. As a result of transient behaviour, stiffness and strength are a function of MC and the MC gradient. That is, at equilibrium conditions for a given material, stiffness and strength are solely functions of MC, but during moisture sorption, the rate of moisture change also affects stiffness and strength.

From these studies, it is obvious that paperboard experiences relatively unpredictable changes in properties during moisture sorption. Static RH tests are not sufficient to predict this behaviour. These mechanisms include transient stiffness loss during moisture sorption, RH frequency effects, and moisture gain during cyclic RH. There does not

appear to be a comprehensive model describing mechanosorptive behaviour, including the behaviour of paperboard during compressive creep in a cyclic humidity environment.

2.2.3 Effect of Storage Time on Box Performance

The time effect, or creep, of RSC containers when loaded by a dead weight for prolonged periods was investigated by Kellicutt & Landt (1951), Moody & Skidmore (1966), Koning & Stern (1977), and Zhao (1993), among several others. They found that the total time from load application to failure at a given RH environment depends strongly on the dead weight applied. If the load is near the ultimate compressive strength of the container, it will usually fail within minutes, while dead loads of about 60% of yield load may cause container failure after 30 days. It is unlikely, however, that chilled horticultural produce could be stored in boxes for this length of time.

Koning & Stern (1977) established an empirical relationship linking the duration to failure, τ , of dead loaded RSC containers in terms of creep rate, C_r :

$$\tau = \frac{4988}{C_r^{1.038}} \quad (2.5)$$

where τ is in hr and C_r is measured in strain units per hour times 10^6 (i.e. (m/m)/hr $\times 10^6$).

The Society of Plastics Industry, Inc., have proposed the following correction factor for corrugated boxes stored for extended duration (SPI, 1980):

$$T_0 = 1 - 0.204t^{0.104} \quad (2.6)$$

where T_0 is the box storage time compression strength correction factor and t is the duration of storage in days.

Hanlon (1984) proposed that one-quarter of the compressive strength of a corrugated box may be used as a rule of thumb when predicting long-term stacking strength, but argued

that a more accurate method would involve calculation of a fatigue factor for the length of time in storage.

2.2.4 Effect of Mechanical Inputs on Box Performance

Adams et al. (1992) conducted tests on various RSC boxes to determine the effect of simulated transit vibration on the compressive strength of corrugated boxes. They subjected boxes to an acceleration amplitude of 0.5 g peak input during resonance for 15 min, using ASTM D 4169 assurance level I (ASTM, 1994). Their results showed that the mean vibrated compression strength was approximately one-third of the mean non-vibrated compression strength. Boxes typically failed within the first 4 min of vibration with a top load of one-third of the mean compression strength of the non-vibrated boxes. They suggested a correction factor of 3 to be appropriate for calculation of the maximum load a box can withstand in a transient vibration environment. In contrast, Marcondes (1994) suggested correction factors of 1.5 and 1.8 for highways and rough roads respectively.

Marcondes (1992b) investigated the effect of static and dynamic load history on the compression strength and shock absorption properties of corrugated fibreboard boxes. His results indicated that dynamic compression forces do, and static compression forces do not, have an influence on these factors. A history of drops can cause a significant reduction in the final compression strength of corrugated fibreboard boxes, with the reduction being a function of the number of drops. Crofts (1989) studied the effect of multiple drops on the compression strength of corrugated fibreboard boxes and concluded that the mean overall box compression strength decreased as the drop heights increased and as the gross weight of the boxes increased.

Pallets also have an effect on the performance of the boxes they carry. Monaghan & Marcondes (1992) conducted experiments to determine the effect of overhang and gap size on the ultimate vertical compression strength of corrugated fibreboard boxes for fresh produce. They found that compression strength decreased with both gap size and overhang. White (1992) studied the influence of pallet design on unit load performance and found that non-uniform stress distribution of pallet decking also reduces stacking

strength. The Society of Plastics Industry, Inc., proposed the following correction factor for corrugated boxes stored on gapped or overhanging pallets (SPI, 1980):

$$P_0 = \frac{\text{(contact area)}}{\text{(face area)}} \quad (2.7)$$

where P_0 is the box pallet pattern compression strength correction factor, that represents the percentage of bottom or top areas of the box in contact with only one other box.

2.2.5 Effect of Contents on Box Performance

Peleg (1985) conducted experiments to determine the effect of content apples on the compressive strength of fibreboard boxes, and found the yield force of full boxes to be greater than that of empty boxes. The initial load was apparently carried by the container sides, and as the box deformed the increased produce's share in bearing the load results in greater yield forces. The internal pressure of the produce enhanced bulging of the container sides, increasing the box deflections. Another aspect of the share of the stacking load borne by the apples was the packing method. The results showed that a face-centred-cubic (fcc) pattern pack caused less bulging than a random jumble pack, thereby enabling the box to bear a greater load before collapsing. This resulted in better protection to the apples and emphasised the greater protective quality of the fcc produce packaging system.

The question now arises concerning the emphasis that should be placed on the load-bearing capability of horticultural products. Some products, such as rockmelons or potatoes, are capable of bearing considerable weight without damage. Other products, such as citrus, can tolerate intermediate loads. However the majority of produce, such as broccoli, lettuce, kiwifruit, strawberries, and tomatoes, can support no load without suffering some mechanical damage.

2.2.6 Effect of Packaging on Horticultural Produce Quality

In considering the effects of the packaging and the distribution environment on the quality of horticultural produce, it is necessary to obtain some quantitative measure of produce damage. One of the most controversial areas encountered in the assessment of damage to fresh horticultural produce centres on how to mechanically model produce. There has been a tendency to use the techniques developed for solid materials, e.g. fracture mechanics (Schoorl & Holt, 1983), or for mechanical products, e.g. damage boundary theory (Newton, 1976).

Little work appears to have been conducted on the effects of packaging on produce in a mechanical sense. Considerable work (e.g. that described by Robertson, 1993) has been conducted on other food materials, particularly processed foods and liquids, but this has mainly been with respect to chemical or physical reactions occurring between the food and the packaging materials (e.g. flavour and odour tainting and discolouration caused by migration of polymer constituents into the foods or scalping of food components by the package).

Vergano et al. (1992) studied the effectiveness of polypropylene film and paper between peaches in reducing vibration bruising, and found that the amount of vibration bruising is proportional to the kinetic coefficient of friction (KCOF) of peaches in contact with packaging materials. They determined that lower KCOF values did correspond to less bruising, and recommended that the use of paper or film to reduce bruising be investigated further.

Considerable research has also been conducted into the quantification of produce damage, and into the development of empirical relationships to predict produce damage during distribution. Mohsenin (1970) suggested the use of the bruise volume, and this has been used to quantify bruising in produce such as apples, peaches, and pears. Peleg (1985) agreed with the bruise volume method for small sample sizes, but suggested that an equivalent bruise index (EBI) would be better to rapidly quantify damage in large samples. Other measurements of bruising that have been suggested include bruise diameter, used by

the US Department of Agriculture for grading apples (Siyami et al., 1988), and bruise area (Bollen & Cox, 1991).

Jones et al. (1991) developed a model to predict damage to horticultural produce during transportation, based on a force-characteristic of the vehicle and load elements to calculate the energy absorbed by the produce. The energy absorbed was then used to calculate physical damage to produce, in this case bruise volume in apples. A parametric study showed that the model gave results in accordance with practice, and they concluded that this approach to predicting damage during transport had considerable potential.

2.3 ENVIRONMENTAL HAZARDS IN PRODUCE DISTRIBUTION

Efficient and effective use of packaging materials implies that there is no waste, either in the form of excessive packaging (overpackaging) with high material costs, or inadequate packaging, with resulting product loss or damage. Loss and damage are a highly visible cost and this is generally an obvious area for improvement. Overpackaging is more difficult to identify and cost, but it can be assumed that this is also an area for improvement. The desired goal is to design a packaging system that will provide adequate protection, but at the lowest possible total cost.

The major inputs required for efficient and effective use of packaging materials include: (i) a knowledge of the distribution environment; (ii) a knowledge of the susceptibility to damage of the product to be packaged; and (iii) a knowledge of the performance characteristics of the packaging materials. Unless adequate and accurate design information of this type is available, alternate, more costly and time consuming approaches, such as trial shipments, must be adopted. This study is concerned with the first of these three inputs, namely an assessment of the physical hazards existing in the produce distribution environment.

It is not possible to precisely predict the exact levels of all physical hazards which occur in the distribution environment. This is due to the variability in conditions to which packaged

products can be exposed while they are transported and handled. Similarly, it is not possible to design a packaging system to protect the product from all possible hazards. However these hazards can be determined with some statistical certainty, and packaging systems can be developed which will protect the product against expected distribution hazards. Because high hazard levels occur rarely, packaging systems are only used for protection up to a certain confidence level. This level depends on the cost of the product and its packaging, and the desired quality of the product when received by the final consumer.

A produce distribution environment is defined to include all the environmental conditions likely to be encountered by produce during movement in typical distribution cycles from the growing area to the ultimate consumer. These movements include transportation by truck, railcar, aircraft, and ship. The conditions of interest are related to the physical requirements of the shipping container associated with different segments of the distribution cycle including handling, vehicle transport, warehousing, or storage. The conditions of interest include impacts, vibration, and compression, and the climatic conditions of temperature and humidity (Ostrem & Godshall, 1979).

A comprehensive summary of studies into common distribution environments which subject packages to distribution hazards is given by Ostrem & Godshall (1979). Although data has been accumulated since, this study is regarded as definitive (Maltenfort, 1989). This is useful as a general reference, however more specific data is required for produce damage simulation, as the load in combination with the transport vehicle determines the dynamic transportation environment (Peleg & Hinga, 1986).

2.3.1 Vibration Hazards

The vibration environment has been studied in greater detail than any other distribution hazard, probably because there is generally little control over the operation of commercial vehicles and the resulting vibrations transmitted to the products. Vibration data from these studies have been reported in several forms, which are related to the end-use of the data and available data analysis equipment. They range from acceleration power spectral

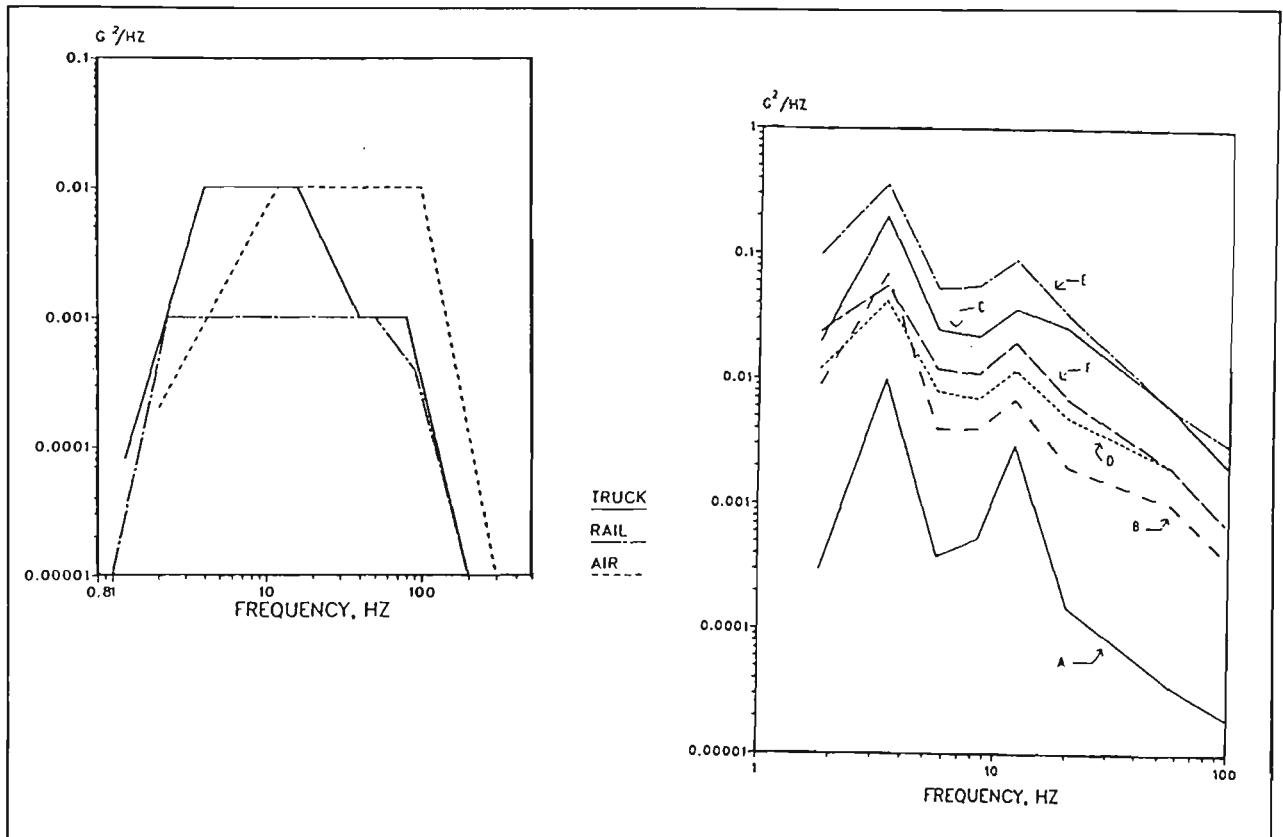
density (PSD), peak hold PSD, overall root mean square (RMS) acceleration, and frequency distribution of acceleration peaks within selected frequency bands. Many of these formats are identical to the PSD format, with only the data rescaled.

The reported acceleration levels, regardless of the format in which they are presented, are dependent on the bandwidths used in the analyses. Modern analysers use constant bandwidth measurements together with techniques such as compression real-time analysis and fast Fourier transform (FFT) analysis. These analysers take snapshots of the amplitude-time history and produce amplitude-frequency spectra at a resolution dependant on the sampling rate required. Spectra are then continually averaged to produce an average spectrum, or autospectrum. Most recent investigations use this approach. Bandwidths are normalised typically to 1 Hz. The analyser outputs also vary, but data is typically presented in PSD form (g^2/Hz). This format is the only one suitable for describing stationary random vibration. The primary advantage of a modern spectrum analyser and the reason for its extensive use is its ability to rapidly and automatically analyse a complex signal and resolve it into basic components, namely frequency and amplitude. Newland (1984), Harris (1988), and Thompson (1993) present detailed discussion on spectral analysis and data reduction procedures.

Figure 1(a) and Figure 1(b) show sample acceleration PSD data from ASTM D 4728 (ASTM, 1994). Figure 1(a) illustrates that there are relative differences in vibration intensity and frequency content for various types of commercial transport: truck, rail, and air. These PSD curves have evolved from a compilation of field measurements made by several organisations over a long time, and do not purport to accurately describe a specific transportation mode or distribution environment. These curves are envelopes that include data from a variety of loading conditions, suspension types, road conditions, weather conditions, and travel speeds.

Figure 1(b) illustrates the various vibration intensities attributed to different road conditions by a single truck/payload combination. In these studies, a truck was instrumented and driven over various routes. Each condition was then reduced to a PSD format and plotted.

Figure 1: (a) Summary of commercial transport random vibration spectra; (b) Comparison of leaf spring truck vertical vibration for different roads.



Source: ASTM D 4728 (ASTM, 1994).

Key: (A) Production area: slow speeds (< 35 km/hr), rough roads; (B) City road: slow speeds (15-25 km/hr), extremely rough, cracks, railway tracks; (C) Expressway: concrete highway, indicative of interstate highway, high speeds (> 85 km/hr); (D) Suburban roads: slow speeds (< 30 km/hr), sharp turns, numerous stops; (E) Main suburban roads: asphalt road, many pitched areas, railway tracks, numerous stops, average speeds (55-75 km/hr); (F) Secondary suburban roads: two lane, asphalt, many bumps, slow speed (< 50 km/hr).

Studies conducted to date have shown that trucks impose the most severe vibration loads on cargo, with railcars next, followed by ships and aircraft. Many transportation vehicles and systems remain to be defined, however the environment appears to have been largely described for the most severe condition, i.e. truck transport, which is present in almost every distribution cycle. Shock and vibration originate from two sources in a truck-trailer system (Harris, 1988):

1. External sources, such as road or surface irregularities, braking, and forward acceleration.
2. Internal sources from the vehicle itself, such as engine vibration, drive mechanism, and wheel imbalance.

The magnitude of vibrations transmitted to the transported product are in turn affected by the type of suspension system that supports the truck-trailer system. The most common systems in use are air-bag suspensions and leaf-spring suspensions.

Early studies on road vehicle vibration include those conducted by Schlue (1966), Foley (1972), Sharpe & Kusza (1973), and Silvers & Caruso (1976).

Schlue (1966) studied air-bag suspension truck-trailers operating over smooth, rough, and irregular road surfaces, and presented summarised data showing the maximum, 95-percent, and 50-percent levels of shock spectra and power spectral densities. His major findings were:

1. Vibration levels at frequencies above 100 Hz were not significant.
2. Lateral and longitudinal vibrations were significantly less than vertical vibrations.

Foley (1972) studied several trucks ranging from well-used flatbed truck-trailers with conventional leaf-spring suspensions to new van truck-trailers with air-bag suspensions, and presented data summarised by an envelope PSD curve covering all vehicles and load conditions investigated.

Sharpe & Kusza (1973) studied three different scheduled common carrier truck-trailers, and presented rear vertical acceleration measurements, and the effects of speed, location, and direction, as PSD curves. Their findings included:

1. Rear vertical vibration was the most severe.
2. Front-vertical vibration levels were between the levels recorded at the mid and rear.
3. Lateral measurements were smaller than the vertical by a factor of two or more.
4. Trucks with lighter loads had lower levels of vibration independent of speed.
5. Speed increased the levels of vibration for all other cases.

Silvers & Caruso (1976) reported on vibration environment studies conducted on truck-trailers. Tests were conducted to determine the effects of suspension system (conventional steel spring, rubber isolator, damped coil springs, and air bags), load, rear wheel position, road type, and driver. Their results were presented as PSD curves. At some times a

0.2 Hz bandwidth resolution was used, and the data analysed to 50 Hz, and at other times a 1 Hz bandwidth was used, and the data analysed to 250 Hz. In all cases, a 3 min segment of data was recorded and analysed. Their main findings were:

1. PSD levels for frequencies above 50 Hz were insignificant.
2. The worst ride with regard to road occurred during high speed operation on interstate highways.
3. The worst ride with regard to location and weight occurred over the rear axle for a lightly loaded trailer.
4. The worst ride with respect to suspension occurred when single-leaf steel suspension springs were used.
5. The individual drivers had little effect on the vibration levels.

Comparisons of the PSD curves from these different sources show similarities in the general shape of the curves. However many variables influence both the magnitude and exact frequency of the excitation. These factors include suspension system, load, speed, road condition, condition of trailer, and location of cargo (Tevelow, 1983). Schlue (1966) also reported that high vibration levels at high frequencies (over 100 Hz) indicate a suspension system in need of repair. A comparison of reported distribution vibration levels is shown in Table 1. One disadvantage of this published information is that the values of maximum acceleration are provided without any reference to the distribution of acceleration over the test duration or the particular method of analysis used. Thus it is difficult to interpret the data in Table 1.

Table 1: Vibration frequencies and maximum acceleration levels encountered in distribution.

Transport Mode	Vibrating System	Frequency Range (Hz)	Max Acceleration (g)
Rail Cars	Suspension, vertical	2 - 7	0.5
	Suspension, lateral	0.7 - 2	0.8
	Structural	50 - 70	0.3
	Roll	≈ 1	0.1
Trucks	Suspension	0 - 7	0.5
	Unsprung suspension	10 - 20	0.3
	Structural and tyres	50 - 100	0.3
	Damaged suspension	100 +	
Trucks on Flat Cars	Vertical	2 - 4.6	1
	Roll	0.7 - 3.1	10
Aircraft	Propeller	2 - 10	0.5
	Jet	100 - 200	0.5
Ships	Sea	0.1 - 0.2, 10	0.2
	Engines	100	0.4

Sources: Schlue (1966), Tevelow (1983), Brandenburg & Lee (1988), Marcondes (1994).

Tevelow (1983) summarised the many different studies done in this area over the previous 20 years and had several major conclusions:

1. Vibration levels in the lateral (sideways) direction are usually the lowest.
2. Vibration levels in the vertical direction are usually the highest, with extreme levels occurring over the rear axle on the footpath-side of the vehicle (i.e. on the right-hand side of vehicles in the United States, and (presumably) on the left-hand side of vehicles in Australia).
3. Vibration levels in the longitudinal axis can be as high as or higher than the vertical vibration levels, but this usually only occurs as a result of resonant frequencies of the truck body.
4. Specific relationships between vertical, lateral, and longitudinal vibration levels are highly dependant upon the particular vehicle and external conditions.

More recent studies are predominantly an extension of these earlier studies. These researchers include Goff et al. (1984), Antle (1989), Marcondes et al. (1990), Singh (1992), Pierce et al. (1992), and Marcondes & Feather (1992).

Goff et al. (1984) studied the effect of different suspension systems on truck vibration levels. Accelerations in the rear of the trucks were recorded during half-hour trips on city roads, country roads, interstate freeways, bridges, and rail crossings. The suspensions

systems studied were a fixed-position air-bag tandem-axle trailer, a moveable leaf-spring tandem-axle trailer with the axle in the rear-most position, and the leaf-spring trailer with the axle in the front-most position. Their major results were:

1. Transient accelerations were more severe than those generated in steady-state vibration.
2. The spring-leaf suspension trailer with the wheels forward gave the roughest ride.
3. The air-bag suspension caused the greatest amplification of vibration by the load.

Antle (1989) and Singh et al. (1992) compared the lateral, longitudinal, and vertical vibration levels in commercial truck shipments in the United States. They concluded:

1. Levels of lateral and longitudinal vibration are generally less than the vertical vibrations in the same trailer at frequencies below 10 Hz.
2. The lateral levels at the top of the trailer may be higher than the vertical levels below 10 Hz.
3. At frequencies greater than 10 Hz, the lateral and longitudinal spectra have contours similar to that of the vertical spectrum.
4. Above 20 Hz the levels of vertical, lateral, and longitudinal vibration are similar.

Marcondes et al. (1990) investigated the use of road roughness index data to estimate levels of vibration in vehicles as an alternative to the direct measurement of vibration levels. They obtained a set of equations to predict PSD based on pavement classification and on the International Roughness Index (IRI).

Pierce et al. (1992) compared the performance of leaf-spring, air-cushion, and damaged air-cushion suspension systems. Their main conclusion was that the undamaged air-bag suspension gave lower power density levels on all road surfaces studied. The damaged air-bag and leaf-spring suspensions were similar in response frequencies, although the damaged air-bag produces higher vibration levels at lower frequencies.

Marcondes & Feather (1992) conducted an assessment of vibration in commercial truck shipments on Highway 1 between Christchurch and Invercargill in New Zealand. Comparisons were made between loaded and empty truck-trailers at three different speeds, between single and double axle for city deliveries at three different speeds, and between

averages for Highway 1 and the ASTM D 4728 standard acceleration profile recommended for the vibration testing of truck shipments. The results were presented in PSD formats and indicated significant differences from previously published data and that currently used in packaging design and laboratory testing. However in this study, transients were not removed from the vibration data before analysis, leading to the possible distortion of the PSDs.

2.3.2 Shock Hazards

The shock environment presents a particularly difficult parameter to characterise because in most cases it must first be separated from vibration type data and then analysed separately. Shocks are transient events, and what may constitute a shock to one investigator may not be so defined by another. The most common definitions of transient events are:

1. Events which occur as a result of the vehicle crossing an obvious physical transient, e.g. potholes and railway crossings.
2. Events for which the peak:RMS acceleration ratio (i.e. crest factor) is greater than a certain value, usually around 3 to 3.3.
3. Events for which the magnitude is greater than a certain statistical probability, e.g. the highest 0.1% of all recorded events.

The last two of these are related to the probability distribution of the signal and are essentially the same.

Mechanical shocks occur when an object's position changes suddenly. A typical shock waveform is characterised by a rapid change in acceleration, over a relatively short period of time (usually a few milliseconds). The three main parameters describing a sampled shock waveform are peak acceleration, duration, and velocity change, although the waveform shape is also important. Peak acceleration, G_m , is the largest (absolute) sampled g-level on the shock waveform, and may be positive or negative depending on the assumed coordinate system. The velocity change, ΔV , is equal to the area under the shock waveform curve, and is a function of G_m , τ , and the waveform shape.

The duration of the shock waveform, τ , is the time duration of the shock, often measured between the points to either side G_m on the waveform which are 10% of G_m in magnitude. There is no scientific reasoning for the choice of 10% limits; this value seems arbitrarily chosen, although it is referred to in ASTM D 3332. IST (1993a) and Lansmont (1990) define duration in this way in their data acquisition and analysis software.

Shock damage to products is dependant on both the maximum shock level and the shock duration, as well as the waveform shape. A true product fragility index must be based on two of the three waveform parameters described above (Brandenburg & Lee, 1988), but only if the shape of the waveform is known. Actual shock waveforms are often approximated by a half-sine waveform, and in this case the velocity change is given by

$$\Delta V = \frac{2}{\pi} G_m g \tau \quad (2.8)$$

Shock data has been presented in a variety of forms. In addition, the data has been recorded either within the product itself, or on the vehicle floor. When data has been recorded on the product, the results have generally been reported in terms of peak acceleration. When data has been recorded on the vehicle floor, the results have been reported in terms of peak acceleration, shock spectrum, or spectral analysis. Depending on the end use of the data, each form of data presentation has advantages and disadvantages.

Peak product acceleration has many advantages in that it can be related to product fragility or 'g' rating, which is often used in the design of protective packaging. However it has not yet been shown that this simple approach can be applied to horticultural products as it generally can for mechanical products.

In most studies, the shock input to the products as a result of various transient events encountered during transport are separated from the continuous-type inputs. This is because PSD analysis assumes that the signal is stationary with Gaussian statistics. The presence of transient events in the data violates these assumptions. These transients may

be identified from the data by means of a voice channel (from observation of physical transients, e.g. potholes) or by a visual review of the data records (i.e. removing events exceeding a predetermined value of acceleration magnitude or crest factor).

The transient inputs result from discrete inputs to the vehicle. For trucks, vertical transients may occur when traversing potholes, tracks, bridges, bumps, or dips, and longitudinal shock inputs may occur when backing into a loading dock. For railcars, vertical transients may occur when crossing intersecting track, switches, roadways, or bridges, and longitudinal inputs may occur during switching or coupling operations. For aircraft, transient inputs may occur during landing and in air turbulence.

Shock data can also be expressed in terms of the statistical distribution of levels of shock events, e.g. a histogram or distribution function of the frequency of occurrence of shocks against their magnitude. This is similar to the approach taken in handling studies where data is often presented in terms of the frequency of occurrence for various equivalent drop heights (EDHs). Hasegawa (1989) compared and evaluated a number of transport shock and vibration data processing formulae proposed in the past. He found that shock and vibration data has generally been considered by applying a regression formula rather than as a distribution function, and proposed three functions for future analyses: (i) the irrational regression function; (ii) the hybrid regression function; and (iii) the Weibull distribution function. The conclusions from this study were:

1. The irrational or hybrid functions or the Weibull distribution are best suited to represent the relationship between the levels of shocks and vibrations and the number of their occurrences.
2. The irrational function or the Weibull distribution are suited to compare transport test data or to describe the status of changing conditions.
3. The irrational or hybrid functions are best for equivalent-level calculations, re-evaluation of criteria or requirements, and where extrapolation is to be used.

For wide-band records, the amplitude, phase, and frequency all vary randomly and an analytical expression is not possible for its instantaneous value (Thompson, 1993). The most likely probability distribution for such records is the Gaussian distribution. When a

wide-band record is put through a narrow-band filter, a constant-frequency oscillation with slowly varying amplitude and phase is obtained. The probability distribution for its instantaneous values is the same as that for the wide-band random function, i.e. a Gaussian distribution, however the absolute values of its peaks will have a Rayleigh distribution (Newland, 1984), where the probability function that any peak chosen at random is less than a is:

$$\text{Prob}\left(\frac{\text{Peak}}{a_0} < \frac{a}{a_0}\right) = 1 - \exp\left(-\ln 2 \left(\frac{a}{a_0}\right)^2\right) \quad (2.9)$$

where a_0 is the median peak height.

However in a number of applications of the theory it has been found that the Gaussian assumption may not be valid and that the distribution of peaks then departs significantly from a Rayleigh distribution. Two such examples are the calculation of wave-induced bending moments in ships (Mansour, 1972) and the wind loading of buildings (Melbourne, 1977). If the exponent 2 in the Rayleigh distribution is replaced by a general coefficient k , the more general two-parameter Weibull probability distribution function is obtained (Newland, 1984):

$$\text{Prob}\left(\frac{\text{Peak}}{a_0} < \frac{a}{a_0}\right) = 1 - \exp\left(-\ln 2 \left(\frac{a}{a_0}\right)^k\right) \quad (2.10)$$

The Weibull distribution can also be expressed with three parameters (Montgomery, 1991):

$$f(x) = \frac{\beta}{\delta} \left(\frac{x-\gamma}{\delta}\right)^{\beta-1} \exp\left[-\left(\frac{x-\gamma}{\delta}\right)^\beta\right] \quad (2.11)$$

where $-\infty < \gamma < \infty$ is the location parameter, $\delta > 0$ is the scale parameter, and $\beta > 0$ is the shape parameter. In the two-parameter model the location parameter is assumed to be zero. The mean and variance of the Weibull distribution are

$$\mu = \gamma + \delta \Gamma\left(1 + \frac{1}{\beta}\right) \quad (2.12)$$

and

$$\sigma^2 = \delta^2 \left[\Gamma\left(1 + \frac{2}{\beta}\right) - \Gamma\left(1 + \frac{1}{\beta}\right)^2 \right] \quad (2.13)$$

respectively. The Weibull distribution is relatively flexible, and by appropriate selection of the parameters γ , δ , and β , the distribution can assume a wide variety of shapes. The cumulative Weibull distribution is

$$F(a) = 1 - \exp\left[-\left(\frac{a - \gamma}{\delta}\right)^\beta\right] \quad (2.14)$$

The Weibull distribution has been used extensively in reliability engineering as a model of the time to failure in electrical and mechanical components and systems.

A review of available shock data with reference to general cargo or package-related problems indicates these transients to be of relatively low level except for railcar coupling (Ostrem & Godshall, 1979). Unfortunately, it appears that several researchers have included shock transients in vibration analyses, and where these have been treated separately they have been recorded at the vehicle floor. Thus these results are only of value if cargo is firmly attached to the floor, which is not the case for general loads that are free to move. If the cargo bounces, which may occur when the cargo is free to move, then it impacts the floor after a free-fall, which produces an impact of a greater intensity.

Researchers in the area of truck shocks include Schlue (1966), Johnson (1971), Foley et al. (1972), Sharpe & Kusca (1973), Grier et al. (1975), and Singh et al. (1993).

Schlue (1966) analysed the transient data recorded in air-bag suspension vans. The data was presented in terms of shock spectra calculated with an assumed amplification factor of 10. The spectrum represents the response of a series of single degree of freedom oscillators, each having a damping ratio of $\xi = c/c_c = 0.05$. This ratio corresponds to typical structural damping for bolted and riveted connections. Typical shock spectra plots are summarised to show the maximum 95- and 50-percentile levels of data samples from events recorded at the rear on the truck floor.

Similarly, Foley et al. (1972) have reported truck shock environments in terms of shock spectra for a number of vehicles and a number of events. The events included trucks traversing bumps, dips, potholes, railway tracks, and backing into loading docks. Composite curves are presented which envelope the shock response for the three directions (vertical, lateral, and longitudinal).

Sharpe & Kusza (1973) have analysed transient data recorded on typical commercial trucks in terms of peak acceleration versus frequency. The study covers several truck-trailers loaded with different weights. Comparisons were made between a curve computed for a transient event and a curve for conditions just prior to the event, and it was found that the general shapes of the curves were similar, but higher acceleration levels were present during the transient. Other transient data were reported in terms of peak acceleration of the composite signal. The conclusions from this study were that transients produce increased low-frequency vibration and not sharp pulses, and that if a random noise generator is to be used to generate a test signal, these higher levels will be produced automatically.

A different format was used by Johnson (1971) to present data from a European study. In this study, acceleration measurements were made directly on a number of packages carried on a commercial truck over a variety of terrains. Packages varying in weight from 20-1000 kg were used, and triaxial accelerometers were attached to the outsides. Transients

due to package bouncing were separated from the continuous vibration data, and the two were analysed separately. It was found that:

1. Terrain, truck speed, and package position had the greatest effect on acceleration levels.
2. Peak acceleration distributions changed when there was a large change in speed.
3. The rear of the truck experienced higher acceleration levels.
4. Heavily loaded vehicles experienced lower levels of vibration than lightly loaded vehicles.
5. There appeared to be only a small effect of package weight of the acceleration levels, with the heavier packages showing lower acceleration levels.

All the pulse shapes were reported to be nearly half-sinusoidal with a pulse duration of 3-5 ms for more than 90% of the values recorded.

Grier et al. (1975) conducted a study to obtain data to be used to develop a method to determine the so-called 'shock index' of commercial trucks. The main results of this study were:

1. A practical method using planned payload and vehicle axle spring rates was developed to determine the shock index of commercial trucks.
2. Vertical accelerations were generally greater than either lateral or longitudinal accelerations during highway travel, and had a major influence on cargo damage.
3. The load as a percentage of maximum payload had a greater influence on the shock index than vehicle speed or tyre pressure.

Singh et al. (1993) studied the dynamic environment inside the cargo holds of refrigerated ships carrying bananas between Central America and Europe and the United States. The variables studied were shock and vibration *g*-levels. The shipment types studied were break-bulk, palletised, and containerised. The results showed that the average *g*-levels are similar to those found on trailers and railcars, and that the palletised method limits the motion of the cargo the best. The vibration levels in the packages themselves were found to be amplified by up to 8 times for break-bulk and containerised shipments, and 1.4 times for the palletised shipments.

A study of longitudinal shocks of palletised loads during forklift handling was conducted by Rodriguez et al. (1994). They described shock acceleration and duration as a function of forklift weight, impact speed, pallet weight, and impact condition. They also showed that typical forklift handling shocks have the product of maximum shock (in g) and duration (in ms) in the range 37.2 - 368 for half-sine shocks. In contrast, ASTM D 4003 recommends either a 40 g, 10 ms (i.e. a product of 400) shock, or a 10 g, 50 ms (i.e. product of 500) shock, to simulate forklift handling.

In conclusion, it can be stated that the general consensus among modern researchers in this field is that stationary random vibration data should be analysed and presented using spectral analysis techniques in a frequency-domain format, and transient data (however it is defined) should be analysed and presented in a time-domain format. As vibration data is usually recorded in a raw form in time domain, it thus follows that transient events should be excluded from further analysis immediately after data collection. It is clear from previous studies that this data separation has not been rigorously attended to, and many random vibration studies involve data that has been 'contaminated' with transient events. Whether or not these transients make any significant difference to the final results is unknown, however their presence is reported to reduce the applicability of statistical models which are assumed during the subsequent frequency-domain processing of the vibration data.

2.3.3 Handling Hazards

Handling occurs at the loading, unloading, and transfer points of a distribution system, and produce damage can occur as a result of either manual or mechanical handling operations. Handling hazards are generally considered to impose the most severe loads on products.

The loads imposed on packages during handling operations have historically been reported in terms of equivalent drop height (EDH). The drop height refers to the vertical distance from the ground or impact surface that the container is released (either intentionally or accidentally) and falls under the influence of gravity. Drop height data has been collected

by several methods, including observation, camera, and instrumented package. The instrumented package is considered the most effective technique for gathering data on the many handling operations of a typical distribution cycle. Experimental studies are performed with an instrument located inside a package that is calibrated to record actual drop heights and free-fall time. Modern instruments have an internal timer, and if the position of the package in the distribution system is time-related, the drop height data can be correlated with particular handling operations.

The EDH is defined as the free-falling drop height required to produce the same total velocity change as measured on the recorded shock waveform. EDHs are particularly useful as a direct measure to compare a horizontal impact, or an impact caused by forces other than gravity, to an ideal vertical drop forced only by gravity. The relationship between the EDH and the total velocity change for an ideal free-falling object is given by

$$\Delta V = (1 + e)\sqrt{2gh_{eq}} \quad (2.15)$$

where e is the coefficient of restitution, g is the acceleration due to gravity, and h_{eq} is the EDH. The coefficient of restitution is a measure of the amount of energy absorbed by the impacted surface during the impact, and is defined as the ratio of the rebound velocity to the impact velocity, or $e = V_r / V_i$. Theoretically, e is limited to values between 0 and 1, but for most real-world cases involving packaged products, e will typically be in the 0.3 - 0.75 range. In packaging design, e is often taken as 1 to give a worst-case value.

Two pioneering studies of drop heights were conducted by the United States Air Force (Bull & Kossack, 1960) and the United States Army Natick Development Centre (Barca, 1975a). The results from these and other studies, while not adequate for package design or test purposes, have indicated some useful trends:

1. Many packages receive many drops at low heights, while few receive more than one drop from higher heights. The probability of a package being dropped from a high height is minimal.
2. The heavier and/or larger the package, the lower the drop height. Unitised loads are subjected to fewer and lower drops than individual packages.

3. Most packages are dropped on their bases.
4. Handholds or vents significantly reduce drop height, but 'handle with care' labels have a minor effect.

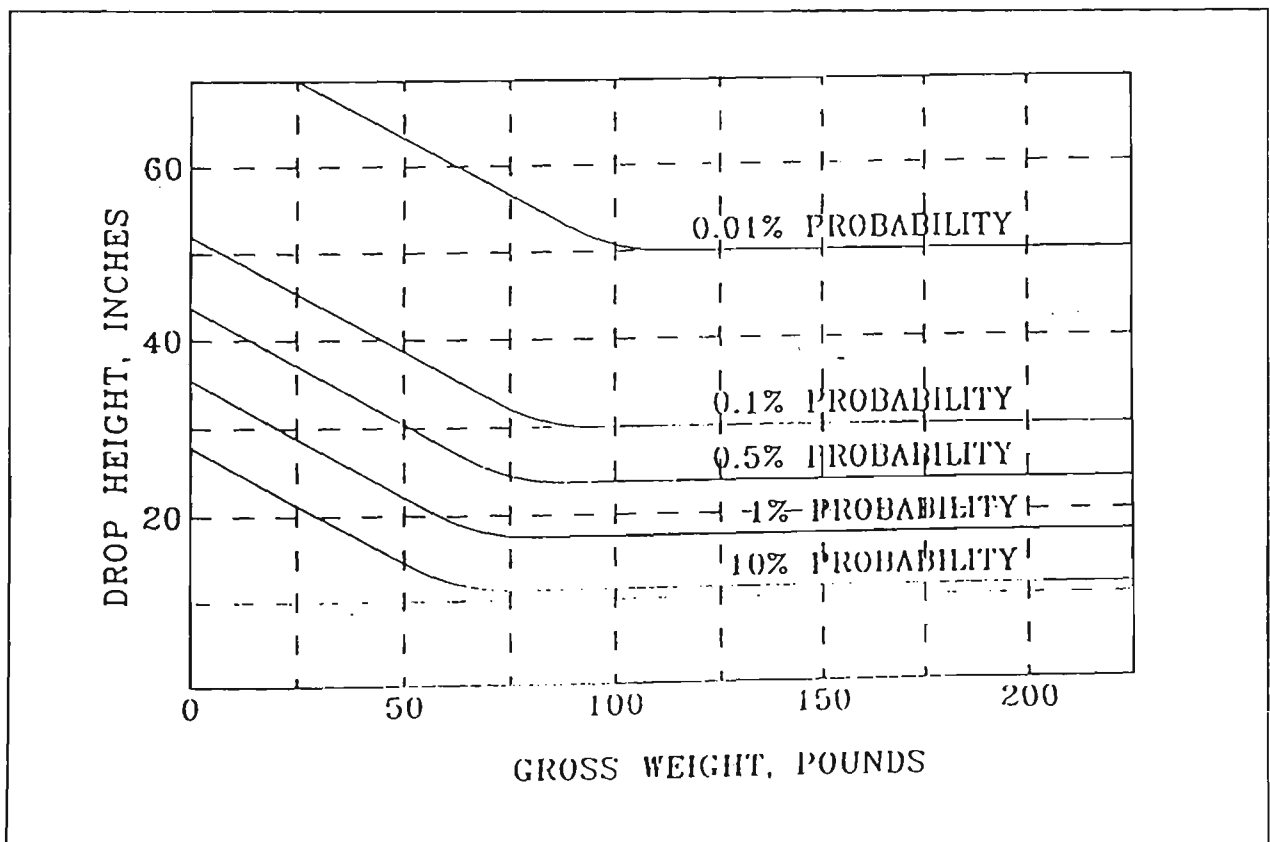
Two examples of the relationship between package weight and drop height are shown in Table 2 and Figure 2.

Table 2: Severest probable handling environments.

Package Weight (lb)	Greatest Dimension (in)	Drop Height (in)	Drop Type or Direction	Handling Type
< 20	48	42	Any side or corner	One person throw
20 - 50	36	36	Any side or corner	One person carry
50 - 100	48	24	Any side or corner	Two people carry
100 - 150	60	21	Any side or corner	Two people carry
150 - 200	60	18	Any side or corner	Two people carry
200 - 600	72	24	Rotating (end roll or tip)	Mechanical
600 - 3000	Unlimited	18	Rotating (end roll or tip)	Mechanical
> 3000	Unlimited	12	Rotating (end roll or tip)	Mechanical

Source: Brandenburg & Lee (1988).

Figure 2: Probability curves for package drops during handling operations.



Source: Brandenburg & Lee (1988).

The available data on manual handling operations provides an indication of the variability and random nature of the drop hazard. Most studies show the same general trends, but the drop heights and probability levels are largely different. Factors relating to these differences could include package size and weight, the presence of handholds, the particular distribution system, data reduction and analysis procedures, and instrumentation sensitivity (Ostrem & Godshall, 1979). In addition, most studies have been conducted for specific distribution systems, for example the United States studies have concentrated on military supply channels for specific container sizes and weights. The applicability of any available data to any other distribution system is largely unknown.

Until recently one major reason for sparse handling data has been the unavailability of a low-cost, self contained instrument capable of recording drops over an extended time period. The requirements of such an instrument would include its ability to measure accurately the drop height, the nature of the impact surface, and the drop orientation. It should also have a time reference and an internal storage capability (Graesser et al., 1992). Today, however, instruments such as the drop height recorder (from Lansmont Corporation) and the environmental data recorder (from Instrumented Sensor Technology, Inc.) are available with these capabilities.

2.3.4 Temperature and Humidity Hazards

The climatic conditions of temperature and humidity are important considerations for both paperboard containers and components and for fresh horticultural produce. The strength of paperboard products is largely affected by moisture content, while temperature is important in determining the quantity of water condensing from the atmosphere. Temperature and humidity can usually be monitored and/or observed directly, particularly in storage and warehouse areas. However, other sections of the distribution cycle, such as when a refrigerated vehicle is on the road, are more difficult to monitor, although modern environmental recording instruments can record temperature and humidity profiles as they record shocks or vibration.

Temperature and humidity conditions encountered in distribution cycles are difficult to summarise because of many factors that influence not only the ambient conditions but the package response as well. A large amount of information has been compiled on ambient temperature and humidity data, and it is a common practice to define the distribution temperature and humidity conditions in terms of ambient conditions and assume that packages are in equilibrium with these conditions. In some cases, laboratory testing is performed to more accurately determine the package response to these inputs. More often, the ambient conditions are assumed synonymous with package conditions. This assumption may be justified, but it is important to be aware of how the data was acquired.

Some of the more important variables that influence the package response to temperature and humidity conditions include package weight, package thermal conductivity, configuration, surface absorptivity and emissivity, and ventilation. Air flow also results from the movement of the vehicle and forced ventilation, and changes in ambient conditions result from changes in locality or time.

The range of possible conditions that can be encountered in a typical distribution cycle has limited the number of studies that have been conducted to acquire general cargo response information. In general, those measurement studies that have been conducted have been performed for a specific situation or set of conditions (Ostrem & Godshall, 1979). Until recently, the unavailability of suitable instrumentation has hampered the acquisition of extensive data, but suitable self-contained instruments and sensors are commercially available today.

Australian Standard 2582.2 (which is technically identical with International Standard ISO 2233) provides a note on the measurement of RH and temperature. As a continuous record of RH or temperature will show a cyclic variation, this standard provides a method of determining precise values to define both the level and the variation of this property. However, cyclic conditions are important, and conditions cannot be suitably expressed in terms of mean and variance values alone.

A problem with many ambient humidity sensors is that they do not measure the moisture content of materials. This is a major disadvantage when studying materials such as corrugated fibreboard, where structural properties are sensitive to MC. The MC of corrugated fibreboard can, however, be related to air RH (Eagleton & Marcondes, 1994), and this relationship is relatively independent of ambient air temperature. However a period of time is required for the board to reach equilibrium, e.g. Peleg (1985) estimates that for practical purposes, at least 8 hr is required, and recommends a minimum conditioning time of 12 hr. Conditioning times of 72 hr are recommended by common testing standards such as ASTM D 4169 (ASTM, 1994) and ISO 2233. If rapid changes in air temperature occur, the air RH will change fast, while the material moisture content would change at a slower rate. In addition, under certain conditions, the moisture in the air may condense on the cargo either as a result of reaching saturation conditions, or because the cargo is slow in following the air temperature and is at or below the dew point temperature. Under these conditions, air RH would not always be an accurate indication of material moisture content.

Barca (1975b) presented data on the conditions of temperature and humidity inside various fibreboard boxes during shipment, warehousing, and outdoor storage. The tests were conducted in Autumn in the United States, and showed temperature swings from 8-21°C and RH variations from 21-85%. Measurements were not correlated with ambient conditions. Similar surveys have been conducted by many other researchers, but the trend has been to concentrate on specific distribution systems. Both temperature and RH can be easily measured to obtain detailed information about any specific distribution system, but obtaining a correlation between distribution systems is difficult.

Ievans (1977) measured the interior humidity of containers in a palletised stack and found that the interior humidity was largely dependant on location within the stack. Thus, palletised stacks should be designed for the most severe moisture condition in the stack, which is typically found at the corners.

Cairns et al. (1971) presented data to show the influence of season and type of distribution system element on quarterly mean temperatures and humidities in the United Kingdom.

Similar data for temperature in six main cities in the United States has also been presented (Labuza, 1985). Little useful information has been published for Australian distribution systems, but ambient temperature and RH conditions for several Australian cities are available from the Bureau of Meteorology in raw form or in terms of trends (Kirkpatrick, 1989).

Singh et al. (1993) studied the climactic environment inside the cargo holds of refrigerated ships carrying bananas between Central America and Europe and the United States. The variables studied were temperature, humidity, and air velocity, and the shipment types studied were break-bulk, palletised, and containerised. The temperature and humidity results were summarised in terms of the average (expected), minimum, and maximum levels in each of the three ships.

Recommended temperatures for the shipment of horticultural produce in Australia are tabulated in a Code of Practice (DPI&E/AQIS, 1990). For example, temperate fruit is usually shipped at about -1°C or 0°C , and tropical fruit at about 13°C .

Generally shippers observe these recommendations and set the delivery air temperature to the recommended value (Sharp, 1993). The return air temperature is usually a few degrees Celsius higher, giving a mean product temperature of about 1°C above the set-point. However due to airflow and heat transfer through the product, the temperature of the centre products in any load may be the same as when they were packed, even though the outside products in the same load are at the temperature demanded by the refrigeration unit. In this case the mean temperature of the produce will be higher than the refrigeration unit can provide. Conversely, if there is perfect airflow and heat transfer throughout an entire load, then all of the produce will be in equilibrium with the airstream, and, providing the capacity of the refrigeration unit is satisfactory, the produce and the air will be at the demanded temperature.

The effectiveness of the system depends on the ability of the refrigeration unit in providing fine temperature control over the desired range. Some older refrigeration units use on-off control to maintain a constant return air temperature near the set-point temperature. To

maintain an average cargo temperature of 2°C, for example, these units may cycle up to 16 times per hour, with a maximum delivery temperature of up to 10°C and a minimum delivery temperature perhaps as low as -6°C (Thermo King, 1992). This cyclic temperature can cause problems such as dehydration or top freeze. Ideally, cyclic temperature should be eliminated, with the delivery air temperature maintained within a narrow band.

The RH inside refrigerated vehicles and containers is not controlled explicitly, despite RHs between 90 and 98% being recommended for the storage of most vegetables (Langbridge, 1983). The MC of the delivery air stream is determined by the temperature of the refrigeration unit's evaporator coil, and depends on the refrigeration load. Sharp (1993) estimates that in general, the RH in refrigerated vehicles will be around 60-70% for temperatures near 0°C, and around 70-80% for temperatures of 8-13°C. These values are below those recommended by Langbridge (1983), which reinforces the need for adequate precooling and storage of the produce prior to final packaging and transport.

2.3.5 Compression Hazards

Package compressive loads are generally associated with warehousing and storage stacking. These static compressive loads are a result of stacking one container on top of another. Stacking height can vary considerably depending on available headroom, storage equipment, stack stability, or restrictions regarding maximum stack height. Warehousing stacking heights can easily be determined by observation of storage facilities, including equipment, ceiling height, and stacking procedures.

Dynamic compressive loads resulting from vibration and shocks in transportation and handling are more difficult to establish. Load amplification can occur as a result of vibrations at critical resonant frequencies, and can result in high dynamic loads at the bottom containers, even for the low stacking heights in vehicles. In addition there are the loads resulting from low frequency vibration, such as ship pitching and rolling, and aircraft response to updraughts or gusts. Other sources of compressive loading include railcar

coupling, mechanical handling equipment such as squeeze clamps on lift trucks, slings, and cargo nets, and compression due to strapping.

Sobczak (1977) reports on side-to-side or end-to-end loads on containers as a result of box clamp by material handling equipment. The side-to-side clamping pressure was found to range from 12.6-15.0 kPa. The side platens are normally self-aligning so that uneven loading of the containers is minimised. The side-to-side compressive load is carried by the containers in a manner similar to the machine compression test, since the platens fully cover the containers. If the platens do not cover the containers, their load-carrying capability is reduced. This is analogous to the reduced stacking capacity (compression in the vertical direction) as a result of pallet overhang.

2.4 LABORATORY TESTING OF PACKAGING SYSTEMS

Package testing is used both in the design of protective packaging and in the determination of compliance with specific regulations. There are four possible ways to approach the testing of transport packaging systems (McDougall, 1992):

1. No testing, i.e. wait and see what happens.
2. Sending a number of packages or unit loads on a 'representative' journey.
3. Performing tests to determine the static strength of the packaging system.
4. Performing laboratory tests to determine the effectiveness of the packaging system under appropriate static and dynamic loads.

The advantages of laboratory testing over the other approaches include:

1. The worst case design parameters may be consistently reproduced in the laboratory, whereas they may not occur in any particular shipment.
2. The scientific nature of laboratory testing enables comparisons to be made between different packages or distribution environments.
3. A greater, more comprehensive range of tests may be performed in a shorter time.
4. The ability to observe failure mechanisms is useful in redesigning the package.

Two organisations that have published performance testing schedules for packaging systems are the International Organisation for Standardisation and the American Society for Testing and Materials.

The International Standard ISO 4180 ('Complete, filled transport packages - General rules for the compilation of performance test schedules') was adopted by ISO in 1980. Taking the ISO approach, ASTM developed the Standard Practice D 4169 ('Performance testing of shipping containers and systems') in 1982, and last revised it in 1993. ASTM D 4169 applies the basic principles presented in ISO 4180 and results in test plans complete with test sequences and test levels and intensities. This is accomplished by delineating typical 'distribution cycles' and their component 'elements'. The elements are environmental hazards replicated in test laboratories using standard test methods and schedules and by listing them in a resulting 'test plan'. ASTM D 4169 accomplishes the objectives of ISO 4169 and reduces the ambiguity and variance in complying with this standard. The approach taken by ASTM D 4169 provides a model for the application of ISO 4180 that can be universally applied (Fiedler, 1993).

After the release of the ISO 4180 standard, ASTM recognised the need to integrate the ASTM standards with ISO standards. Like ISO 4180, ASTM D 4169 develops package tests based on test intensities and conditions products experience in normal shipments. However, in contrast to the open-ended approach used in ISO 4180, ASTM D 4169 develops predefined schedules for the most common (US domestic and US import/export) shipping sequences to establish a common basis for the standardisation of comparative testing. Because such distribution channels treat products flowing through them in the same manner, it is unnecessary to redefine the hazard conditions for each shipment. It is, however, necessary to define the events that occur and the hazard elements the shipping units will encounter for each unique distribution channel. The result is the development of 18 partial or full pre-established distribution cycles consistent with normal shipping methods.

Other performance testing procedures have been published by the Standards Association of Australia (SAA) (AS 2584 Parts 1 and 2: 'Complete, Filled Transport Packages -

General Rules for the Compilation of Performance Schedules'), and the Technical Association of Pulp and Paper Industries (TAPPI) (UM 800: 'Performance Testing of Corrugated Fibreboard Shipping Containers') (TAPPI, 1991a). These are described in the following sections.

Appendix A contains a table of some common international (ISO) transport packaging test standards, and their equivalents in other systems.

2.4.1 International Standard ISO 4180

This International Standard has been prepared to fulfil a need of organisations concerned with the compilation of test schedules for complete, filled transport packages. It is intended to set guidelines for the compilation of appropriate test schedules, rather than to provide a rigid framework or to be specified by regulatory or other authorities. This standard may be used to compile both single-test and multi-test schedules.

ISO 4180/1 ('Part 1: General Principles') states the general rules to be used for the compilation of performance test schedules. It also gives the factors to be considered in assessing the criteria of acceptance of such packages after they have been subjected to a package performance test schedule. Values of intensities of tests appropriate to the different modes of transport (road, rail, sea, and air) and storage are given in ISO 4180/2 ('Part 2: Quantitative Data'). The two parts are intended to be read in conjunction with one another.

The values given are 'basic' values associated with common distribution systems and have been based on consideration of a package of 'average' mass and size. Modifying factors may be applied to the basic values of intensity to take account of the characteristics of the distribution system, the design of the package, the degree of assurance, the nature of the contents, and the frequency and value of the consignment. These factors are detailed in ISO 4180/2. Test intensities should be selected according to the hazards of the distribution system, the nature of the goods involved, and the particular mode of transport used.

In compiling a multi-test schedule, the following steps are conducted:

1. Identify the simple elements in the distribution system.
2. Decide what hazards these simple elements involve.
3. Decide which tests are necessary to represent or simulate these hazards.
4. Decide what are the appropriate basic values of the test intensities.
5. Decide what test intensity modifying factors should be applied.
6. Place the tests thus identified into the following recommended sequence: conditioning for testing, stacking, impacts, climatic treatment, vibration, stacking, and impacts.

The relevant ISO test methods and the factors requiring quantification before testing are shown in Table 3.

Table 3: ISO test methods and factors requiring quantification before testing.

Method of Test	Relevant Standard	Factors Requiring Quantification
Conditioning	ISO 2233	Temperature, relative humidity, time, pre-drying conditions (if any)
Stacking test	ISO 2234	Load, duration of load, package attitude(s) ¹ , temperature, relative humidity, number of replicates
Vertical impact test by dropping	ISO 2248	Drop height, package attitude(s) ¹ , temperature, relative humidity, number of replicates, number of impacts
Horizontal impact tests	ISO 2244	Horizontal velocity, package attitude(s) ¹ , temperature, relative humidity, impact surface profiles, use (if any) of an interposed hazard, number of replicates
Vibration test	ISO 2247	Test duration, package attitude(s) ¹ , temperature, relative humidity, superimposed load (if any), number of replicates
Compression test	ISO 2872	Maximum load (where applicable), package attitude(s) ¹ , temperature, relative humidity, upper platen mounting, number of replicates
Low pressure test	ISO 2873	Pressure, test duration, temperature, number of replicates
Stacking test using compression tester	ISO 2874	Load applied, test duration, package attitude(s) ¹ , temperature, relative humidity, number of replicates
Water spray test	ISO 2875	Test duration, package attitude(s) ¹ , number of replicates
Rolling test	ISO 2876	Temperature, relative humidity, number of replicates

Note: (1) When specifying the package attitude(s), reference should be made to ISO 2206.

Basic test intensities, which are considered normal for a common distribution system and which are based upon a package of 'average' mass and size (i.e. of mass 20 kg and dimensions 400 mm × 400 mm × 400 mm), are provided in the Standard, for the road, rail, water, and air modes of transport and for storage. When a test intensity other than the

basic value is appropriate, the value selected should be chosen, as far as is practicable, from the provided list of preferred values.

Guidelines for modifying basic values of test intensity, due to known features of the distribution system or of the package, are given in ISO 4180/2, and consider the following variables: (i) stacking height; (ii) stacking duration; (iii) vibration duration; (iv) vibration stack height; (v) horizontal impact velocity; (vi) number of horizontal impacts; (vii) vertical impact drop height; (viii) number of drops; (ix) attitude of package; and (x) use of palletisation or freight containers.

2.4.2 Standard Practice ASTM D 4169

This Standard Practice provides a uniform basis of evaluating, in a laboratory, the ability of shipping units to withstand the distribution environment. This is accomplished by subjecting them to a test plan consisting of a sequence of anticipated hazard elements encountered in various distribution cycles. This practice provides a guide for the evaluation of shipping units according to a uniform system, using established test methods at levels representative of those occurring in actual distribution. The recommended test levels are based on available information on the shipping and handling environment, and current industry practice and experience. For government application, D 4169 also complies with the packaging design provisions of MIL-STD-2073-1 (USDoD, 19??), including those elements peculiar to the distribution of military material.

ASTM D 4169 and its referenced standards are generally regarded as being particularly strict. This is due to the fact that in the United States, the onus is on the freight carrier for any product damage sustained during transport (Uniform Freight Classification Rule 41). This has led to the adoption of relatively strict performance standards for transport packaging in the United States, of which freight handling organisations having a large input into the content. In Australia, however, there is no clear change of ownership of, or responsibility for, the product as it passes through the distribution system, and transport companies therefore do not necessarily have to specify performance standards to protect themselves from litigation. Thus product loss during distribution in Australia is generally

borne by the grower, because it is often too difficult to prove negligence at later stages of the distribution system.

The following steps are used to conduct a performance test:

1. Define the shipping unit in terms of size, weight, and form of construction.
2. Establish the assurance level, or level of test intensity.
3. Determine the acceptance criteria for the product and package.
4. Select the appropriate distribution cycle from the available standard cycles.
5. Write the test plan, including test sequences and intensities.
6. Select the samples for test.
7. Condition the test samples to standard conditions or to a special climate.
8. Perform the tests as directed.
9. Evaluate and document the test results, and obtain feedback

The recommended distribution cycles and the corresponding test sequences are shown in Table 4. The key to the element test sequences together with the element descriptions and relevant ASTM test methods are shown in Table 5.

Table 4: ASTM D 4169 distribution cycles and element test sequences.

DC No.	Distribution Cycle Description	Element Test Sequence
1	General schedule - undefined distribution system.	I, A/B, D, E, F, H, A/B
2	Special - controlled environment, user specified.	I, user specified
3	Single package environment, up to 45.4 kg.	I, A, D, F, G, A
4	Motor freight - single package over 45.4 kg.	I, B, D, F, G, B
5	Motor freight - truckload, not unitised.	I, A/B, D, E, G, A/B
6	Motor freight - truckload or less-than-truckload unitised.	I, B, D, E, B, C
7	Rail only, carload - bulk loaded.	I, A, D, E, H, A
8	Rail only, carload - unitised.	I, B, D, E, H, B, C
9	Rail and motor freight - not unitised.	I, A/B, D, G, H, F, A/B
10	Rail and motor freight - unitised.	I, B, D, E, H, B, C
11	Rail, trailer-on-flatcar and container-on-flatcar.	I, A/B, D, H, E, F, A/B
12	Air (intercity) and motor freight (local) - over 45.4 kg or unitised.	I, A/B, D, E, G, A/B
13	Air (intercity) and motor freight (local) - single package up to 45.4 kg.	I, A, D, F, G, A
14	Warehousing, partial cycle.	I, A/B, C
15	Export/import shipment by intermodal container or roll on/roll off trailer, partial cycle, to be added to other cycles as needed.	I, B, D, B
16	Export/import shipment of unitised cargo by ship, partial cycle to be added to other cycles as needed.	I, A/B, D, A/B
17	Export/import shipment by break bulk cargo ship, partial cycle to be added to other cycles as needed.	I, A, D, A
18	Government shipments	I, A/B, C/D, A/B, J, F, H, A/B

Table 5: ASTM D 4169 hazard elements and ASTM test methods.

Element	Element Description	Test Simulation Hazards	Test Method(s)
A	Manual handling up to 90.7 kg.	Drop	D 5276
B	Mechanical handling over 45.4 kg.	Drop, stability	D 1083
C ¹	Warehouse stacking.	Compression	D 642
D ¹	Vehicle stacking.	Compression	D 642
E ²	Truck and rail transport stacked or unitised load.	Vibration	D 999 (C), D 4728 (A, B, or C)
F	Loose-load vibration.	Repetitive shock	D 999 (A1, A2)
G ²	Vehicle vibration.	Vibration	D 999 (C) D 4728 (A, B, or C)
H	Rail switching.	Longitudinal shock	D 4003 (A), D 5277 ³
I	Climate, atmospheric condition.	Temp, moisture, RH	D 4332, D 951
J ⁴	Environmental hazard	Cyclic exposure	MIL-P-116

Notes: (1) D 642 deforms the container at a constant rate until a predetermined load is achieved. In contrast, D 4577, which is not referenced in D 4169, subjects the container to a constant load for a predetermined time.

(2) Both sine (D 999) and random (D 4728) vibration tests are permitted.

(3) D 5277 is used for railcars with standard draft gear only (not long-travel draft gear).

(4) Only generally required for conditions associated with the distribution of military material.

The hazard elements relevant to the testing of corrugated fibreboard boxes and unit loads are described in detail in ASTM D 4169.

2.4.3 TAPPI Useful Method UM 800

This method describes pre-shipment testing procedures for the evaluation of packaged products to simulate actual transit conditions. The test procedures are performance tests to ascertain the resistance of a packaged product to damage during distribution. For the purposes of this procedure, packaged products are divided into two categories: group A, about 45 kg and over; and group B, up to about 45 kg. Group A includes heavy packages that are not readily subjected to free dropping; the test cycles for this group consist primarily of vibration and incline impact tests. Group B includes packages of a lesser weight that may be subjected to vibration and drops during distribution.

For group A, the test cycle consists of a vibration test followed by an incline impact test. For group B, the test cycle consists of a vibration test followed by drop tests. However for group B packaged products over about 23 kg, the group A test cycle may be used.

In the vibration test, the vibration table frequency is such that the packaged product leaves the table momentarily at some interval during the vibration cycle. The test is conducted for a minimum of 1 hr.

In the drop tests, the packaged product is dropped ten times, in a specific sequence, onto its faces, edges, and corners. The height of drop for packaged products under about 23 kg is 450 mm, and for packaged products between about 23 and 45 kg, the height of drop is 300 mm.

TAPPI has also published Official Test Methods for testing loaded fibreboard shipping containers (e.g. T 801 om: 'Impact Resistance of Fibreboard Shipping Containers'; T 802 om: 'Drop Test for Fibreboard Shipping Containers'; and T 817 om: 'Vibration Test for Fibreboard Shipping Containers') (TAPPI, 1991b). UM 800 is based on the National Safe Transit Committee Test Procedures, and is not necessarily compatible with the Official Test Methods, hence its 'Useful Method' status. TAPPI has not published an official test method for the compilation of performance test schedules.

2.4.4 Australian Standard AS 2584

This standard establishes general rules to be used for the compilation of performance test schedules for complete, filled transport packages intended for use within any distribution system, whether transported by road, rail, sea, air, or inland waterway, or by a combination of these modes of transport.

AS 2584 is technically identical with International Standard ISO 4180. AS 2584.1 ('Part 1 - General Principles') states the general principles entailed in compiling test schedules. It also gives the factors to be considered in assessing the criteria of acceptance of such packages after they have been subjected to a package performance test schedule. AS 2584.2 ('Part 2 - Quantitative Data') incorporates all of the quantitative data necessary to establish test intensities and other quantitative features of test schedules. AS 2584.1 and AS 2584.2 are intended to be read in conjunction with one another.

The test compilation procedure and the recommended test sequence are identical to those in ISO 4180. The referenced AS test methods and the factors requiring quantification are given in Table 6.

Table 6: AS test methods and factors requiring quantification.

Method of Test	Relevant Standard	Factors Requiring Quantification
Conditioning ²	AS 2582.2	Temperature, relative humidity, time, pre-drying conditions (if any).
Stacking, compression ³	AS 2582.3	Load or maximum load (where applicable), duration of time under load, maximum bulge in mm (where applicable), attitude(s) of the package(s) ¹ , atmospheric temperature and relative humidity, number of replicate packages.
Vertical impact by dropping	AS 2582.4	Drop height, attitude(s) of the package(s) ¹ , atmospheric temperature and relative humidity, number of replicate packages, number of impacts.
Horizontal impact	AS 2582.5	Horizontal velocity, attitude(s) of the package(s) ¹ , atmospheric temperature and relative humidity, profiles of impacting surfaces and use (if any) of an imposing hazard, number of replicate packages.
Vibration	AS 2582.6	Duration of test, attitude(s) of the package(s) ¹ , atmospheric temperature and relative humidity, load (if any) superimposed on the package(s), number of replicate packages.
Low pressure	AS 2582.7	Pressure, duration of time at reduced pressure, temperature within test chamber, number of replicate packages.

Notes: (1) When specifying the attitude(s) of the package(s), reference should be made to AS 2582.1.
(2) Other Australian standards for conditioning are APPITA P414m and APPITA P415m (endorsed as part of AS 1301).
(3) An Australian standard for the compression resistance of *unfilled* fibreboard boxes is APPITA 800s (endorsed as part of AS 1301).

The basic test intensities, the preferred range of test intensities, and the test intensity modifying factors are the same as for ISO 4180/2, and are described in detail in AS 2584.2.

2.5 SUMMARY

Gunderson (1991) summarised corrugated box testing and corrugated box performance in the ‘real world’ and found that “today’s tests for corrugated board do not adequately predict a container’s performance in actual use”, and that the “move toward performance based criteria for corrugated containers will better serve producers and users and will encourage engineering and process innovations”. New test methods must account for extended duration of load (progressive creep deformation) and humidity changes (hygroexpansion) that are part of the distribution environment. Only with the development of suitable test methods, environmental profiles, material databases, and advanced

structural models, can the efficiency of design and the reliability of corrugated containers in the distribution environment be improved.

3. AIMS AND OBJECTIVES

A typical distribution system for fresh produce involves long transport distances, relatively short storage times, and reasonably constant (or involving few cycles) temperature and relative humidity conditions. Most packaging performance test methods in current use seem to be intended for products with longer storage times, and generally rely on some static or quasi-static mechanical property as a measure of the performance of the packaging system. In a fresh produce distribution system, however, where transportation times are about the same as storage times, and hence the transportation phase constitutes a larger proportion of the total distribution system, some form of dynamic measure may be more relevant.

The hypothesis of this project is that a dynamic test method for packaging performance is more appropriate for fresh produce packaging systems than the static or quasi-static test methods in current use.

The aim of this project is to develop a performance-based test method for corrugated fibreboard boxes for fresh horticultural produce, using an engineering fatigue-type approach to the prediction and evaluation of packaging performance.

A box is generally deemed to have failed once it deflects a certain critical distance, i.e. static or dynamic creep is the failure criterion, rather than the force required to produce this deflection. The survival time (or time to deflect the critical distance) under dynamic loading will be used as the performance indicator, rather than the compression strength (or resistance to applied force) as used in quasi-static test methods. This approach is expected to have the advantage of simulating the forces most significant in the produce distribution environment, i.e. road transport vibration at high humidity, rather than extended static storage under cycling humidity conditions. These results will then be correlated to quasi-static performance indicators. Ideally this test method should link the performance of the fibreboard boxes with laboratory test results at standard conditions, and at the same time reproduce the damage potential encountered in the field in the laboratory.

The specific objectives of this project can be summarised as follows:

1. *Field experiments*: To measure the levels of physical inputs expected to occur in a typical fresh horticultural produce distribution environment, i.e. shock and vibration, temperature and relative humidity, and shocks during manual and mechanical handling.
2. *Laboratory experiments*: To develop a dynamic performance-based method for the testing, evaluation, and comparison of corrugated fibreboard boxes for the packaging of fresh horticultural produce, using these observed environmental conditions.

The experiments conducted to meet these two major objectives, and the results obtained, are described in detail in Chapters 4 and 5 respectively. Overall conclusions for the project are given in Chapter 6.

4. FIELD EXPERIMENTS

This section describes field experiments which were conducted to measure and analyse the levels of physical inputs expected to occur in a typical distribution system for fresh horticultural produce in the Melbourne and East Gippsland regions of Victoria. It is organised into four main sections as follows:

1. *Shock and vibration*: The measurement of acceleration PSD, peak acceleration, velocity change, and crest factor for a typical produce transportation environment.
2. *Temperature and relative humidity*: The measurement of temperature and relative humidity for a typical produce distribution environment.
3. *Manual and mechanical handling*: The measurement of peak acceleration, duration, velocity change, equivalent drop height, and drop impact direction for a typical produce handling environment.
4. *Summary of results*: summarised observations from the measurement and analysis of shock, vibration, temperature, relative humidity, and handling.

4.1 SHOCK AND VIBRATION

This set of experiments consisted of obtaining typical shock and vibration profiles of the fresh produce transportation environment around the Melbourne and East Gippsland regions of Victoria. These experiments were conducted using an Instrumented Sensor Technology (IST) model EDR-1 Environmental Data Recorder (EDR), the IST EDR1S and EDR2S operating software packages, three PCB Piezotronics (PCB) Integrated Circuit Piezoelectric (ICP) accelerometers, and at least one IBM-compatible personal computer (PC). The accelerometers and EDR were attached to a mounting rig, which was then bolted to the chassis structure of several trucks which transport produce around the greater Melbourne and East Gippsland regions.

There were two main objectives to these experiments:

1. To obtain a set of typical PSD curves for the Melbourne and East Gippsland transport vibration environments.
2. To obtain typical distributions of peak acceleration, velocity change, and crest factor for the Melbourne and East Gippsland transport shock environments.

4.1.1 Methodology

Trucks with refrigerated trailers were used for the measurement of transport shock and vibration data. These trucks operated from Costa's Wholesale Fruit and Vegetable Distribution Centre in Sunshine, Victoria, which delivers to about 90 supermarkets around Melbourne and country Victoria. These supermarkets, and the order in which they were visited, were largely unpredictable, so it was intended to study a variety of Costa's trucks over several weeks to obtain a general view of typical produce distribution environments.

It was initially planned to study four trucks, as follows:

1. A new, medium-sized trailer (PT298) operating in the Melbourne area overnight.
2. An older, large trailer (PT279) which operates between Melbourne and East Gippsland (Bairnsdale) overnight, and around the Melbourne area during the day.
3. A small van which operates around the Melbourne area overnight.
4. A large trailer operating overnight in other areas of country Victoria overnight.

However due to equipment failure before the completion of the experiments, it was only possible to study the first two of these trucks. The testing can therefore be divided into three trailer/location combinations: PT298 operating in Melbourne, PT279 operating in Melbourne, and PT279 operating between Melbourne and Bairnsdale.

Trailer PT298 is a two-axle, leaf-spring suspension trailer manufactured in 1993 by Freighter Australia Manufacturing Pty. Ltd. Together with its truck it has a combined tare weight and combined maximum gross weight of 5850 kg and 35,000 kg respectively. Trailer PT279 is a two-axle, leaf-spring suspension trailer manufactured in 1988 by Freighter Australia Manufacturing Pty. Ltd. Together with its truck it has a combined tare weight and combined maximum gross weight of 7250 kg and 42,500 kg respectively.

The shock and vibration information was measured and recorded using an IST EDR-1 Environmental Data Recorder and three PCB ICP accelerometers mounted onto a custom-built test rig. This experimental equipment is described in more detail in Appendix B. The software set-up and verification of the equipment is described in Appendix C.

After set-up and verification, the EDR and accelerometers were mounted onto the test rig, which was then clamped around the I-section beams running the length of the trailer. The three external accelerometers were attached to the plate in-line to record vertical acceleration. Acceleration in the lateral and longitudinal axes were not studied as (i) vertical acceleration is generally regarded as being the worse case for trucks, and (ii) lateral and longitudinal acceleration could not be later simulated on the single-axis laboratory vibration system.

Once the test rig was secured to the trailer, it was activated, and then securely wrapped in plastic to protect it from dust and moisture. The design of the test rig meant that the three accelerometers were in firm contact with the I-section below the truck, and, ignoring any acceleration amplification or attenuation through the structure of the trailer, this was regarded as being equivalent to recording accelerations on the deck of the trailer. The rig was mounted on the left hand side of the trailer as close as possible to the rear axle, where vertical vibration is reported to be the most severe.

The raw acceleration data were uploaded from the EDR daily, and processed using a PC with the IST EDR1S and EDR2S software packages. The shock and vibration results were then analysed in two ways, in terms of (i) vibration, and (ii) shock.

The transport vibration results were analysed and presented as PSD curves; one PSD curve for each journey that each truck made, and an average PSD curve for each trailer/location combination. Traditionally PSD information has been presented on a logarithmic frequency scale, due to the use of logarithmic increments of the frequency interval. In this case, however, the frequency interval was constant, and a linear frequency range was used.

The transport shock results were analysed and presented as the distributions of the peak acceleration and velocity change for each recorded acceleration event, both for each individual journey, and overall distributions for each trailer/location combination. The distributions of peak acceleration and velocity change were also modelled using several cumulative probability density functions.

4.1.2 Results and Discussion

The transport shock and vibration recording was conducted as shown in Table 7.

Table 7: EDR files generated during transport shock and vibration recording.

Journey No.	Trailer	Location	No. Events
1	PT298	Melbourne	1000
2	PT298	Melbourne	1000
3	PT279	Bairnsdale	650
4	PT279	Melbourne	349
5	PT279	Bairnsdale	124
6	PT279	Bairnsdale	261
7	PT279	Melbourne	66
8	PT279	Bairnsdale	147
9	PT279	Melbourne	145
10	PT279	Bairnsdale	471
11	PT279	Bairnsdale	466
12	PT279	Bairnsdale	1000

The number of events listed for any journey is the number of events recorded in the EDR file (out of 1000 total events) corresponding to that journey. Often more than one journey was recorded in the same EDR file over two or more consecutive days, due to (i) the unpredictable times the truck would be at the distribution centre, and (ii) the occasional malfunction of the portable PC battery pack during data upload which meant that the data could not be retrieved until the following day. Some events were also disregarded when there was a clear discrepancy between the recorded data from the three channels. This was found to be due to loosening of one or more of the external leads.

4.1.2.1 Vibration

Before discussing the vibration study results, it should be noted that the terminology used in this study occasionally differs from that used in random vibration and spectral analysis texts. This is done for the sake of clarity, as this study was performed with a specific application of random vibration theory in mind, using instrumentation and software designed for this purpose. For example, what is referred to here as an ‘event’ is more accurately a ‘record’ or ‘sample’; a ‘journey’ is more accurately an ‘ensemble of records’, and a ‘sample’ is more accurately an ‘instantaneous value’. A ‘journey’ is the period in which the truck under study leaves and returns to Costa’s Distribution Centre. An ‘event’ is a collection of 500 consecutive samples, i.e. digitised instantaneous values measured and recorded by the EDR’s ADC at a rate of 500 Hz. The use of journeys, events, and samples is summarised in Table 8.

Table 8: Number of journeys, events, and samples for each trailer/location combination.

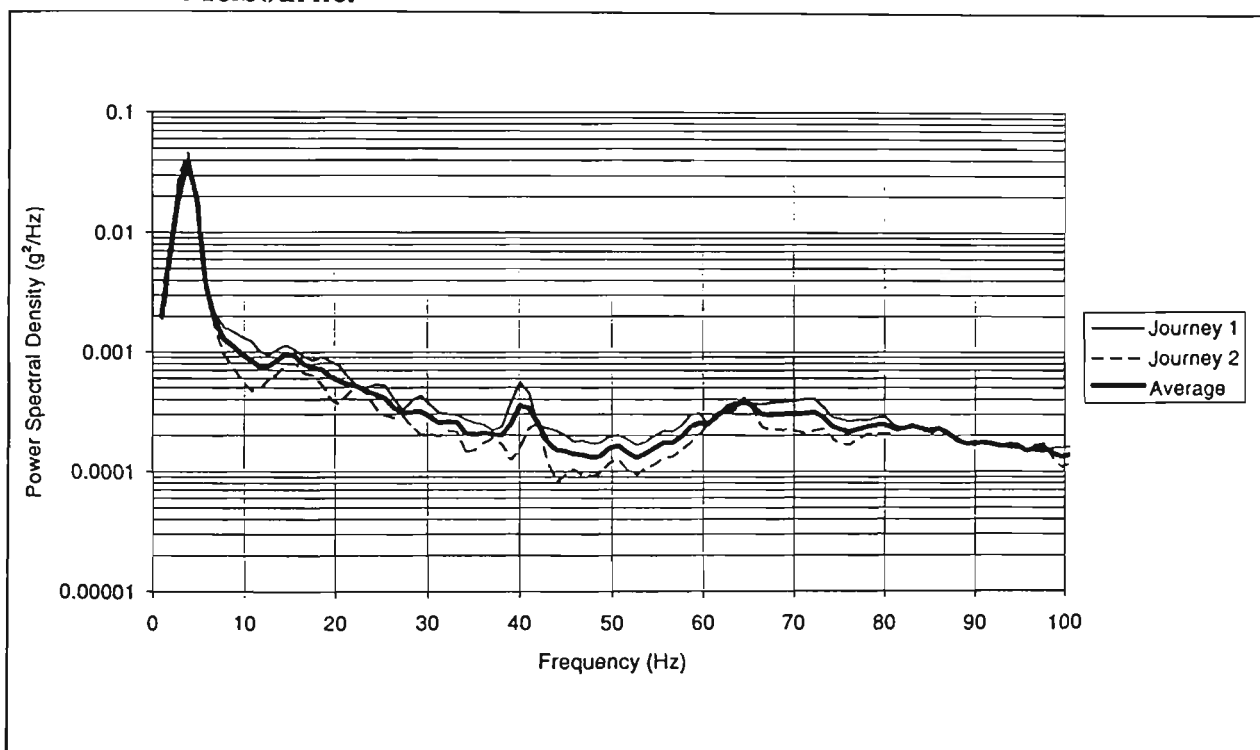
Trailer/Location Combination	Number of Journeys	Number of Events in Each Journey	Total Number of Events	Total Number of Samples
PT298 Melb	2	1000, 1000	2000	1,000,000
PT279 Melb	3	349, 66, 145	560	280,000
PT279 B`dale	7	650, 124, 261, 147, 471, 466, 1000	3119	1,559,500

The PSD curves for each of the trailer/location combinations listed in Table 8 are shown in Figure 3, Figure 4, and Figure 5. These Figures show the PSD curves for each journey by trailers PT298 in Melbourne, PT279 in Melbourne, and PT279 to Bairnsdale respectively. Each Figure contains the PSD curve generated for each individual journey using the channel 3 (high resolution, low range) accelerometer. In addition, each Figure contains the arithmetic average PSD curve for each trailer/location combination. These three average curves, and the ASTM truck profile from ASTM D 4728, are also shown in Figure 6 for comparison.

Figure 3, Figure 4, and Figure 5 all show that the recorded PSD curves for each trailer/location combination follow each other reasonably closely. Figure 6 shows that the recorded PSD curves for each of the three trailer/location combinations differs notably

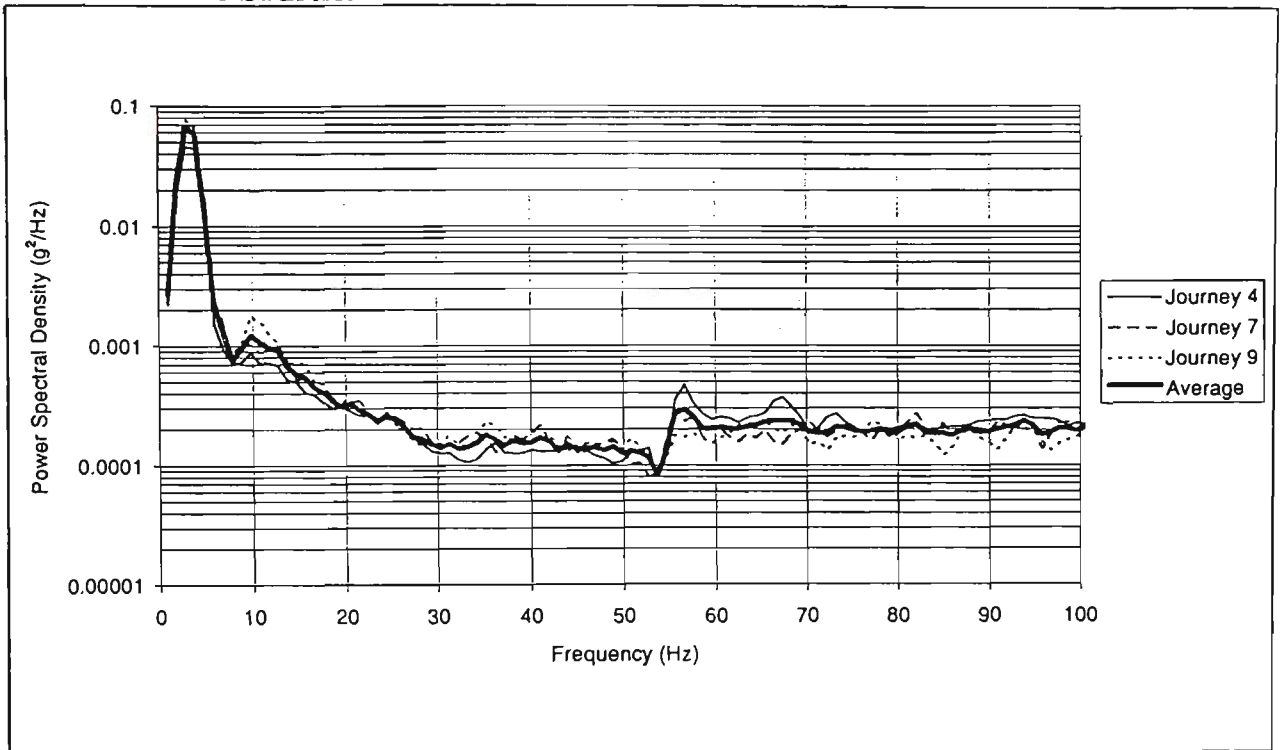
from the ASTM truck profile. The ASTM truck profile is commonly used as a laboratory standard, as it is a compilation of results covering a wide range of variables and does not purport to accurately describe any specific transport environment. Hence the ASTM truck profile is useful for comparing the vibration performance of different products and packaging systems. However, for the specific case of produce transport around greater Melbourne and East Gippsland, the other PSD curves in Figure 6 more accurately describe the transport vibration environment.

Figure 3: Power spectral density: Average of all journeys, trailer PT298 in Melbourne.



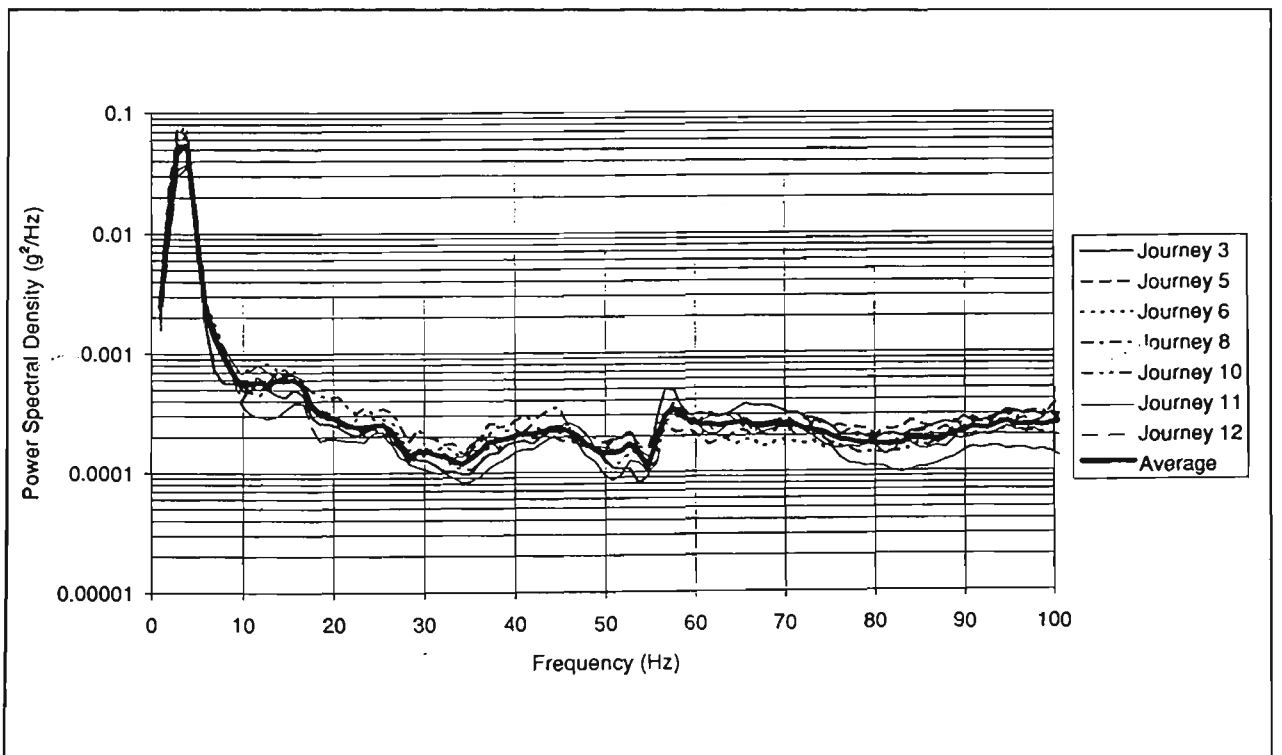
Note: Data from channel 3 accelerometer.

Figure 4: Power spectral density: Average of all journeys, trailer PT279 in Melbourne.



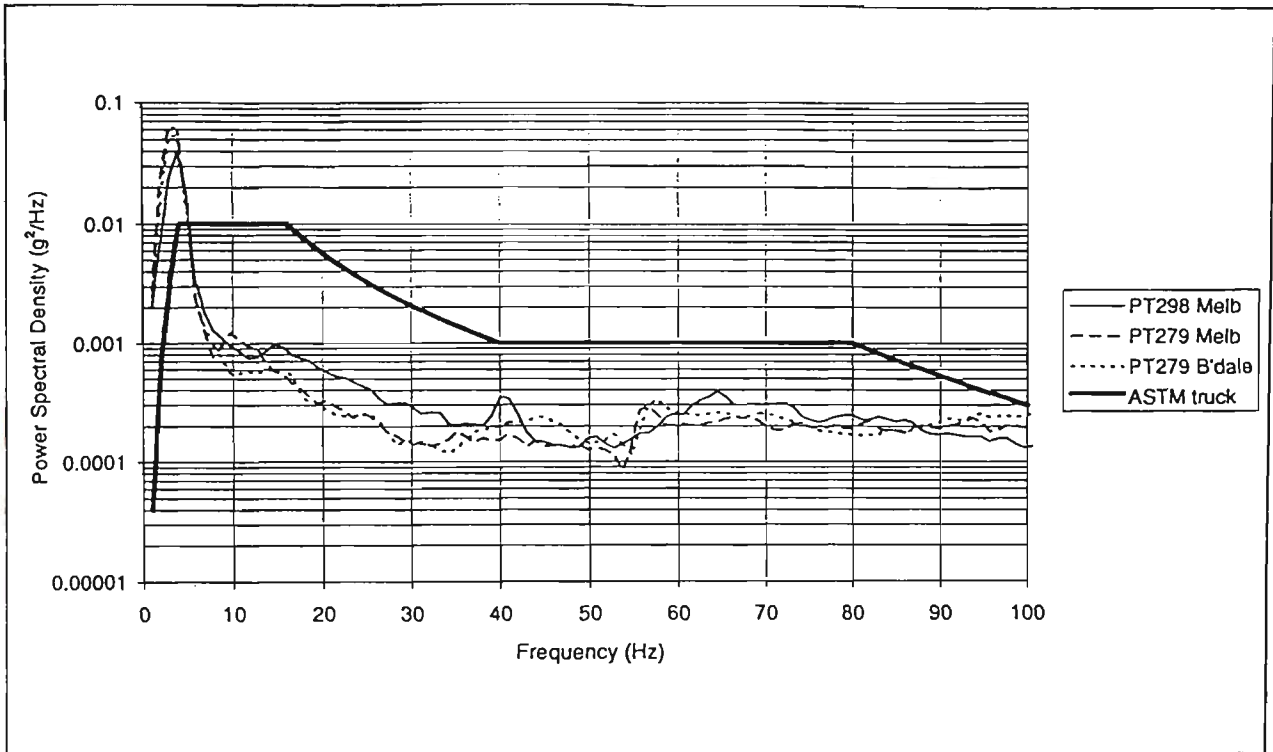
Note: Data from channel 3 accelerometer.

Figure 5: Power spectral density: Average of all journeys, trailer PT279 to Bairnsdale.



Note: Data from channel 3 accelerometer.

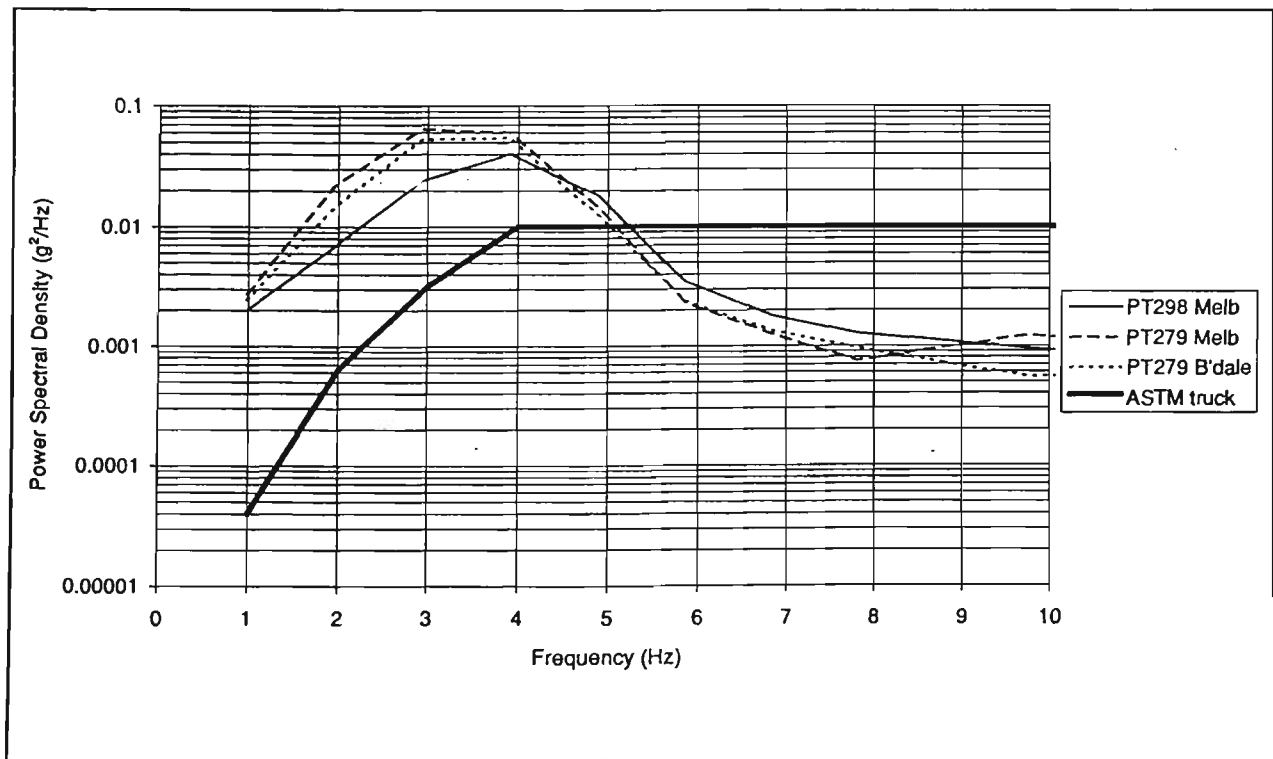
Figure 6: Power spectral density: Average of all trailer/location combinations (1 - 100 Hz).



Note: Data from channel 3 accelerometer.

Figure 7 shows the same information as Figure 6, but is zoomed to show detail in the 1 - 10 Hz range.

Figure 7: Power spectral density: Average of all trailer/location combinations (1 - 10 Hz).



Note: Data from channel 3 accelerometer.

Table 9 shows the RMS acceleration level (g -RMS) for each journey. The RMS acceleration level is represented by the area below the PSD curve, and has the units of g . Only frequencies from 1 - 100 Hz are included in the analyses.

Table 9: RMS acceleration levels for each journey.

Journey No.	Trailer	Location	No. Events	g -RMS
1	PT298	Melbourne	1000	0.35
2	PT298	Melbourne	1000	0.38
3	PT279	Bairnsdale	650	0.35
4	PT279	Melbourne	349	0.39
5	PT279	Bairnsdale	124	0.46
6	PT279	Bairnsdale	261	0.46
7	PT279	Melbourne	66	0.45
8	PT279	Bairnsdale	147	0.45
9	PT279	Melbourne	145	0.48
10	PT279	Bairnsdale	471	0.39
11	PT279	Bairnsdale	466	0.40
12	PT279	Bairnsdale	1000	0.32

Table 10 shows the average RMS acceleration levels for each of the PSD curves in Figure 6. It can be seen that the RMS levels for each of the three recorded PSD profiles are less than the ASTM truck profile, except at assurance level 3. However this does not infer that the recorded vibration is less severe than ASTM D 4169 demands, as the shape of the profiles also has a large influence on the resultant severity of vibration.

Table 10: Average RMS acceleration levels for each trailer/location combination.

Trailer	Location	RMS acceleration (g -RMS)
PT298	Melbourne	0.37 ¹
PT279	Melbourne	0.44 ¹
PT279	Bairnsdale	0.40 ¹
ASTM truck (assurance level 1)		0.73 ²
ASTM truck (assurance level 2)		0.52 ²
ASTM truck (assurance level 3)		0.37 ²

Notes: (1) Average g -RMS acceleration levels obtained from Figure 6 and Table 9.

(2) g -RMS acceleration levels obtained from ASTM D 4169.

Considering these results, the ASTM truck PSD profile appears to be inappropriate for the laboratory testing of produce transport around the Melbourne and East Gippsland regions of Victoria. A more suitable profile would be that obtained from trailer PT279 in

Melbourne with an RMS acceleration of 0.44 g-RMS, as this would provide the worst-case conditions of the three recorded profiles above.

4.1.2.2 Shock

4.1.2.2.1 Peak Acceleration and Velocity Change Distributions

The peak acceleration distributions for each individual journey are shown in Table 11. This Table shows the occurrence of peak accelerations in intervals of 4 g, where the tabulated interval value is the lower limit of the interval. The total number of events and the maximum, mean, and median peak acceleration recorded on that journey are also shown.

Table 11: Shock event peak acceleration distributions: Distribution for each journey.

Trailer and Location:	PT298 Melbourne	PT298 Melbourne	PT279 Melbourne	PT279 Melbourne	PT279 Melbourne	PT279 Bairnsdale
Journey:	1	2	4	7	9	3
0 g	984	983	349	65	145	648
4 g	4	7	0	0	0	1
8 g	9	4	0	0	0	0
12 g	0	1	0	1	0	0
16 g	1	2	0	0	0	0
20 g	0	1	0	0	0	0
24 g	1	1	0	0	0	0
28 g	0	0	0	0	0	0
32 g	0	0	0	0	0	0
36 g	0	0	0	0	0	0
40 g	1	1	0	0	0	0
44 g	0	0	0	0	0	1
> 48 g	0	0	0	0	0	0
Count:	1000	1000	349	66	145	650
Maximum:	40.26	43.80	3.36	12.86	3.66	47.54
Mean:	1.27	1.21	1.01	1.27	1.17	1.01
Median:	0.99	0.92	0.90	0.99	1.04	0.84

Trailer and Location:	PT279 Bairnsdale					
Journey:	5	6	8	10	11	12
0 g	122	258	146	469	463	990
4 g	2	2	0	2	1	7
8 g	0	1	0	0	1	0
12 g	0	0	0	0	0	0
16 g	0	0	1	0	0	2
20 g	0	0	0	0	0	0
24 g	0	0	0	0	0	1
28 g	0	0	0	0	0	0
32 g	0	0	0	0	0	0
36 g	0	0	0	0	0	0
40 g	0	0	0	0	0	0
44 g	0	0	0	0	0	0
> 48 g	0	0	0	0	1	0
Count:	124	261	147	471	466	1000
Maximum:	5.20	8.26	16.92	6.00	93.44	24.36
Mean:	1.23	1.17	1.22	1.19	1.40	1.08
Median:	1.10	1.04	1.02	1.06	1.08	0.92

Note: Data from channel 2 accelerometer.

The velocity change distributions for each individual journey are shown in Table 12. This Table shows the occurrence of velocity changes in intervals of 20 cm/s, where the tabulated interval value is the lower limit of the interval. The total number of events and the maximum, mean, and median velocity change recorded on that journey are also shown.

Table 12: Shock event velocity change distributions: Distribution for each journey.

Trailer and Location:	PT298 Melbourne	PT298 Melbourne	PT279 Melbourne	PT279 Melbourne	PT279 Melbourne	PT279 Bairnsdale
Journey:	1	2	4	7	9	3
0 cm/s	951	947	342	62	121	637
20 cm/s	27	25	1	2	15	9
40 cm/s	9	20	1	2	7	2
60 cm/s	5	5	3	0	1	1
80 cm/s	1	1	1	0	0	0
100 cm/s	0	0	1	0	1	0
120 cm/s	1	1	0	0	0	0
140 cm/s	0	0	0	0	0	0
160 cm/s	3	0	0	0	0	0
180 cm/s	1	0	0	0	0	1
200 cm/s	1	0	0	0	0	0
220 cm/s	1	0	0	0	0	0
> 240 cm/s	0	1	0	0	0	0
Count:	1000	1000	349	66	145	650
Maximum:	224	287	112	58	107	198
Mean:	5	5	5	8	12	4
Median:	3	3	3	5	8	3

Trailer and Location:	PT279 Bairnsdale					
Journey:	5	6	8	10	11	12
0 cm/s	115	232	137	440	437	962
20 cm/s	7	20	6	15	20	25
40 cm/s	2	6	4	11	4	10
60 cm/s	0	3	0	3	2	2
80 cm/s	0	0	0	2	2	1
100 cm/s	0	0	0	0	1	0
120 cm/s	0	0	0	0	0	0
140 cm/s	0	0	0	0	0	0
160 cm/s	0	0	0	0	0	0
180 cm/s	0	0	0	0	0	0
200 cm/s	0	0	0	0	0	0
220 cm/s	0	0	0	0	0	0
> 240 cm/s	0	0	0	0	0	0
Count:	124	261	147	471	466	1000
Maximum:	48	74	51	94	107	84
Mean:	8	10	8	7	7	4
Median:	8	5	5	3	3	3

Note: Data from channel 3 accelerometer.

These distributions could be of use in confirming that any laboratory simulations of the transport environment (e.g. on a vibration table) are providing shocks of the appropriate quantity and magnitude. The distributions of shock duration were not determined as the vast majority of events were of a low-amplitude vibrational nature rather than of a transient shock-pulse nature, and hence for most cases the event duration was approximately equal to the event length (1 s).

The overall peak acceleration distribution for each trailer/location combination is shown in Table 13. Again this Table shows the occurrence of peak accelerations in intervals of 4 g, with the tabulated interval value being the lower limit of the interval.

Table 13: Shock event peak acceleration distributions: Overall distribution for each trailer/location combination.

Trailer and Location:	PT298 Melbourne		PT279 Melbourne		PT279 Bairnsdale	
Peak Accel. (g)	Number	(Percent)	Number	(Percent)	Number	(Percent)
0	1967	(98.4%)	559	(99.8%)	3096	(99.3%)
4	11	(0.6%)	0		15	(0.5%)
8	13	(0.7%)	0		2	(0.1%)
12	1	(0.1%)	1	(0.2%)	1	(0.0%)
16	3	(0.2%)	0		2	(0.1%)
20	1	(0.1%)	0		0	
24	2	(0.1%)	0		1	(0.1%)
28	0		0		0	
32	0		0		0	
36	0		0		0	
40	2	(0.1%)	0		0	
44	0		0		1	(0.1%)
> 48	0		0		1	(0.1%)
Count:	2000		560		3119	
Maximum (g):	43.80		12.86		93.44	
Mean (g):	1.24		1.08		1.15	
Median (g):	0.94		0.96		0.98	

Notes: (1) Data from channel 2 accelerometer.
 (2) Percentages do not add up to 100% due to rounding.

It can be seen from Table 13 that for all three trailer/location combinations, approximately 99% of all events had a peak acceleration less than 4 g. These events are mainly (low-amplitude) vibrational in nature. PT298 in Melbourne had approximately 1% of peak accelerations above 8 g, with a maximum of 43.8 g. PT279 in Melbourne had only 1 event (0.2%) with a peak acceleration above 8 g, with a maximum of 12.9 g. PT279 to Bairnsdale had approximately 0.2% of peak accelerations above 8 g, with a maximum of 93.4 g.

The median peak accelerations for all three trailer/location combinations were all approximately equal. Overall, PT298 in Melbourne and PT279 to Bairnsdale had higher levels of maximum and mean peak acceleration than PT279 in Melbourne. PT298 had

higher mean peak accelerations than PT279, and the Bairnsdale journeys had higher maximum peak accelerations than the Melbourne journeys. The maximum peak acceleration also tended to increase as the number of events increased.

The overall velocity change distribution (and EDH distribution) for each trailer/location combination is shown in Table 14. Again this Table shows the occurrence of velocity changes in intervals of 20 cm/s, with the tabulated interval value being the lower limit of the interval. It should be noted that these drop heights are calculated EDHs for the impacts recorded by the EDR. As the EDR was securely bolted to the trailer structure, it was unlikely that any of these events were the result of free-fall drops. The EDH refers to the ideal free-fall drop height required to achieve the same total velocity change as the velocity change of the impact waveform.

Table 14: Shock event velocity change distributions: Overall distribution for each trailer/location combination.

Trailer and Location:	PT298 Melbourne		PT279 Melbourne		PT279 Bairnsdale	
Velocity Change (cm/s) (Equiv. Drop Height, cm)	Number	(Percent)	Number	(Percent)	Number	(Percent)
0 (0.0 cm)	1898	(94.9%)	525	(93.8%)	2960	(94.9%)
20 (0.2 cm)	52	(2.6%)	18	(3.2%)	102	(3.3%)
40 (0.8 cm)	29	(1.5%)	10	(1.8%)	39	(1.3%)
60 (1.8 cm)	10	(0.5%)	4	(0.7%)	11	(0.4%)
80 (3.3 cm)	2	(0.1%)	1	(0.2%)	5	(0.2%)
100 (5.1 cm)	0		2	(0.4%)	1	(0.0%)
120 (7.3 cm)	2	(0.1%)	0		0	
140 (10.0 cm)	0		0		0	
160 (13.0 cm)	3	(0.2%)	0		0	
180 (16.5 cm)	1	(0.1%)	0		1	(0.0%)
200 (20.4 cm)	1	(0.1%)	0		0	
220 (24.7 cm)	1	(0.1%)	0		0	
> 240 (29.4 cm)	1	(0.1%)	0		0	
Count:	2000		560		3119	
Maximum (cm/s, cm):	287	(42.0 cm)	112	(6.4 cm)	198	(20.0 cm)
Mean (cm/s, cm):	5	(0.0 cm)	7	(0.0 cm)	6	(0.0 cm)
Median (cm/s, cm):	3	(0.0 cm)	3	(0.0 cm)	3	(0.0 cm)

Notes: (1) Data from channel 3 accelerometer.

(2) Percentages do not add up to 100% due to rounding.

It can be seen from Table 14 that for all three trailer/location combinations, approximately 95% of all events had a velocity change less than 20 cm/s, about 3% had a velocity change between 20 and 40 cm/s, and about 1.5% had a velocity change between 40 and 60 cm/s.

The maximum recorded velocity changes for PT298 in Melbourne, PT279 in Melbourne, and PT279 to Bairnsdale were 287, 112, and 198 cm/s respectively. Using the Equation (2.15) for EDH, assuming a worst-case coefficient of restitution $e = 0$, the maximum EDHs for these three trailer/location combinations are about 42, 6, and 20 cm respectively.

The mean and median velocity changes for all three trailer/location combinations were all approximately equal. Overall, PT298 in Melbourne and PT279 to Bairnsdale had higher levels of maximum velocity change than PT279 in Melbourne, however PT279 in Melbourne had a higher mean velocity change.

The crest factor distribution for each trailer/location combination is shown in Table 15. This Table shows the occurrence of crest factors in intervals of 1, with the tabulated interval value being the lower limit of the interval. The crest factor is the ratio of peak acceleration to RMS acceleration for each event, and hence is dimensionless.

Table 15: Shock event crest factor distributions: Overall distribution for each trailer/location combination.

Trailer and Location:	PT298 Melbourne	PT279 Melbourne	PT279 Bairnsdale
Crest Factor	Number (Percent)	Number (Percent)	Number (Percent)
0	0	0	0
1	27 (1.4%)	25 (4.5%)	31 (1.0%)
2	1340 (67.0%)	353 (63.0%)	2006 (64.3%)
3	465 (23.3%)	151 (27.0%)	927 (29.7%)
4	85 (4.3%)	25 (4.5%)	128 (4.1%)
5	19 (1.0%)	3 (0.5%)	12 (0.4%)
6	15 (0.8%)	1 (0.2%)	7 (0.2%)
7	8 (0.4%)	1 (0.2%)	2 (0.1%)
8	10 (0.5%)	0	0
9	9 (0.5%)	1 (0.2%)	2 (0.1%)
10	11 (0.6%)	0	1 (0.0%)
11	8 (0.4%)	0	1 (0.0%)
> 12	3 (0.1%)	0	2 (0.1%)
Count:	2000	560	3119
Maximum:	13.76	9.42	99
Mean:	3.02	2.86	2.94
Median:	2.72	2.72	2.80

Notes: (1) Data from channel 3 accelerometer.

(2) Percentages do not add up to 100% due to rounding.

It can be seen from Table 15 that for all trailer/location combinations, the large majority of crest factors were less than 4. PT298 in Melbourne had about 92% of crest factors less

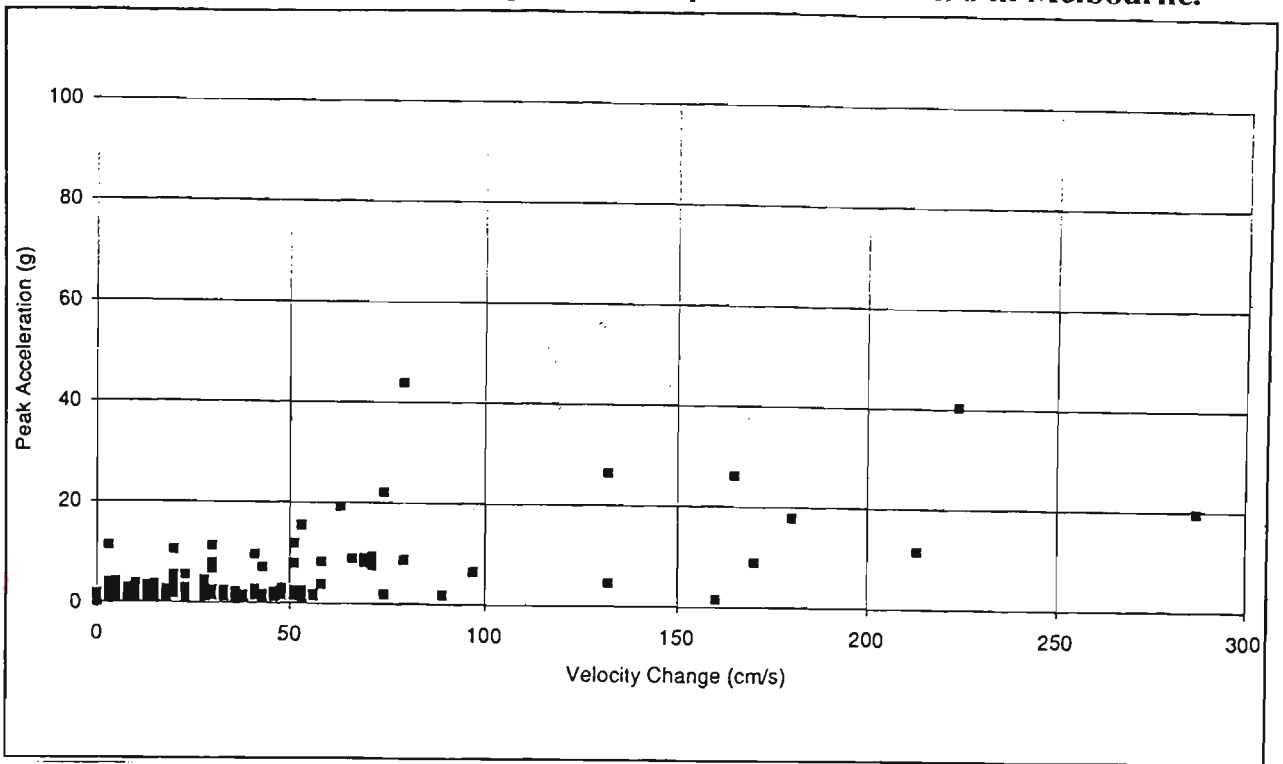
than 4, with 98% less than 7. Both PT279 in Melbourne and PT279 to Bairnsdale had about 95% and 99.7% of crest factors less than 4 and 7 respectively. The highest crest factors recorded for PT298 in Melbourne, PT279 in Melbourne, and PT279 to Bairnsdale were about 14, 9, and 99 respectively.

Overall, PT298 had higher levels of both maximum and mean crest factors than PT279, and PT279 to Bairnsdale had a higher level of maximum crest factor than PT279 in Melbourne. The median crest factors were all approximately equal for each trailer/location combination.

The distributions of peak acceleration and velocity change for each trailer/location combination have also been plotted against each other in what is referred to as, for lack of a better term, an environmental damage potential plot, as shown in Figure 8, Figure 9, and Figure 10. These can be thought of as an inverse damage boundary curve. A damage boundary curve (DBC) relates the combinations of acceleration and velocity change which are likely to cause damage to mechanical products (i.e. products modelled by a simple spring-mass system); the environmental damage potential plot relates the combinations of acceleration and velocity change which were measured in the product distribution environment.

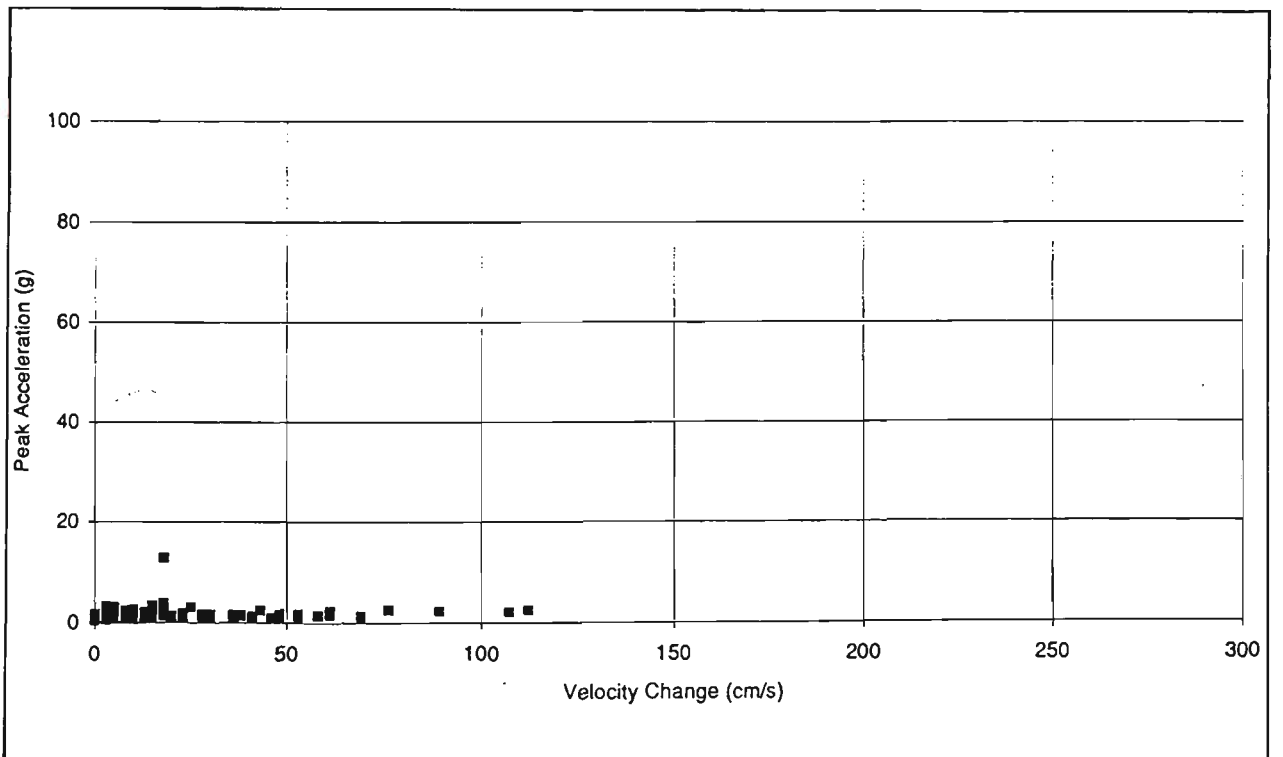
The severity of environmental shock hazards is largely a function of both peak acceleration and velocity change, and these plots could make it easier to visualise the relationship between the two parameters. Events with either a large peak acceleration or a large velocity change may not cause product damage if the other parameter is below some critical threshold. However, if both parameters are above some critical threshold values, then the shock event has the potential to cause damage. The environmental damage potential plot for a distribution system could then conceivably be used in conjunction with the damage boundary curve for a product to observe the likely occurrence of potentially damaging shocks.

Figure 8: Environmental damage potential plot: Trailer PT298 in Melbourne.



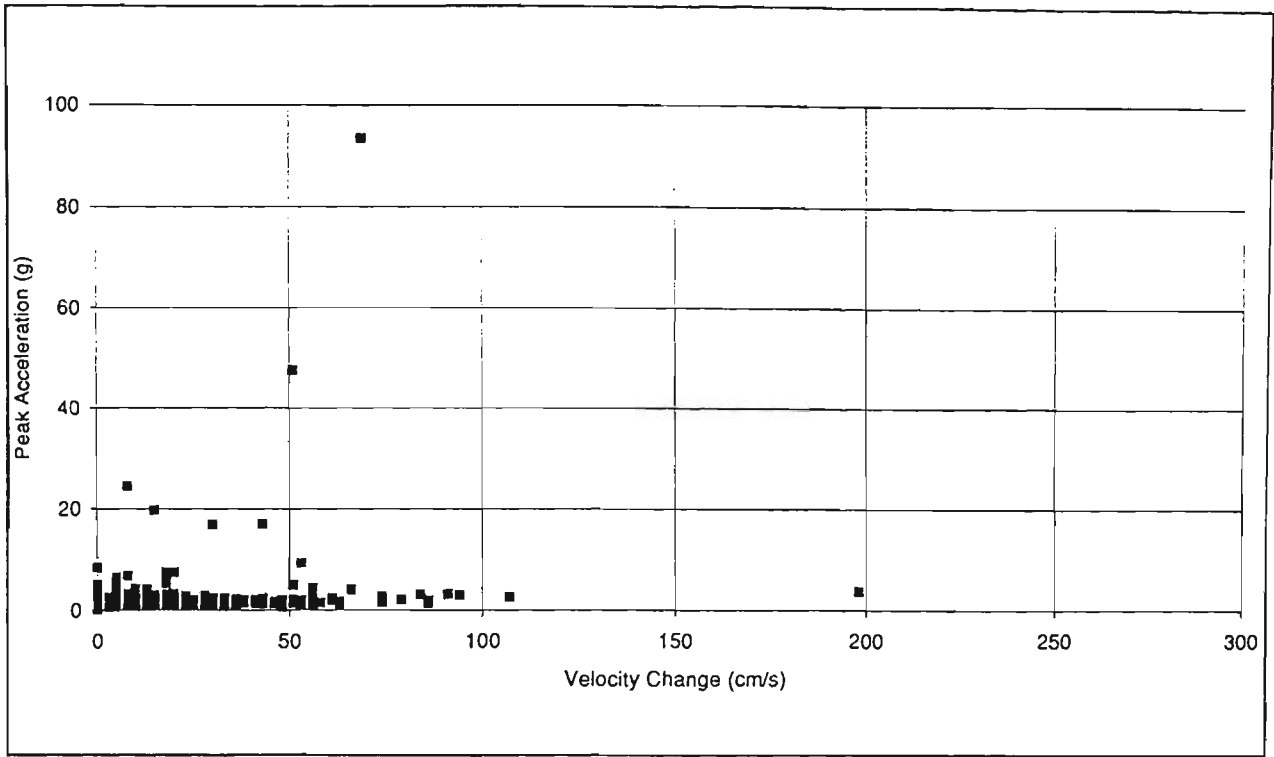
Notes: (1) Peak acceleration data from channel 2 accelerometer.
(2) Velocity change data from channel 3 accelerometer.

Figure 9: Environmental damage potential plot: Trailer PT279 in Melbourne.



Notes: (1) Peak acceleration data from channel 2 accelerometer.
(2) Velocity change data from channel 3 accelerometer.

Figure 10: Environmental damage potential plot: Trailer PT279 to Bairnsdale.



Notes: (1) Peak acceleration data from channel 2 accelerometer.
(2) Velocity change data from channel 3 accelerometer.

Figure 8 shows the relationship between peak acceleration and velocity change for PT298 in Melbourne. It can be seen that the majority of data points (2000 points total) are in the region bounded by about 20 g and 70 cm/s. The remaining points are within 35 g and 230 cm/s, with the exception of three points at (45 g, 80 cm/s), (40 g, 220 cm/s), and (20 g, 290 cm/s). These are the three points likely to be of the most interest when comparing this environmental damage potential plot to a product damage boundary curve. The second of these points, at (40 g, 220 cm/s), is probably the single point most likely to be within the damage envelope on a damage boundary curve, as it has both a high peak acceleration and a high velocity change.

Similarly, Figure 9 shows the vast majority of data points (560 points total) to be within about 10 g and 90 cm/s. The three data points outside this region are at (15 g, 20 cm/s), (5 g, 110 cm/s), and (5 g, 120 cm/s). These values of peak acceleration and velocity change are smaller than for PT298 in Melbourne, and are unlikely to be of concern when compared to a product damage boundary curve.

Figure 10 shows the vast majority of data points (3119 points total) to be within about 25 g and 110 cm/s. The three points outside this region are at (95 g, 70 cm/s), (50 g, 50 cm/s), and (5 g, 200 cm/s). Although high peak accelerations and high velocity changes are present at these points, no point has both a high peak acceleration and a high velocity change. Therefore these points are unlikely to lie within the damage envelope on a product damage boundary curve, even if one of the parameters is above the critical threshold value.

4.1.2.2.2 Modelling of Shock Event Distributions

The distributions of peak acceleration, velocity change, and crest factor were modelled using two common cumulative probability density functions: the Weibull distribution and the gamma distribution. The derivation of the Weibull distribution and its applicability to random processes was described in Chapter 2. The gamma distribution has no analytical derivation for random processes, but is considered here for comparative purposes. The Rayleigh distribution was also fitted to the data, but due to huge model residuals the use of this distribution was soon discontinued.

The gamma distribution can assume a more skewed shape than the Weibull distribution (Montgomery, 1991), but it does not appear to have been considered to model the distribution of peaks in random vibration, which are known to have a skewed shape. The probability distribution of the gamma random variable is

$$f(x) = \frac{1}{\beta\Gamma(\alpha)} (x/\beta)^{\alpha-1} e^{-x/\beta}, \quad x \in \mathbb{R} \mid x \geq 0 \quad (4.1)$$

where $\alpha > 0$ is the shape parameter and $\beta > 0$ is the scale parameter. The mean and variance of the gamma distribution are

$$\mu = \alpha\beta \quad (4.2)$$

and

$$\sigma^2 = \alpha\beta^2 \quad (4.3)$$

The cumulative gamma distribution is

$$F(a) = 1 - \int_a^{\infty} \frac{1}{\beta \Gamma(\alpha)} (t/\beta)^{\alpha-1} e^{-t/\beta} dt \quad (4.4)$$

or

$$F(a) = 1 - \sum_{k=0}^{\alpha-1} e^{-a/\beta} \frac{(a/\beta)^k}{k!}, \quad \alpha \in \mathbb{N} \quad (4.5)$$

The gamma distribution can assume many different shapes, depending on the values chosen for α and β and it is useful as a model for a wide variety of continuous random variables. The gamma distribution has been used to study variables that may have a skewed distribution, and is commonly used in queuing analysis.

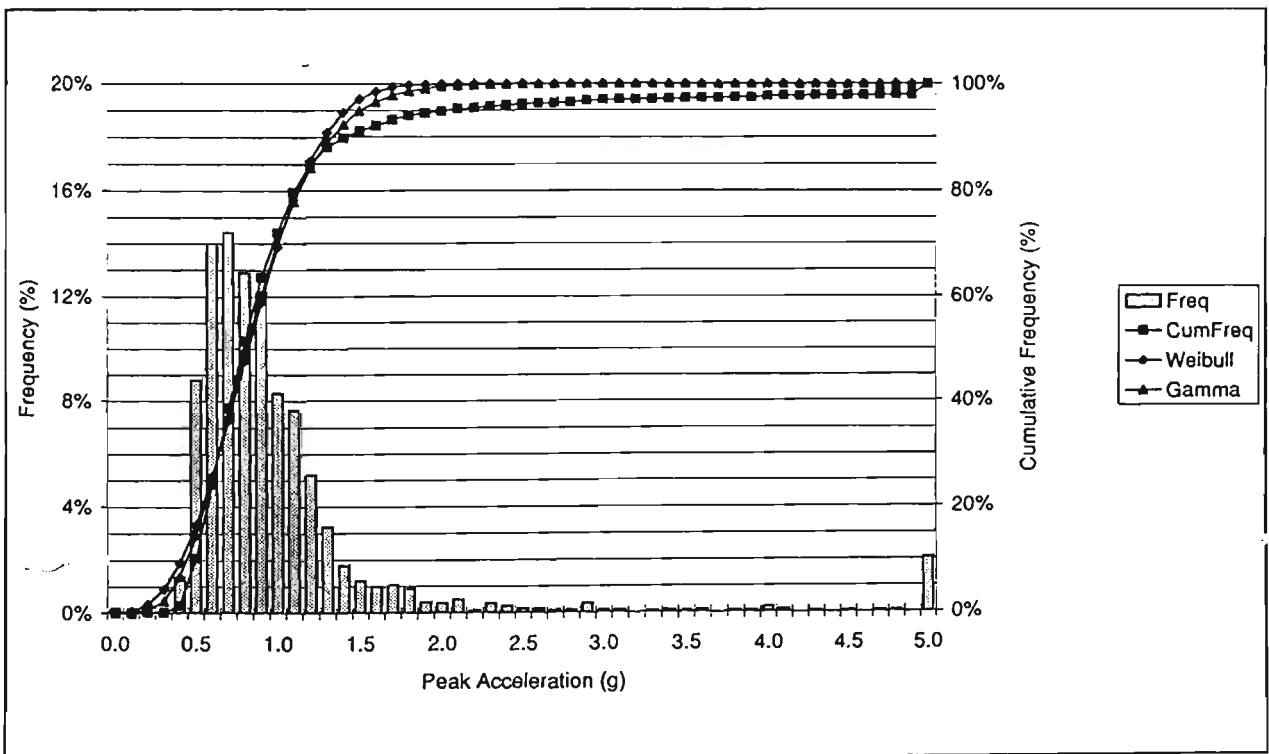
The following Figures illustrate the modelling of the peak acceleration, velocity change, and crest factor distributions using the Weibull and gamma distributions. Figure 11, Figure 14, and Figure 17 show these distributions for PT298 in Melbourne, Figure 12, Figure 15, and Figure 18 show these distributions for PT279 in Melbourne, and Figure 13, Figure 16, and Figure 19 show these distributions for PT279 to Bairnsdale. The bin labels on the x-axis are the minimum values for that interval.

For the model fitting, the channel 3 accelerometer data was used. This was to achieve the greatest resolution for acceleration values (0.02 g). The histogram bin intervals selected for the model fitting were 0.1 g for peak acceleration, 2.5 cm/s for velocity change, and 0.2 for crest factor. The whole range of values for these distributions is not plotted; the maximum histogram bins shown are 5.0 g, 125 cm/s, and 10.0 for peak acceleration, velocity change, and crest factor respectively. The last bin in each Figure also contains all values greater than the range shown. The events in the last bin number less than 0.5%, with the exceptions of Figure 11 (peak acceleration of PT298 in Melbourne), which has about 2% of values in the last bin, and Figure 17 (crest factor of PT298 in Melbourne), which has about 1% of values in the last bin. The fact that all events outside the range of

the histogram are included in the last bin does not affect the fitted model parameters, as the fitted cumulative distribution equates to 100% approximately halfway along the range.

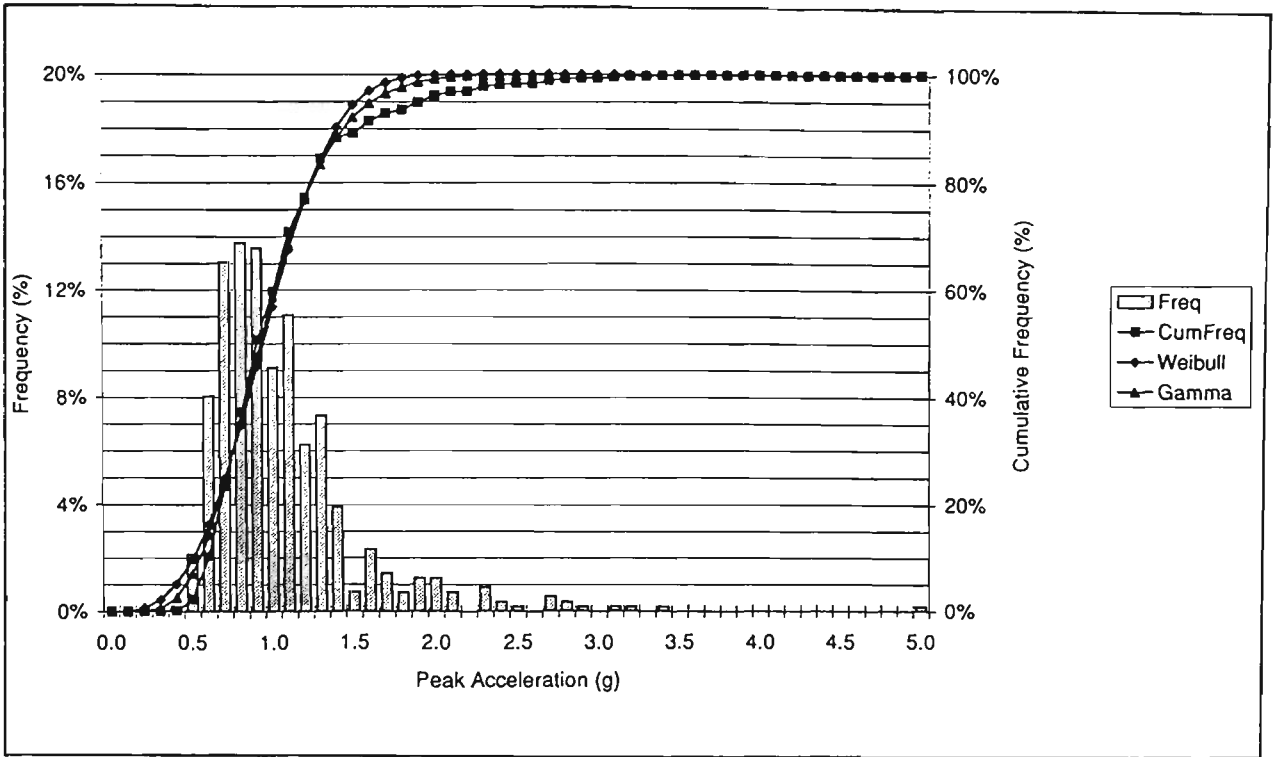
For the purposes of the model fitting, the values in each histogram bin were assumed to all have the value of the bin label. For example, in Figure 11 approximately 14% of all events are in the range 0.60-0.68 g (due to the resolution of the accelerometer and EDR, the greatest possible acceleration less than 0.70 g is 0.68 g). When fitting the models, all values were assumed to be 0.60 g. Ideally model fitting should be conducted using the actual acceleration values rather than artificial intervals, or at worst using the midpoints of the intervals. However a resolution of 0.1 g is satisfactory for practical purposes and any error introduced here would be negligible.

Figure 11: Modelling of shock event peak acceleration distribution: Trailer PT298 in Melbourne.



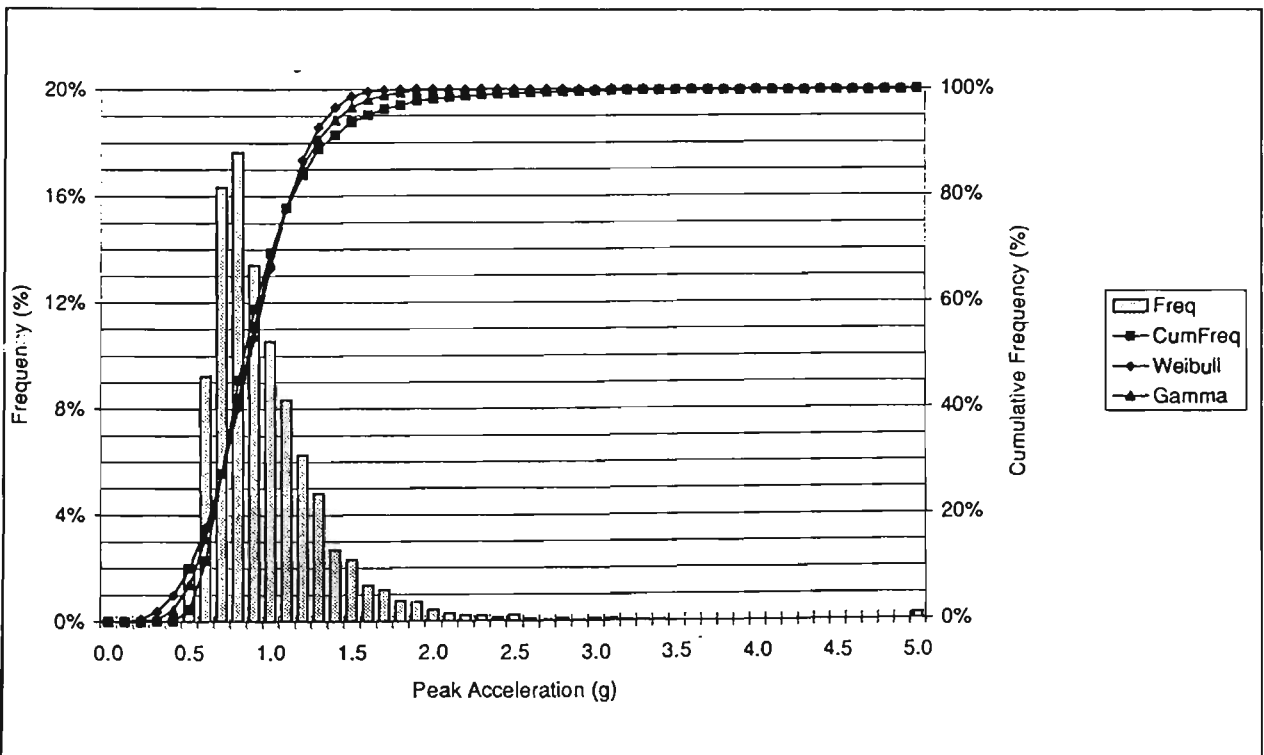
Note: Data from channel 3 accelerometer.

Figure 12: Modelling of shock event peak acceleration distribution: Trailer PT279 in Melbourne.



Note: Data from channel 3 accelerometer.

Figure 13: Modelling of shock event peak acceleration distribution: Trailer PT279 to Bairnsdale.

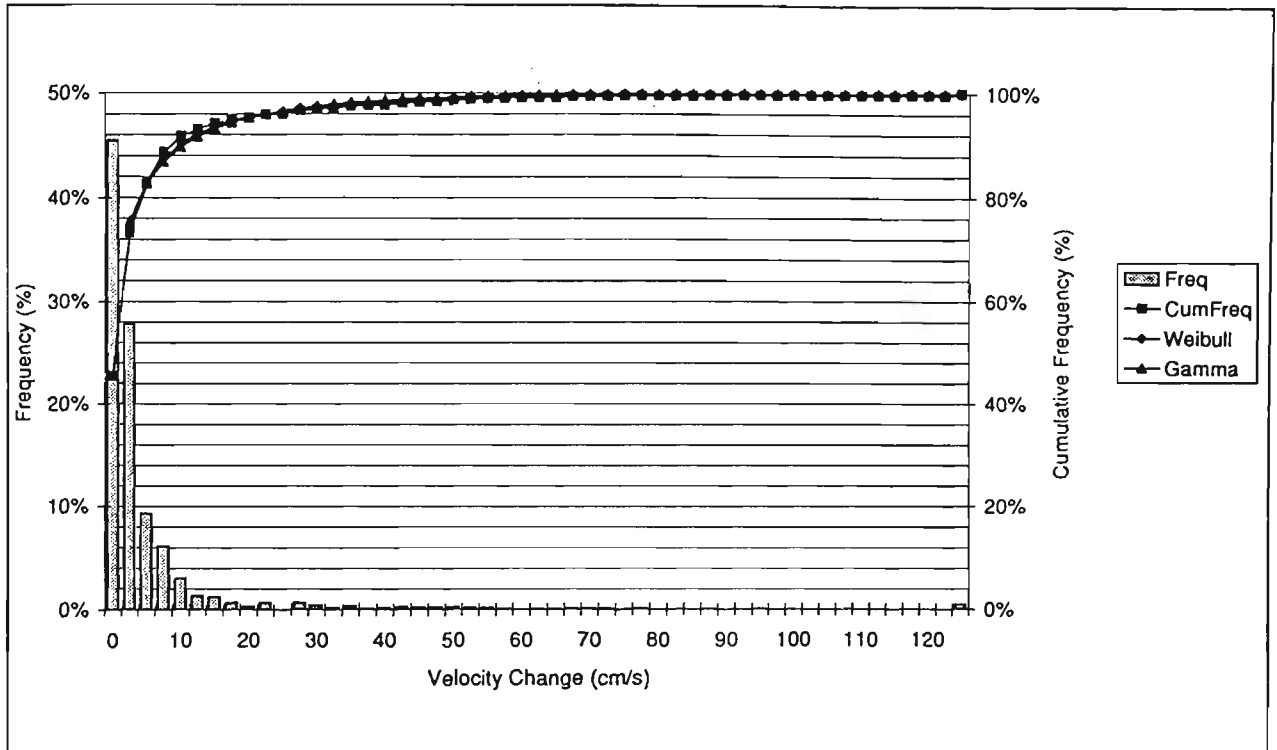


Note: Data from channel 3 accelerometer.

Figure 11, Figure 12, and Figure 13 indicate that the two distribution functions appear to fit the experimental data fairly closely, with the gamma distribution appearing more

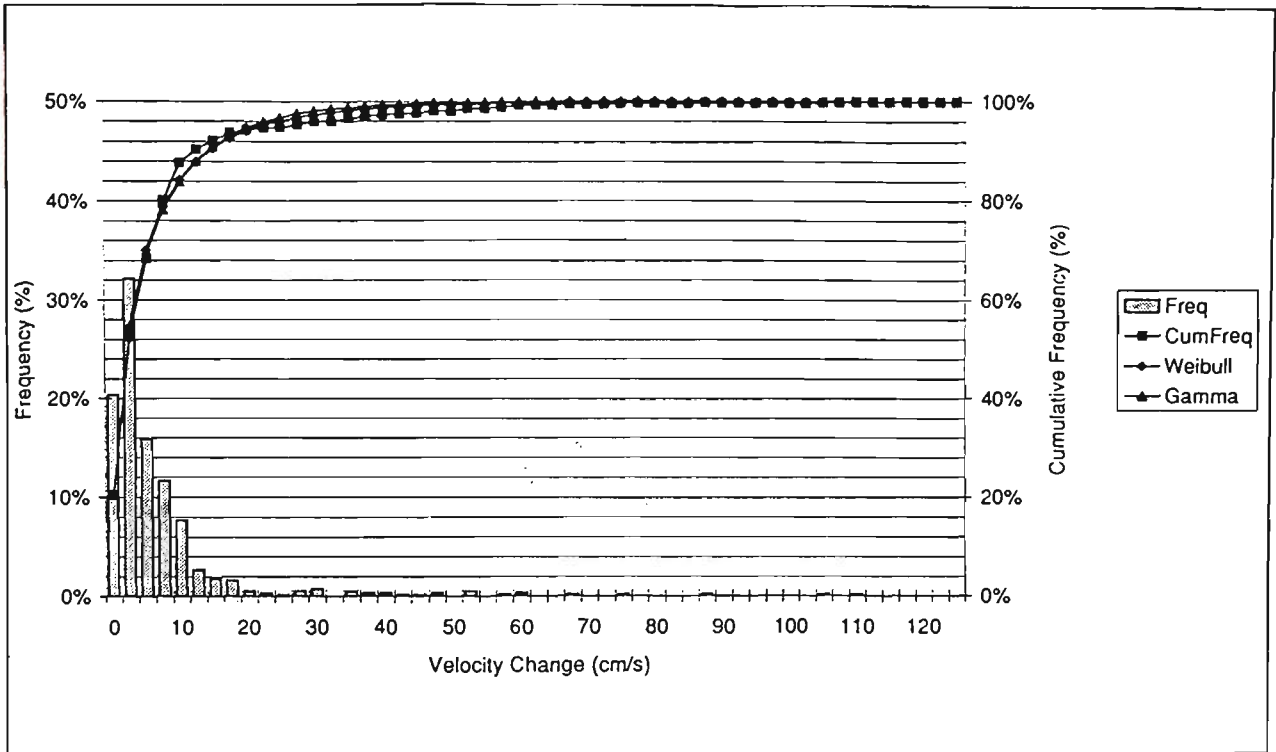
adequate than the Weibull. Both functions appear to better model PT279 than PT298, possibly due to the high number of peak accelerations greater than 5 g recorded on PT298.

Figure 14: Modelling of shock event velocity change distribution: Trailer PT298 in Melbourne.



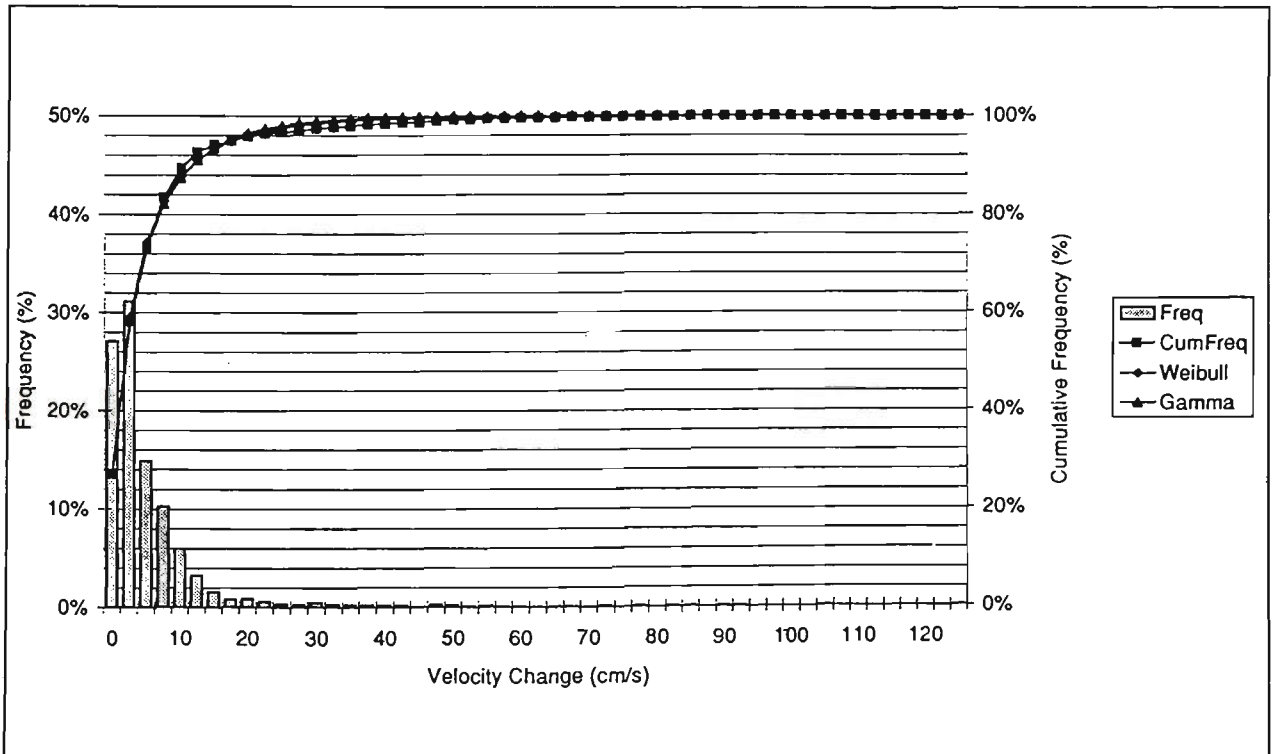
Note: Data from channel 3 accelerometer.

Figure 15: Modelling of shock event velocity change distribution: Trailer PT279 in Melbourne.



Note: Data from channel 3 accelerometer.

Figure 16: Modelling of shock event velocity change distribution: Trailer PT279 to Bairnsdale.

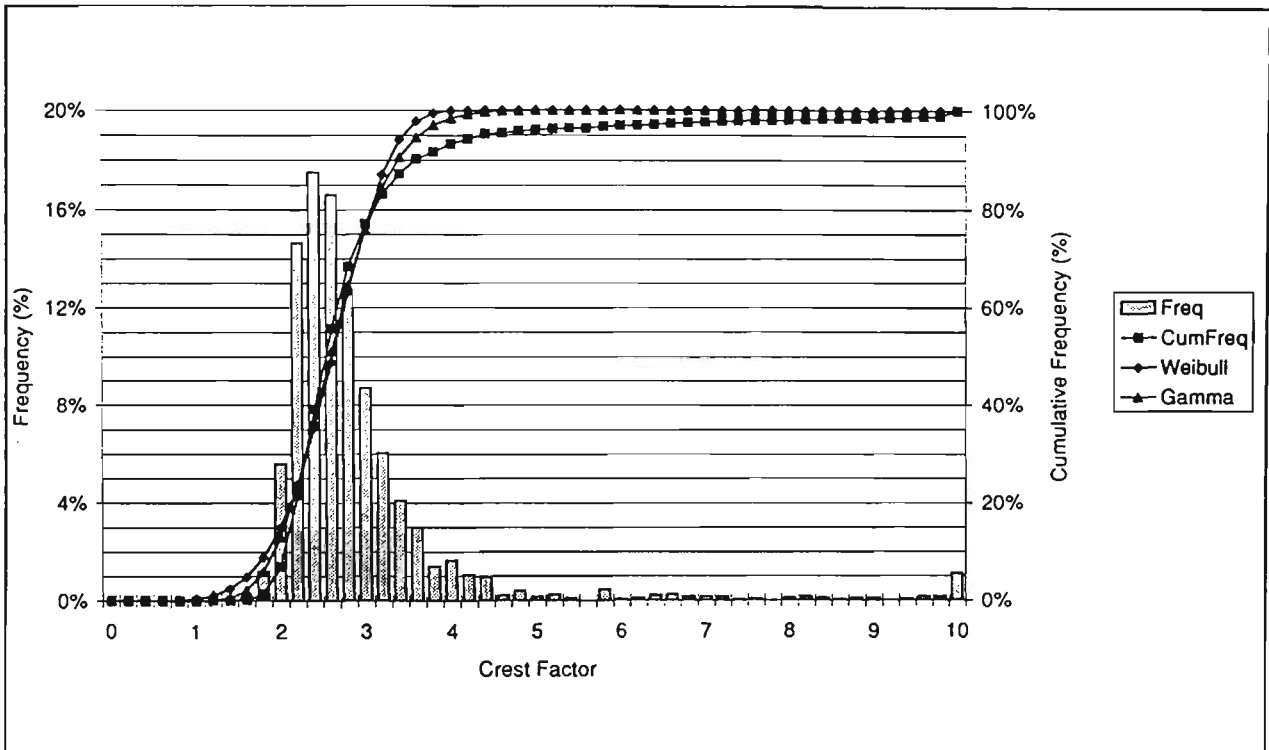


Note: Data from channel 3 accelerometer.

Figure 14, Figure 15, and Figure 16 indicate that both distribution functions appear to fit the experimental data fairly closely. There does not appear to be any difference between

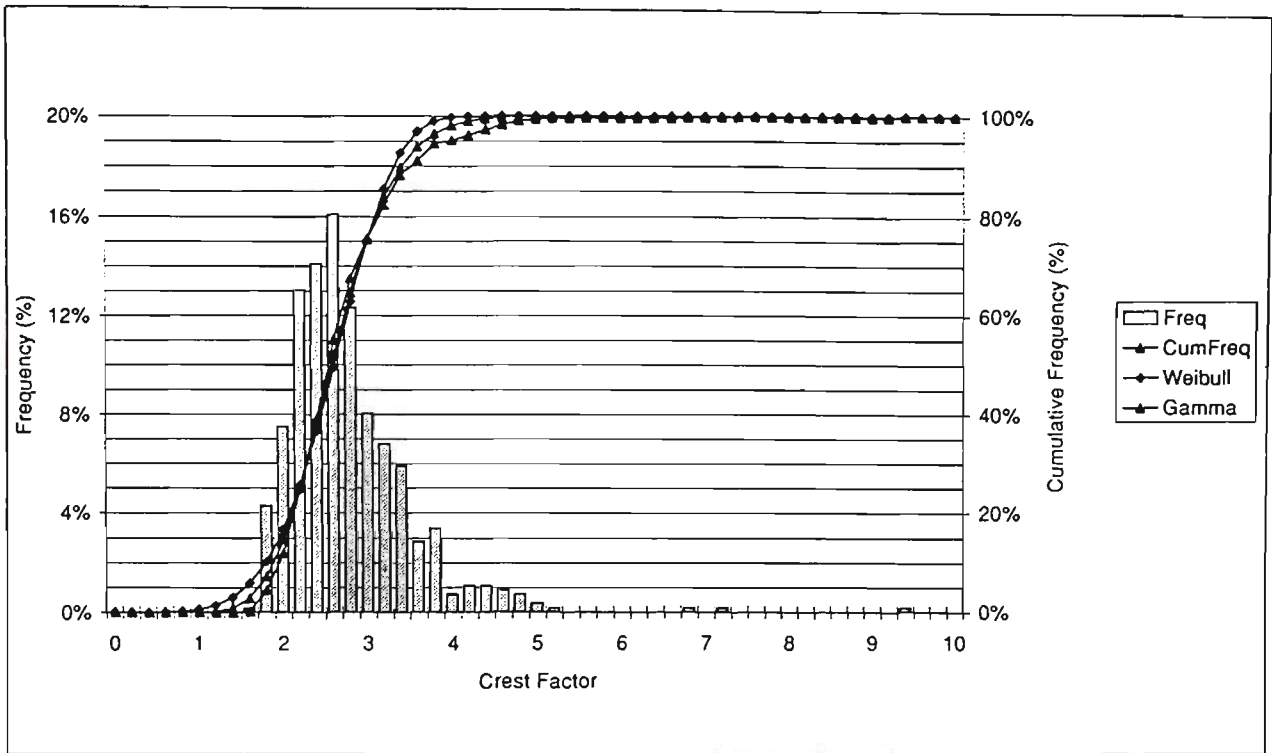
either the fit of the two models, or between the models themselves. The model fits on PT279 in Melbourne appear less adequate than for PT298 in Melbourne and PT279 in Bairnsdale, but this is probably due to the smaller number of recorded events.

Figure 17: Modelling of shock event crest factor distribution: Trailer PT298 in Melbourne.



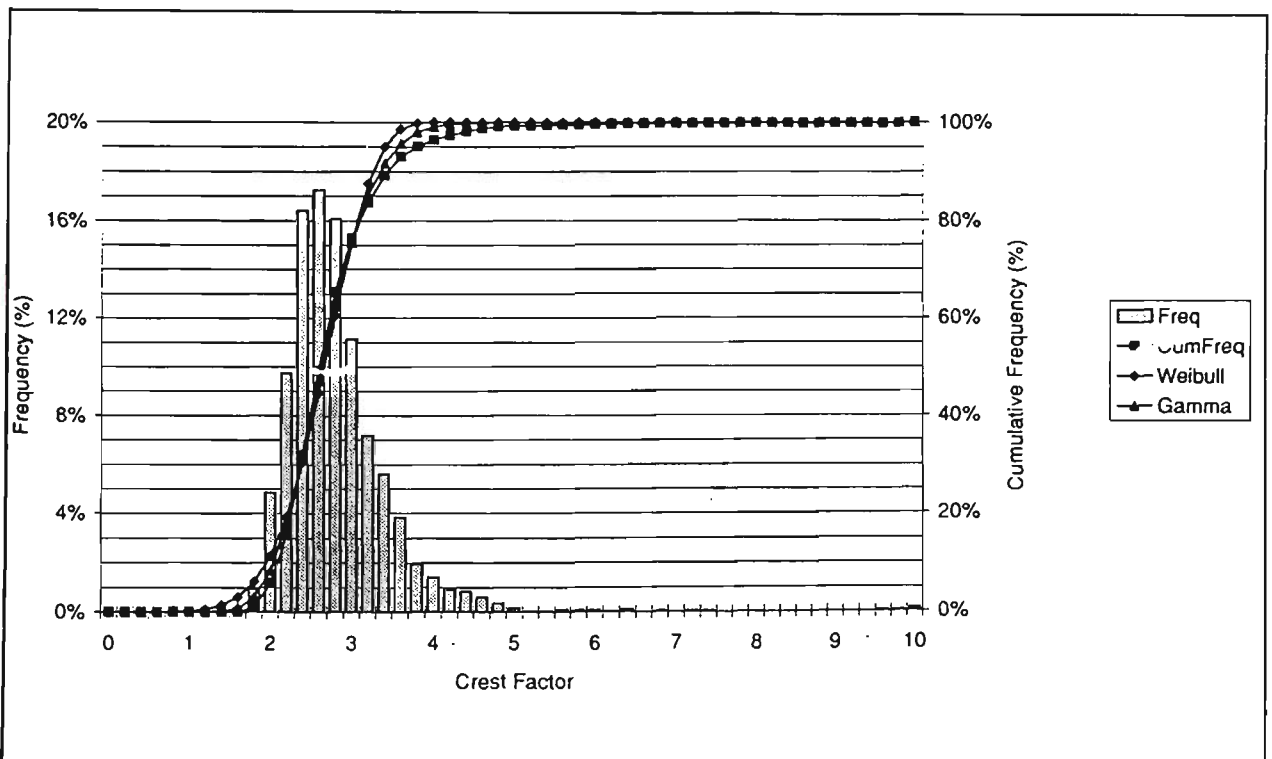
Note: Data from channel 3 accelerometer.

Figure 18: Modelling of shock event crest factor distribution: Trailer PT279 in Melbourne.



Note: Data from channel 3 accelerometer.

Figure 19: Modelling of shock event crest factor distribution: Trailer PT279 to Bairnsdale.



Note: Data from channel 3 accelerometer.

Figure 17, Figure 18, and Figure 19 indicate that both distribution functions appear to fit the experimental data fairly closely, with the gamma distribution appearing more adequate

than the Weibull. Like the peak acceleration modelling described above, the two distributions appear to better model PT279 than PT298, possibly due to the high number of crest factors greater than 10 recorded on PT298.

The Weibull distribution model fitting used the cumulative distribution in Equation (2.14), with the assumption that the location parameter, γ , was zero, effectively making the two-parameter distribution. The gamma distribution model fitting used the cumulative distribution in Equation (4.4). Both distributions were fitted using Microsoft Excel for Windows' built in distribution functions and model fitting tools. The results were then checked using the above equations. As mentioned before, the values of the independent variable a are the histogram bin x-axis labels.

The fitted model parameters for both the Weibull and gamma distributions are shown in the following Tables. Table 16 provides the parameters for the peak acceleration distributions, Table 17 provides the parameters for the velocity change distributions, and Table 18 provides the parameters for the crest factor distributions. These parameters are suitable for use in either the cumulative distribution functions in Equations (2.14) and (4.4), or in the probability density functions in Equations (2.11) and (4.1).

No analyses of significant differences between the three trailer/location combinations have been performed, but these could be used to quantitatively compare different distribution systems for transportation environments.

Table 16: Fitted model parameters: Shock event peak acceleration distributions.

Distribution	Parameters	PT298 Melbourne	PT279 Melbourne	PT279 Bairnsdale
Sample	\bar{x} (mean) (g)	1.12	1.10	1.02
	s^2 (variance) (g)	1.31	0.26	0.21
Weibull	SSR	0.0681	0.0380	0.0325
	β (shape)	2.695	3.032	3.369
	δ (scale)	0.9403	1.059	0.9749
	r (correlation)	0.9971	0.9976	0.9978
	max resid. (%)	8.1%	7.4%	7.8%
	μ (mean) (g)	0.84	0.95	0.88
	σ^2 (variance) (g)	0.11	0.12	0.08
Gamma	SSR	0.0464	0.0170	0.0130
	α (shape)	5.839	7.344	9.093
	β (scale)	0.1465	1.132	0.0981
	r (correlation)	0.9983	0.9989	0.9991
	max resid. (%)	5.4%	4.6%	4.8%
	μ (mean) (g)	0.86	0.97	0.89
	σ^2 (variance) (g)	0.13	0.13	0.09

Note: Data from channel 3 accelerometer.

Table 16 indicates that the gamma distribution appears to model the experimental peak acceleration data more adequately than the Weibull distribution (e.g. a SSR of 0.0681 and r of 0.9971 for the Weibull compared to a SSR of 0.0464 and r of 0.9983 for the gamma). The maximum residual is 8.1% for the Weibull compared to 5.4% for the gamma. Also, it appears that both more adequately model PT279 than PT298.

The mean and variance of the peak acceleration as explained by each of the two models are both similar for a given trailer/location combination, but different from the calculated sample mean and variance. However the mean and variance vary between the different trailer/location combinations. From the mean of the two distributions, it appears that PT279 in Melbourne has the highest mean peak acceleration, followed by PT279 in Bairnsdale, with PT298 in Melbourne having the lowest mean peak acceleration. However the variance of the distributions indicates that these differences are not necessarily significant.

Table 17: Fitted model parameters: Shock event velocity change distributions.

Distribution	Parameters	PT298 Melbourne	PT279 Melbourne	PT279 Bairnsdale
Sample	\bar{x} (mean) (cm/s)	5.28	7.17	5.85
	s^2 (variance) (cm/s)	245	144	95.8
Weibull	SSR	0.0009	0.0057	0.0019
	β (shape)	0.3905	0.6158	0.6188
	δ (scale)	1.145	3.964	3.043
	r (correlation)	0.9962	0.9929	0.9969
	max resid. (%)	1.4%	3.5%	1.7%
	μ (mean) (cm/s)	4.07	5.38	4.40
	σ^2 (variance) (cm/s)	177	83.8	55.5
Gamma	SSR	0.0030	0.0087	0.0032
	α (shape)	0.1491	0.4256	0.4119
	β (scale)	23.78	11.86	10.13
	r (correlation)	0.9890	0.9902	0.9952
	max resid. (%)	2.3%	3.7%	1.9%
	μ (mean) (cm/s)	3.54	5.05	4.17
	σ^2 (variance) (cm/s)	84.3	59.9	42.2

Note: Data from channel 3 accelerometer.

Table 17 indicates that neither distribution appears to model the experimental velocity change data more adequately than the other. The values for SSR, r , and maximum residual are similar. Also, there appears to be no difference in adequacy of modelling the different trailer/location combinations.

The means of the velocity change as explained by each of the two models are both similar for a given trailer/location combination, and are similar to the calculated sample mean. Also, the mean does not significantly vary between the different trailer/location combinations. However the variance of the velocity change as explained by the gamma distribution appears to be less than the variance explained by the Weibull distribution, which in turn is less than the calculated sample variance.

Table 18: Fitted model parameters: Shock event crest factor distributions.

Distribution	Parameters	PT298 Melbourne	PT279 Melbourne	PT279 Baimsdale
Sample	\bar{x} (mean)	3.02	2.86	2.94
	s^2 (variance)	1.64	0.54	3.41
Weibull	SSR	0.0720	0.0295	0.0260
	β (shape)	5.377	5.008	6.058
	δ (scale)	2.802	2.807	2.835
	r (correlation)	0.9975	0.9985	0.9987
	max resid. (%)	8.1%	5.8%	5.8%
	μ (mean)	2.58	2.58	2.63
	σ^2 (variance)	0.31	0.35	0.26
Gamma	SSR	0.0430	0.0086	0.0074
	α (shape)	21.27	19.10	27.42
	β (scale)	0.1235	0.1370	0.0973
	r (correlation)	0.9987	0.9996	0.9997
	max resid. (%)	6.0%	3.3%	2.9%
	μ (mean)	2.63	2.62	2.67
	σ^2 (variance)	0.32	0.36	0.26

Note: Data from channel 3 accelerometer.

Table 18 indicates that the gamma distribution appears to model the crest factor data more adequately than the Weibull distribution (e.g. a SSR of 0.0720 and r of 0.9975 for the Weibull compared to a SSR of 0.0430 and r of 0.9987 for the gamma). The maximum residual is 8.1% for the Weibull compared to 6.0% for the gamma. Also, it appears that these models more adequately model PT279 than PT298.

The mean and variance of the peak acceleration as explained by each of the two models are both similar for a given trailer/location combination. The distribution means appear similar to the calculated sample mean, but the distribution variances appear smaller than the calculated sample variances. Also, neither distribution mean nor variance appears to vary between the different trailer/location combinations.

4.2 TEMPERATURE AND RELATIVE HUMIDITY

These experiments consisted of obtaining typical temperature and relative humidity profiles of the fresh produce distribution environment around the Melbourne and East Gippsland regions of Victoria. The experiments were conducted using a Datataker data logger manufactured by Data Electronics (Australia) Pty Ltd, 12 ANSI type T thermocouples, and two HMP 35 humidity and temperature probes manufactured by Vaisala Sensor

Systems. The data logger, thermocouples, and probes were installed inside a refrigerated trailer which transports produce around the greater Melbourne and East Gippsland regions.

The main objective of these experiments was to obtain typical distributions for temperature and relative humidity for the Melbourne and East Gippsland refrigerated distribution environment.

4.2.1 Methodology

These measurements of temperature and RH were conducted in a refrigerated trailer operating from Costa's Wholesale Fruit and Vegetable Distribution Centre in Sunshine, Victoria. The truck travelled daily from Melbourne to East Gippsland, making produce deliveries to supermarkets as distant as Bairnsdale. The selection of this truck-trailer for the temperature and RH measurements was advantageous as it regularly travelled a large distance and was ideal for providing worst-case information.

Temperature and RH information was not collected in the storage areas of Costa's Distribution Centre, even though produce can expect to spend approximately 6 hr in storage (or up to two days for less perishable items). When not in use, the trailer was backed up to one of the distribution centre loading bays, and both the trailer and distribution centre environments were close to ambient conditions. Temperature and RH recording was conducted continuously over 24 hr periods, and hence the recorded data includes conditions for both the transportation and storage and storage over this time.

The temperature and RH information was measured and recorded using a Datataker DT100F data logger, twelve ANSI type T thermocouples, and two Vaisala HMP 35 humidity and temperature probes. This experimental equipment is described in more detail in Appendix B. The software set-up and verification of the equipment is described in Appendix C.

The experiments were conducted in trailer PT279, used both for the transport of fresh produce between Melbourne and East Gippsland over night, and also for the distribution of produce around the Melbourne region during the day. The Datalogger data logger was installed in the front of the trailer beside the refrigeration unit outlet vent, and the thermocouples and RH sensors were run along the walls and taped firmly in place. The Datalogger and the thermocouple reference junction connector block were both in the refrigerated airstream. While it was likely that there would be some variation in temperature as the refrigerator was switched on and off, it was expected that there would be sufficient thermal equilibrium between the Datalogger case and the thermocouple reference junctions to provide reference junction temperature compensation and zero voltage compensation.

Twelve locations in the trailer were used to collect the temperature RH data. These were the upper-left, upper-right, lower-left, and lower-right corners for each of the rear, centre, and front sections of the trailer. As 12 thermocouples were available, all 12 locations were sampled during each temperature recording journey. However only two RH sensors were available, and the sensor locations were changed for each journey so that all 12 locations could be sampled. A total of 15 journeys were used to record temperature data. These were randomly selected from 33 consecutive working days over the months of June and July. The other 18 days in this 33 day period were used to record RH data. Hence each location in the trailer was sampled for temperature on 15 journeys and for RH on three journeys.

Each journey consisted of a 24 hr period, whether the trailer was in use (i.e. the measurements were of the normal refrigerated conditions) or backed up to the distribution centre docking bays (i.e. the measurements were of the ambient distribution centre conditions). Samples were taken every 3 min over this 24 hr period.

The results were then analysed and presented as confidence intervals for the mean temperature and RH at each location in the trailer.

4.2.2 Results And Discussion

4.2.2.1 Temperature

Analysis of the data collected after a few journeys revealed large fluctuations in the measurements between (i) different thermocouple locations, (ii) consecutive samples at the same location, and (iii) subsequent journeys at the same time and thermocouple location. The air temperature was found to fluctuate, with the range of measurements at any one location over a 60 min (20 samples) period generally being between 6°C and 10°C (i.e. a fluctuation about the hourly mean temperature of up to $\pm 5^\circ\text{C}$).

The nature of the test rig contributed partly to this variation, especially if the assumption of thermal equilibrium between the data logger case and the thermocouple reference junctions connector block was false. However if this assumption was false, it was expected that the error would more systematic than random, and so not contribute to the data variation. The remainder of the variation was probably due to the dynamic nature of the airflow through the trailer. Some factors identified as possibly affecting the airflow include: (i) the initial temperature and respiration of the load, (ii) the quantity and stacking pattern of the load, (iii) the airstream from the refrigeration unit and air delivery chute, and (iv) the condition of the trailer walls and insulation.

It was decided that due to this variation, the results for each individual journey were not suitable for presentation, so each of the 15 journeys were aggregated and presented together. The mean and 95% confidence interval for the individual air temperature data at each measurement location was then determined. The most effective method of presentation was found after fitting 5th order polynomial curves to smooth the raw data. These confidence intervals are shown in Figure 20 and Figure 21. The individual data points are not shown, as a total of 86,400 measurements were taken (12 samples every 3 min over 24 hr for 15 journeys).

Figure 20 shows the fitted 5th order polynomials for the mean air temperature, aggregated by the vertical and lateral position of the thermocouple in the trailer, (i.e. each of the four

plots is the aggregate of three sets of measurements from the rear, centre, and front of the trailer). It can be seen that overall there is little difference between the mean air temperatures at any of these locations. All of the air temperatures appear to follow the general pattern of ambient air temperature (highest temperature at around 3 PM and lowest at around 6 AM). In general, the 95% confidence interval for the individual data is approximately $\pm 3^{\circ}\text{C}$ around the mean.

Figure 21 shows similar information, except the mean air temperatures are aggregated for longitudinal location in the trailer (i.e. each is the aggregate of four sets of measurements). The overall air temperature profile is also shown, where this is an aggregate of all 12 sets of measurements (i.e. all 86,400 data points). Again there appears to be little difference between the mean air temperatures at any location, and the 95% confidence interval for the individual data is approximately $\pm 3^{\circ}\text{C}$ around the mean.

Figure 20: Mean and 95% confidence intervals for temperature by vertical and lateral position in trailer.

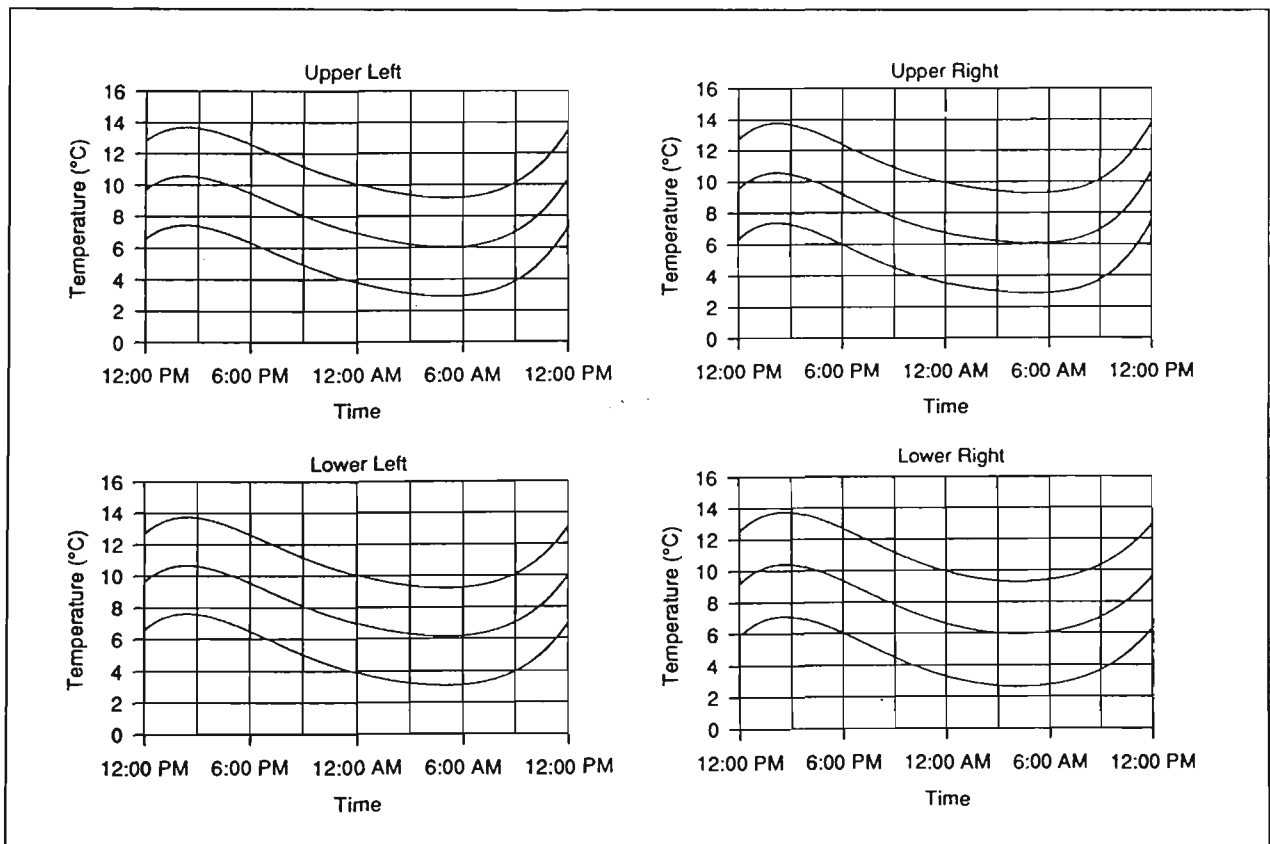
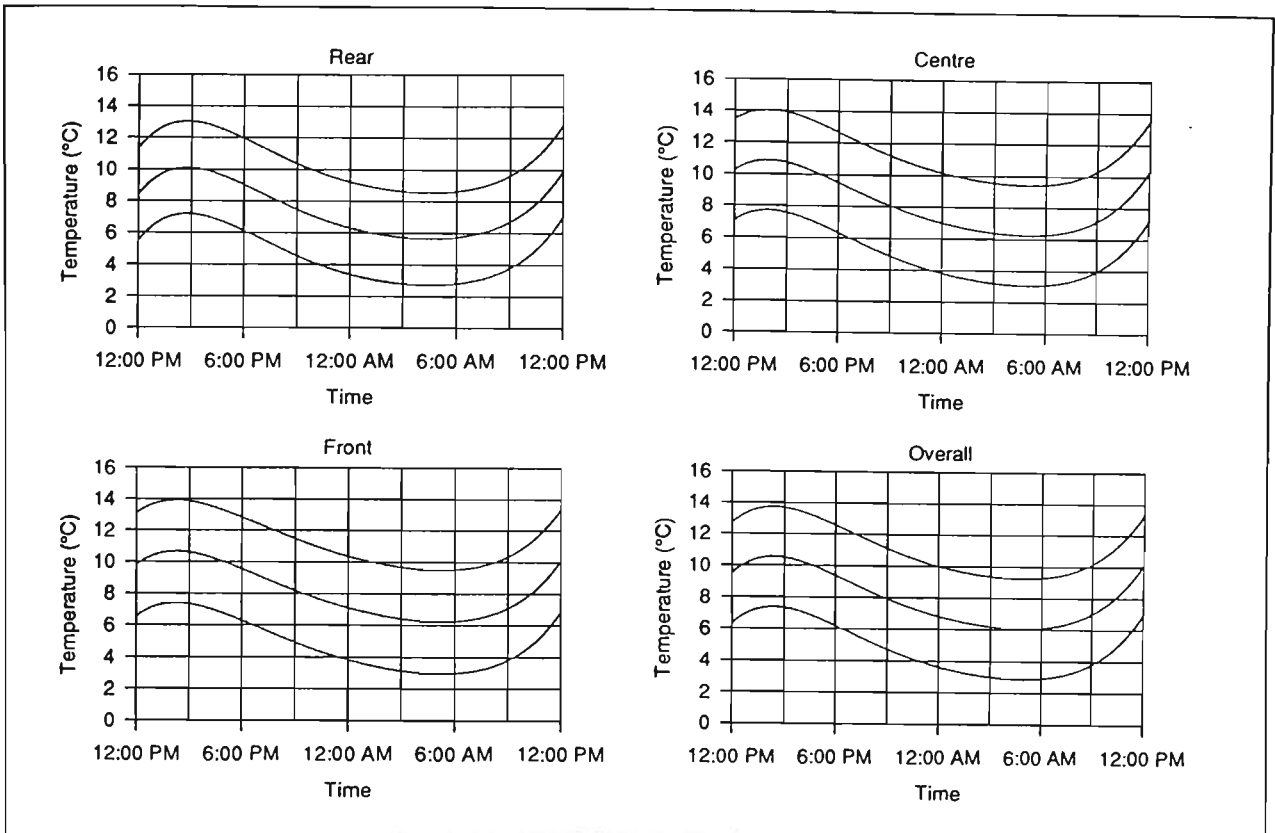


Figure 21: Mean and 95% confidence intervals for temperature by longitudinal position in trailer.



Generally, the air temperatures profiles shown above are all in excess of maximum recommendations for the shipment of non-tropical horticultural products (DPI&E/AQIS, 1990). The 95% confidence limit ranges of measured temperature at no time reached as low as 2°C, the recommended maximum. Not even at the coolest time of the day did the mean air temperature even approach the recommended maximum loading temperature, let alone the maximum carriage temperature. In addition, these measurements were taken in June and July, and are probably best case. Summer temperatures would further increase the demand on the trailer refrigeration unit. Furthermore, these measurements are for the air temperature only. The mean temperature of the load would be expected to be greater than the mean air temperature unless adequate precooling was performed.

Basic recommendations, such as (i) precooling of the load, (ii) precooling of the trailer, (iii) maintenance of thermal insulation, and (iv) efficient stowage of the load, did not, in general, appear to have been followed. Additionally, it was observed that several other trailers operating out of the same facility did not comply with recommendations for the air-return bulkhead and air delivery chute. However the use of only one trailer from one

facility, and the limited number of days during which measurement was undertaken, do not make these results necessarily representative of conditions in all refrigerated trailers. However they do further highlight the need to follow basic recommendations for the precooling and stowage of loads in order to achieve optimum temperature conditions.

4.2.2.2 Relative Humidity

Like the air temperature data, analysis of the RH data again revealed large fluctuations between measurements. The distribution of RH fluctuated, with the range of measurements at any one location over a 60 min (20 samples) period generally being between 15% and 30% (i.e. a fluctuation about the mean hourly RH of up to $\pm 15\%$).

The nature of the test rig was expected to contribute less error than for the air temperature measurements, since the voltage output of the RH probes were not as dependent on temperature. This is reflected in that the variation of the results were generally closer to the expected error ($\pm 10\%$ at the 95% level of confidence) than for the air temperature measurements ($\pm 2^\circ\text{C}$ at the 95% level of confidence). Again, the remainder of the variation was probably due to transpiration of the produce, and the dynamic nature of the airflow through the trailer.

Despite the fluctuation of the RH measurements being less than for the air temperature measurements, it was again decided to present aggregated results for the 18 journeys. The mean and 95% confidence interval for the individual RH data at each measurement location was then determined. The most effective method of presentation was found after fitting 5th order polynomial curves to smooth the raw data. These confidence intervals are shown below in Figure 22 and Figure 23. The individual data points are not shown, as a total of 17,280 measurements were taken (2 samples every 3 min over 24 hr for 18 journeys).

Figure 22 shows the fitted 5th order polynomials for the mean RH, aggregated by the vertical and lateral position of the RH probe in the trailer, (i.e. each of the four plots is the aggregate of three sets of measurements from the rear, centre, and front of the trailer). It

can be seen that overall there is little difference between the mean RH at any of these locations. All of the RHs appear to follow the general pattern of ambient RH (highest at around 6 AM and lowest at around 3 PM). In general, the 95% confidence interval for the individual data is approximately $\pm 12\%$ around the mean. It must also be remembered that the statistics of RH measurement are unusual in that RH can never exceed 100%. This suggests a skewness of the samples with means close to 100%, and a difficulty in calculating the upper bands as drawn.

Figure 23 shows similar information, except the mean RHs are aggregated for longitudinal location in the trailer (i.e. each is the aggregate of four sets of measurements). The overall RH profile is also shown, where this is an aggregate of all 12 sets of measurements (i.e. all 17,280 data points). Again there appears to be little difference between the mean RH at any location, and the 95% confidence interval for the individual data is approximately $\pm 12\%$ around the mean.

Figure 22: Mean and 95% confidence intervals for relative humidity by vertical and lateral position in trailer.

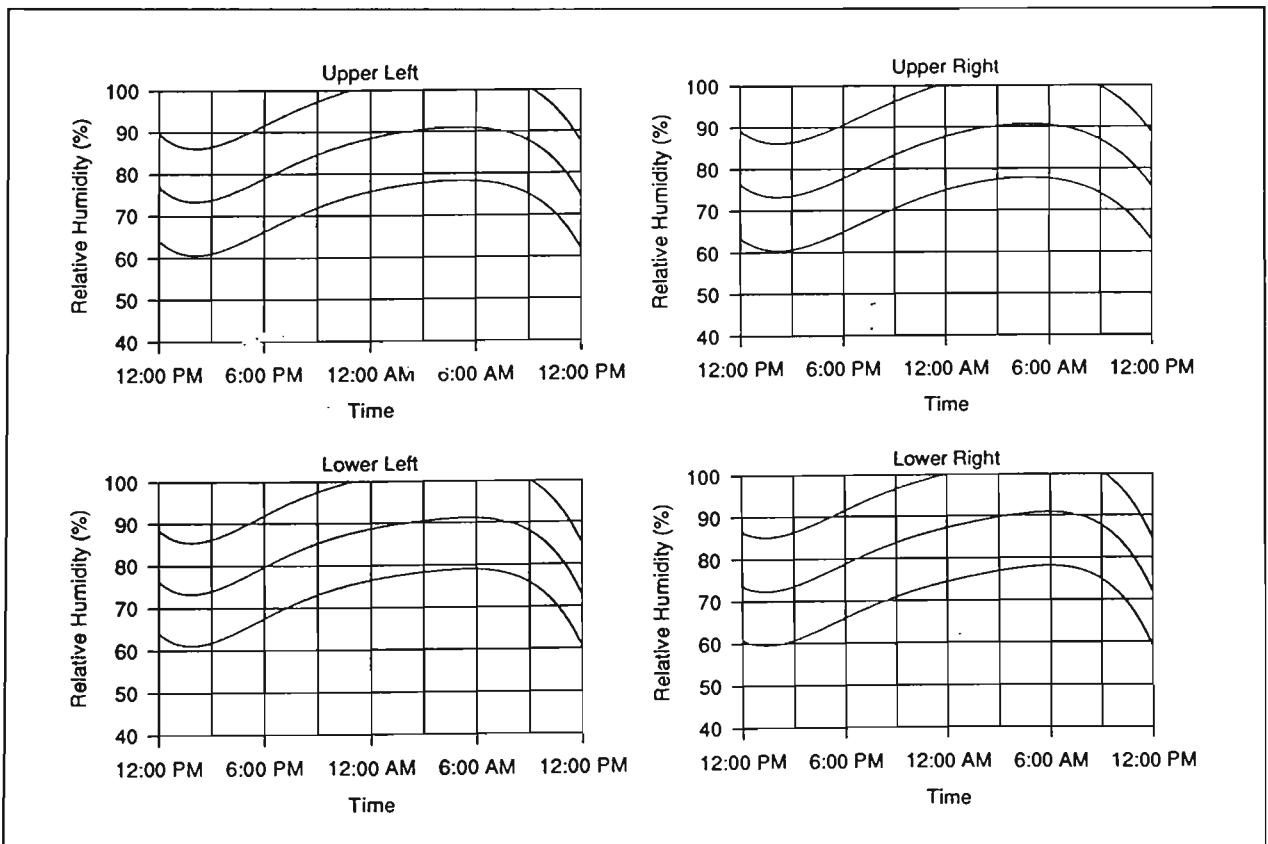
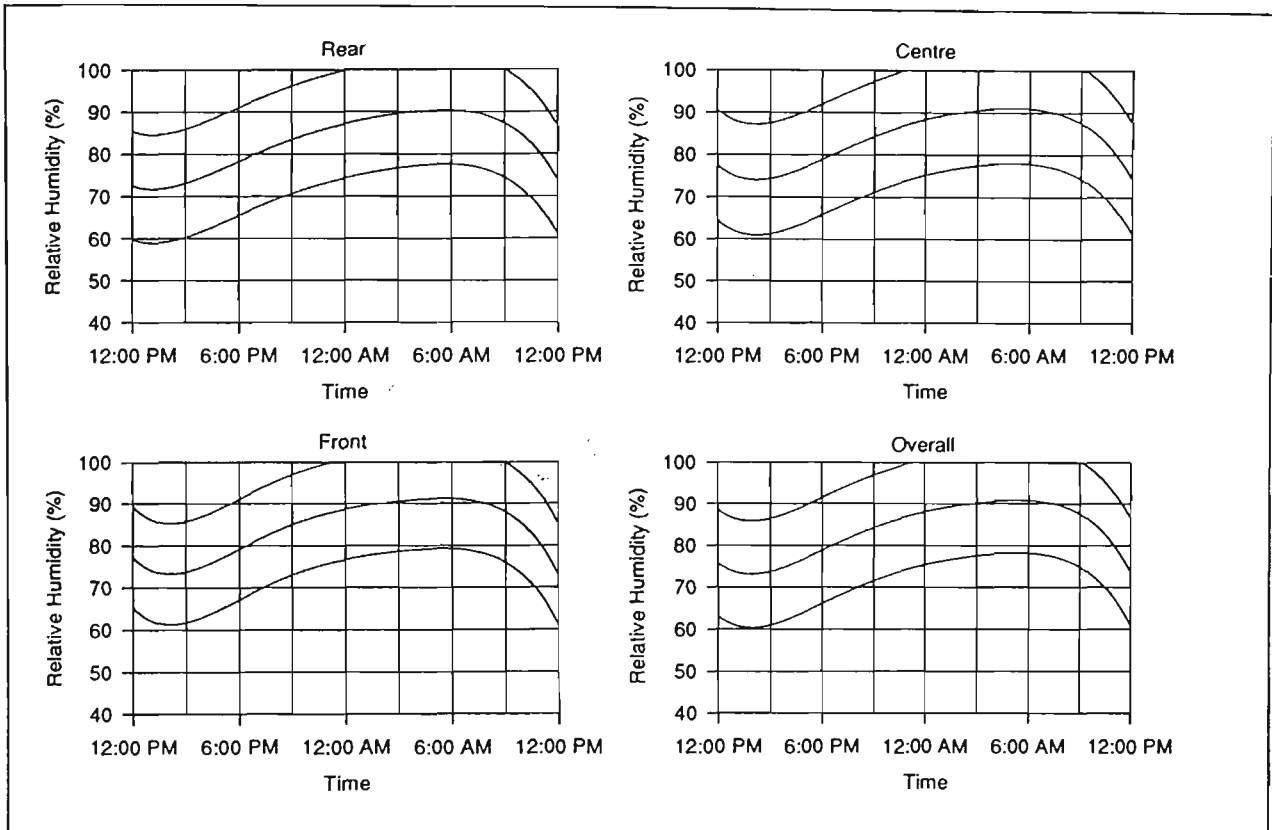


Figure 23: Mean and 95% confidence intervals for relative humidity by longitudinal position in trailer.



Generally, the RH profiles shown above are below minimum recommendations for the shipment of horticultural products (Langbridge, 1983). The mean RH exceeded the recommended minimum of 90% for only around 6 hr, and the mean RH was below 80% for at least 6 hr. However, for all but 6 hr of the day, the recommended minimum RH of 90% was within the 95% confidence limits for the individual data. In addition, the RH measurements seem higher than those observed by Sharp (1993), although again the time of the year in which these measurements were taken could have had some influence as RH is generally greatest during May to July (Kirkpatrick, 1989).

The basic recommendations for temperature management are also important for RH management, as the RH of the delivery airstream depends on the refrigeration load. Moisture from packaging materials and produce transpiration also tend to increase the RH. Again these results highlight the need to ensure optimum precooling of the load and trailer.

4.3 MANUAL AND MECHANICAL HANDLING

These experiments consisted of obtaining typical impact profiles of the fresh produce handling environment around the Melbourne and East Gippsland regions of Victoria. The experiments were conducted using an IST model EDR-3 Environmental Data Recorder together with the EDR1S operating software package. The EDR was either attached to the side of the pallet for handling by forklift, or placed inside a filled corrugated fibreboard box for manual handling.

There were two main objectives to these experiments:

1. To obtain the distributions of peak acceleration, duration, and velocity change for a typical produce package handling environment.
2. To obtain the distributions of equivalent drop height and drop impact direction for a typical produce package handling environment.

4.3.1 Methodology

Manual and mechanical handling operations occur at various stages of any fresh produce distribution system. Typically these operations include packing, loading, unloading, palletisation, depalletisation, and transfer points of the distribution system. Unlike distribution systems for many other products and commodities, fresh produce distribution systems are generally not well defined. The various elements of the distribution system are usually determined independently of each other, and these distribution elements often change daily, depending on, for example, the quantity and availability of produce, and the compatibility of the produce mix (Leng, 1994).

While such a system has several advantages, one major disadvantage is that it is difficult to clearly determine the handling operations that produce will be subjected to during distribution. As a result, a large number of measurements, well beyond the scope of this project, would be required to completely define the forces to which produce packages would likely be subjected to during distribution. For this reason, it was decided to study a

few typical handling operations in detail, rather than many handling operations in less detail.

These handling measurements were undertaken at Costa's Wholesale Fruit and Vegetable Distribution Centre in Sunshine, Victoria. In this distribution centre, the produce is received in unit loads from the grower at the loading docks in the morning, unloaded with a forklift, and racked, either in the main racking area or in one of several coolrooms. In the early afternoon, the orders for each supermarket are made up by 'picking' individual boxes or tubs from the racks and placing them on mixed pallets. During picking, each pallet takes approximately 10 min to make up. The completed pallets are then placed in the storage areas adjacent to the dispatch docks, where they are loaded into trucks and distributed to supermarkets in the late afternoon.

The experiments were conducted using an IST model EDR-3 Environmental Data Recorder together with the EDR1S operating software package. This experimental equipment is described in more detail in Appendix B. The software set-up and verification of the equipment is described in Appendix C.

Initially, all handling of the produce was divided into 10 discrete operations, each of which was to be measured several times. After the first sets of measurements were made, it was observed that there were no differences between many of these operations. Subsequently it was decided to divide the handling into only two main operations, 'unloading' and 'loading', and to make several sets of measurements of each operation.

The unloading operation consisted of all operations from the time the pallet or bulk bin was unloaded from the grower's truck to the time it was racked in the distribution centre, either in the main storage area or in a coolroom. After racking, the pallet or bin was removed from the rack and lowered, so that the EDR unit could be removed. Five sets of unloading measurements were made, which considered a variety of forklifts, drivers, load weights, rack heights, and distances and times of travel. All other variables, such as speed, were kept as close as possible to normal conditions. The duration of these measurements varied from about 30 s to about 2 min.

The loading operations consisted of all operations from the time the pallet or bin was removed from the rack, or the time a box was removed from the racked pallet and manually placed on the mixed pallet being made up, to the time the pallet was placed into the trailer. However, rather than remaining in the storage area for a length of time as usual, the pallet was instead dropped, picked up again, and then immediately placed into the trailer. This was in order to save time during the measurements. In addition, some pallets had to be moved round in the trailer after final placing in order to facilitate the removal of the EDR unit. Five sets of loading measurements were made, which considered the same variables as for the unloading measurements above.

Approximately half of the unloading and loading measurements were made with the EDR mounted directly onto the pallet. The other measurements were made with the EDR placed inside a box on the top of the pallet. There appeared to be no difference between measurements made inside the boxes and measurements made on the pallet, so both sets of results were combined for these analyses. This was unexpected, as manual handling of individual boxes is reported to be more severe than mechanical handling of unit loads. The act of observation and measurement may have had an influence on the behaviour of the workers involved.

The results were processed using the EDRIS software package, and analysed and presented in two ways: (i) the distributions of peak acceleration, duration, and velocity change for each shock event, and (ii) the distributions of equivalent drop height and drop direction.

4.3.2 Results And Discussion

4.3.2.1 Peak Acceleration, Duration, and Velocity Change Distributions

Table 19 and Figure 24 show the shock event peak acceleration distributions for the unloading and loading handling operations. In the unloading operations, the majority of shock events had a peak acceleration less than 1 g, with only 7% greater than 3 g. Only

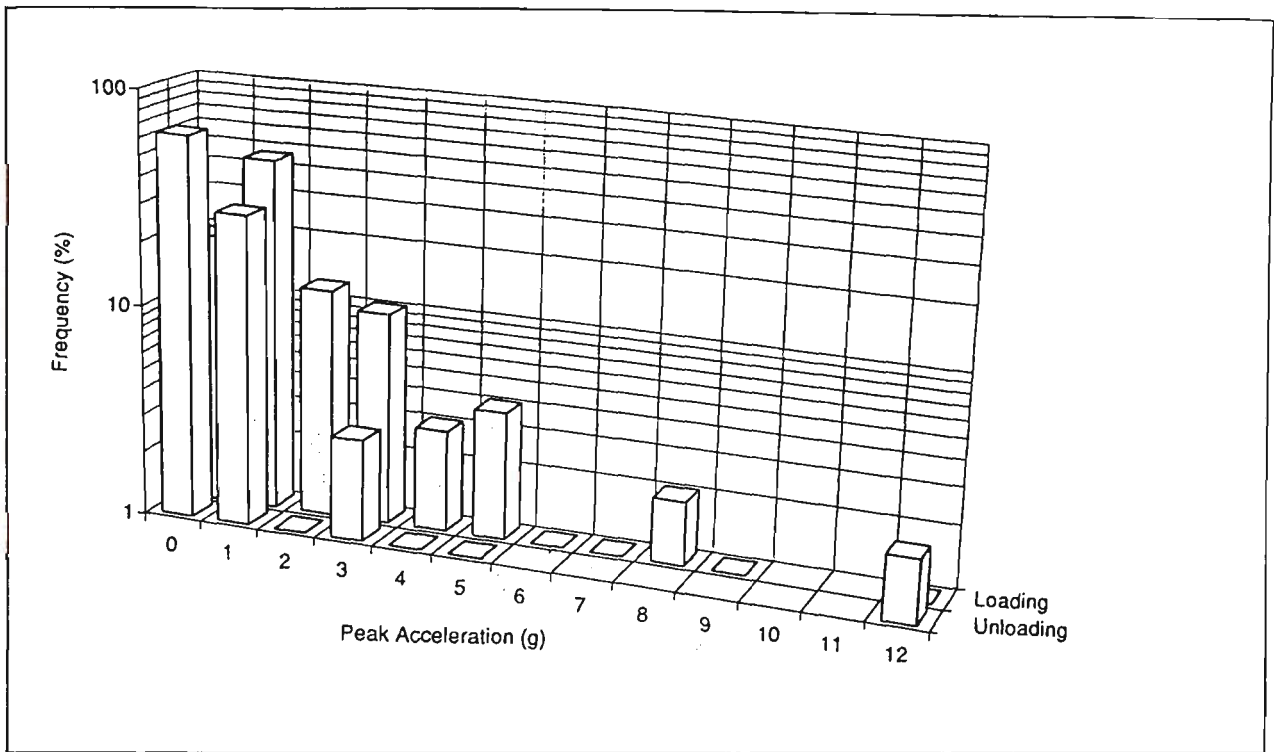
2% of the events had a peak acceleration greater than 6 g, all of which were greater than 12 g, and the maximum was 16 g. In contrast, the loading operations had 23% of shock events greater than 3 g, and 2% greater than 9 g, with the highest being 16 g. From these results it appears that unloading operations generally result in lower peak accelerations than loading operations, although the maximum peak acceleration was the same in both cases.

Table 19: Shock event peak acceleration distributions.

Handling Operation:	Unloading	Loading
Peak Accel. (g)	Frequency (%)	Frequency (%)
0	63	19
1	29	46
2	1	12
3	3	10
4	1	3
5	1	4
6	0	1
7	0	1
8	0	2
9	0	1
10	0	0
11	0	0
> 12	2	1
Count:	500	500
Maximum (g):	15.92	15.82

Note: All percentages are rounded up to the nearest integer.

Figure 24: Shock event peak acceleration distributions.



Note: All percentages are rounded up to the nearest integer.

Table 20 and Figure 25 show the shock event duration distributions for the unloading and loading handling operations. Not all events are represented, as the majority of events in both cases had durations which were equal to the event length (i.e. 400 ms). This was because the peak acceleration of the event was so low that the duration threshold (i.e. 10% of the peak acceleration) was less than the normal fluctuation of the trailing and leading edges of the waveform, and the EDR could not determine where the shock pulse began and ended in the waveform. These events were disregarded for all further analyses involving event duration.

The unloading operation events had low shock durations, with the highest being about 40 ms. The loading operation events had higher shock durations than the unloading operations, with the maximum being about 70 ms.

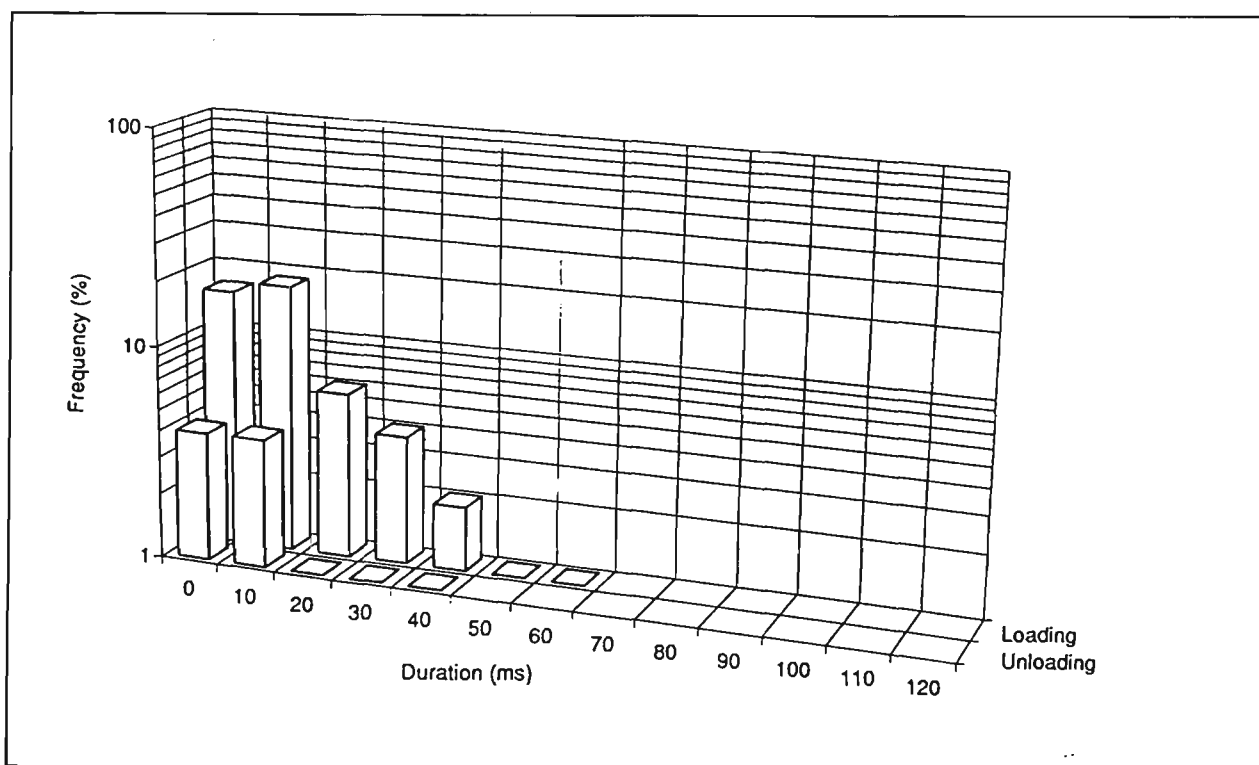
Table 20: Shock event duration distributions.

Handling Operation:	Unloading	Loading
Duration (ms)	Frequency (%)	Frequency (%)
0	4	16
10	4	18
20	1	6
30	1	4
40	1	2
50	0	1
60	0	1
70	0	0
80	0	0
90	0	0
100	0	0
110	0	0
> 120	0	0
Count:	11	48
Maximum (ms):	45	65

Notes: (1) All percentages are rounded up to the nearest integer.

(2) Percentages do not add up to 100% as durations equal to the event length are omitted.

Figure 25: Shock event duration distributions.



Notes: (1) All percentages are rounded up to the nearest integer.

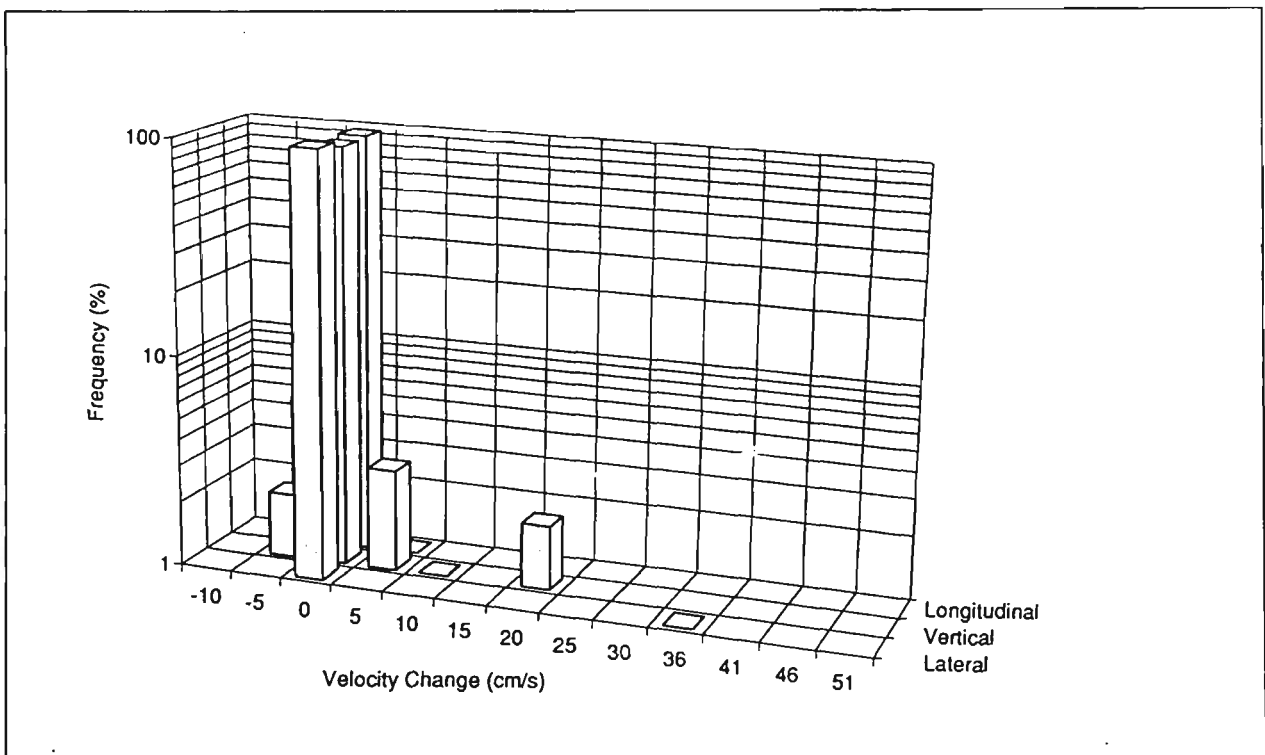
(2) Percentages do not add up to 100% as durations equal to the event length are omitted.

Figure 26 and Figure 27 show the shock event velocity change distributions for the unloading operations and loading operations respectively. Each series in the graphs refers to each of the EDR axes, where the lateral axis is side-to-side movement (relative to the

forklift direction), vertical is up-and-down movement, and longitudinal is forward-backward movement. The positive and negative signs of velocity change refer to the direction of movement along each axis. The sign directions are arbitrarily chosen and not important for this analysis. The histogram bins in these Figures are in intervals of 2 in/s, as the resolution of the EDR is 1 in/s.

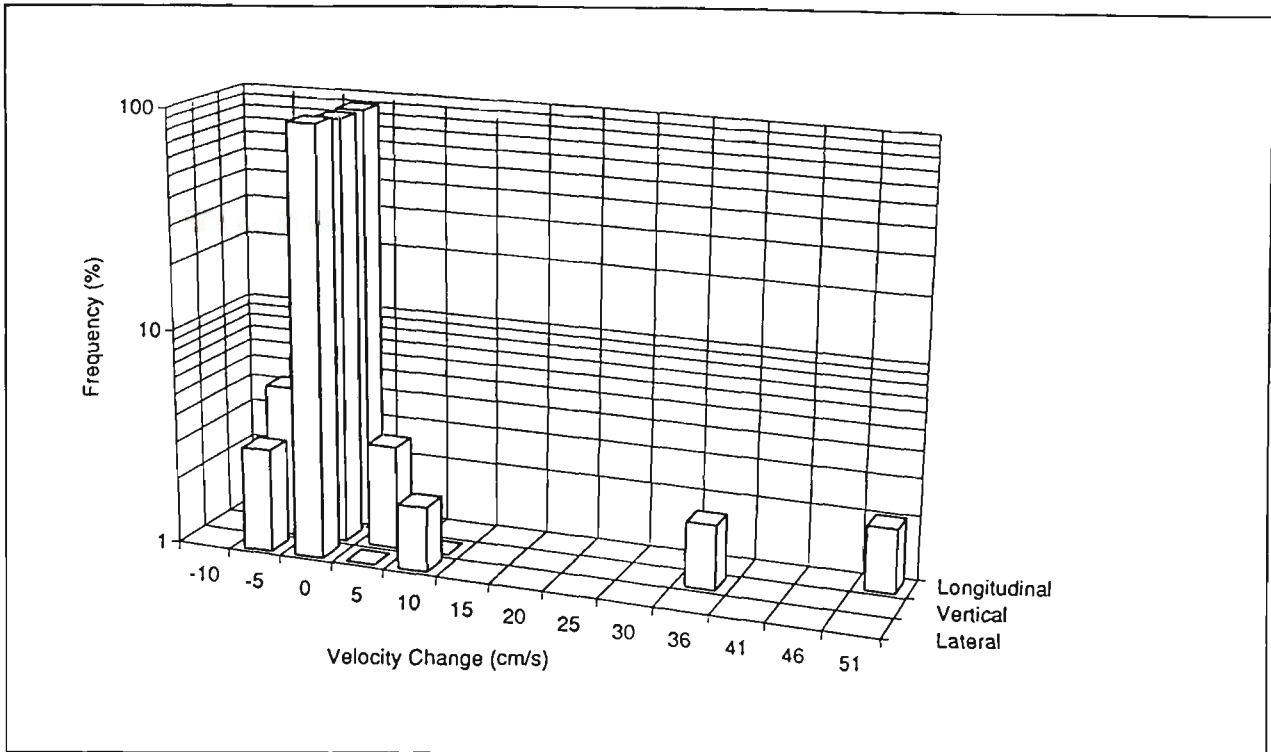
It can be seen that the large majority of events for all axes have velocity changes less than 5 cm/s (absolute), with few event velocity changes greater than 10 cm/s, for both the unloading and loading operations. The largest velocity changes for the unloading operations were recorded on the lateral axis, followed by the vertical axis. The largest velocity changes for the loading operations were recorded on the longitudinal axis, followed by the vertical axis. In general, higher velocity changes were recorded on the loading operations than on the unloading operations.

Figure 26: Shock event velocity change distributions: Unloading operations.



Note: Histogram bins for velocity change are in intervals of 2 in/s.

Figure 27: Shock event velocity change distributions: Loading operations.



Note: Histogram bins for velocity change are in intervals of 2 in/s.

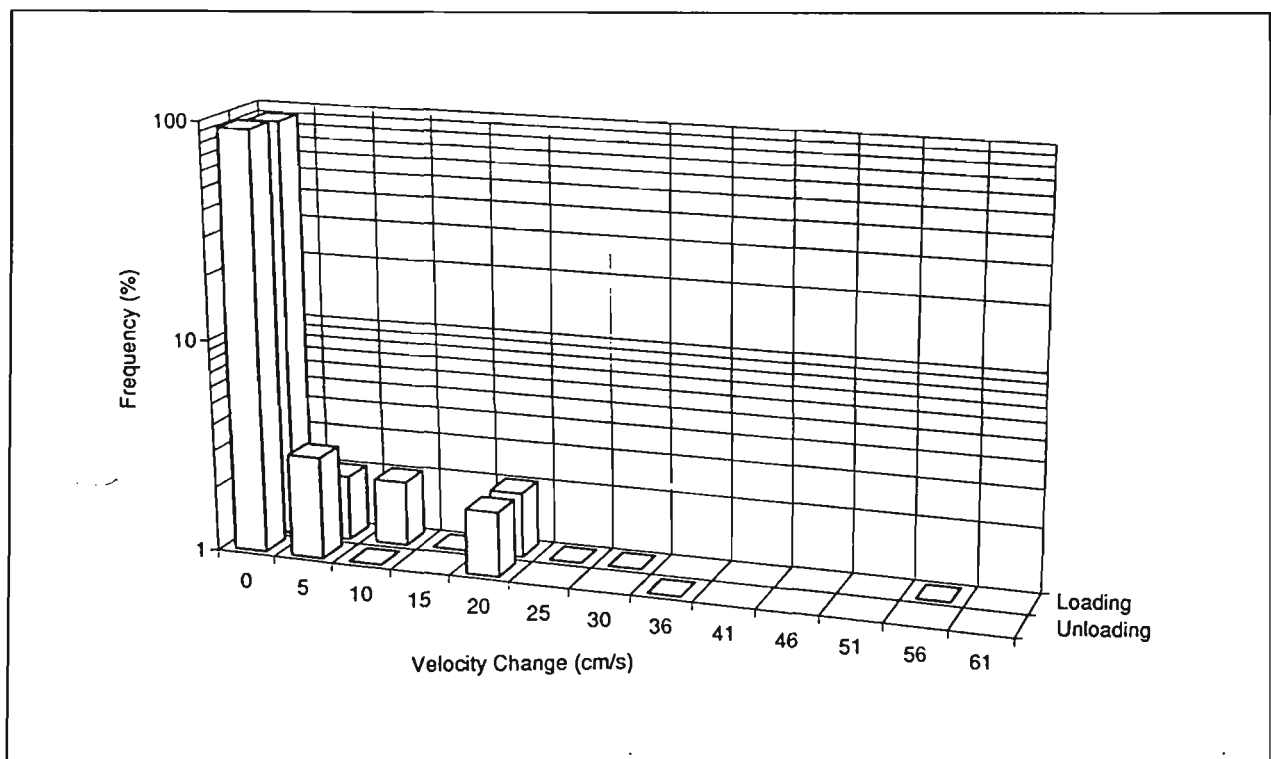
Table 21 and Figure 28 show the shock event resultant velocity change distributions for the handling operations. The resultant velocity changes are calculated from the individual axis velocity changes by Equation (C.1). It can be seen that the resultant velocity change distributions are similar for both sets of handling operations, with a 3% difference in the interval 0-5 cm/s, and about a 1% difference at most other velocity change intervals. The maximum recorded resultant velocity changes were 38 and 58 cm/s for the unloading and loading operations respectively. Using Equation (2.15), and assuming a worst-case coefficient of restitution of zero, the EDH for a velocity change of 58 cm/s is only 2 cm, which is less than the drop height calculation resolution of the EDR (i.e. 1 in).

Table 21: Shock event velocity change distributions: Resultant of all directions.

Handling Operation:	Unloading	Loading
Velocity Change (cm/s)	Frequency (%)	Frequency (%)
0	93	90
5	3	2
10	1	2
15	0	1
20	2	2
25	0	1
30	0	1
36	1	0
41	0	0
46	0	0
51	0	0
56	0	1
> 61	0	0
Count:	500	500
Maximum (cm/s):	38	58

Notes: (1) Histogram bins for velocity change are in intervals of 2 in/s.
 (2) All percentages are rounded up to the nearest integer.

Figure 28: Shock event velocity change distributions: Resultant of all directions.



Notes: (1) Histogram bins for velocity change are in intervals of 2 in/s.
 (2) All percentages are rounded up to the nearest integer.

The distributions of peak acceleration and velocity change for each handling impact have been plotted against each other in Figure 29, for the unloading operations, and Figure 30,

for the loading operations. As with the transport shock and vibration study, these plots are referred to here as environmental damage potential plots.

Figure 29: Environmental damage potential plot: Unloading operations.

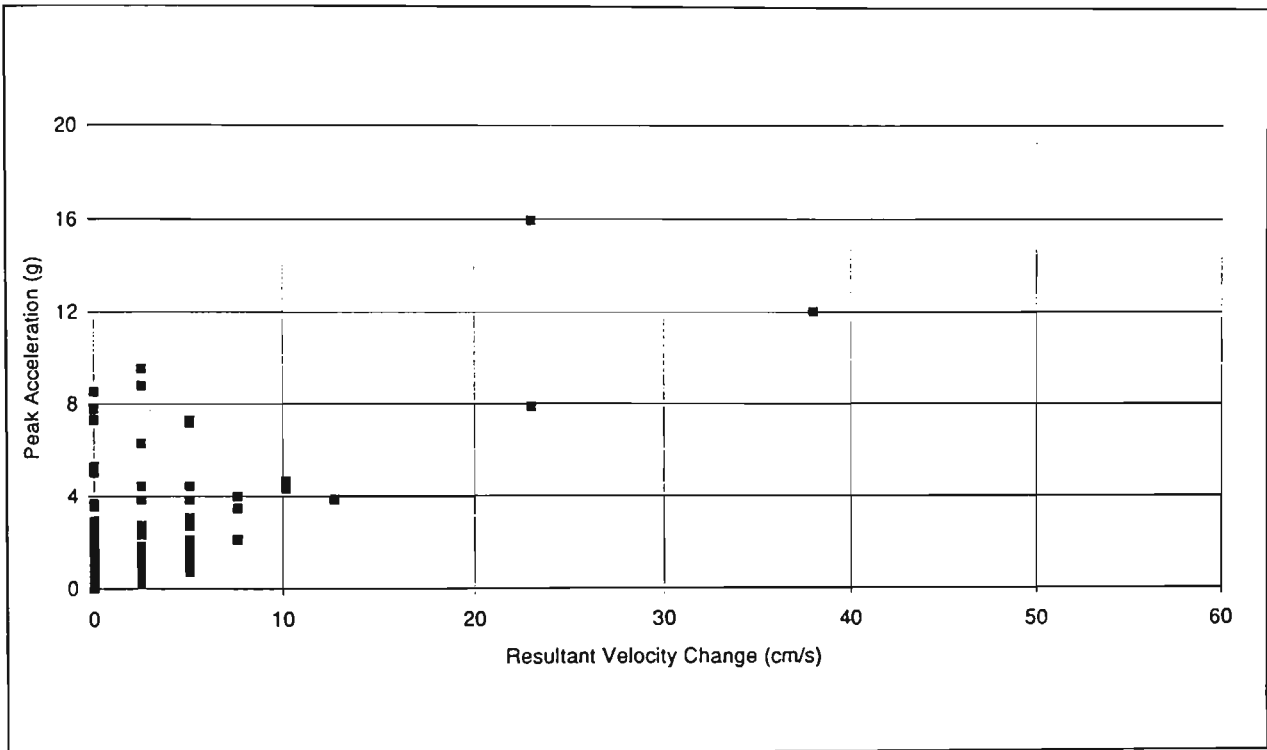
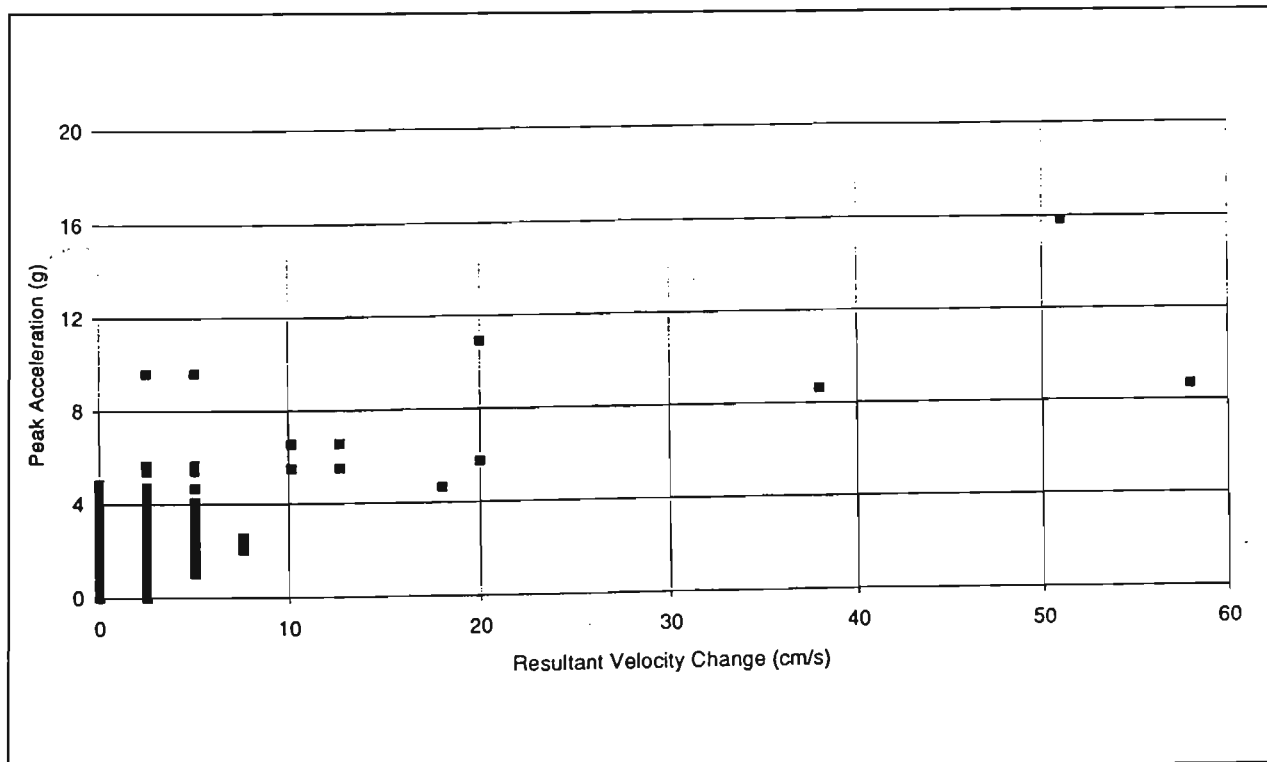


Figure 30: Environmental damage potential plot: Loading operations.



As these environmental damage potential plots indicate, the loading operations appear to be more severe than the corresponding unloading operations. This is probably due to the large impacts the pallets receive when being loaded over ramps into the trailers at the dispatch area. In both cases, the majority of data points are within about 8 g and 10 cm/s. The loading operations recorded more data points outside this range, but more points were recorded overall for loading operations as the unloading operations had many recorded events with durations equal to the event length. However it appears that both the loading and unloading operations are less severe than shocks in the transport environment.

4.3.2.2 Equivalent Drop Height and Direction Distributions

The impact direction distributions for the handling operations are shown in Table 22, Figure 31, Figure 32, and Figure 33. The directions of impact are obtained using the component velocity changes along each of the three axes in the EDR. The directions of impact shown are relative to the forklift driver, so that left and right are the driver's left and right when driving forward, front is the side of the pallet or box closest to the forklift mast, and back is the side furthest from the forklift mast. For example, an impact to the bottom would result from a free-fall drop, and an impact on the back would result from the forklift driving forwards into a wall.

The impacts are further classified into the type of impact, namely flat drops, edge drops, and corner drops. An impact is termed a flat drop if the velocity change along any one of the three axes exceeds 90% of ΔV_R , an edge drop if the velocity change along any two of the three axes exceeds 95% of ΔV_R , and a corner drop if it is neither a flat drop nor an edge drop. The impact direction is then determined by the direction in which the greatest velocity change occurred during the event.

Table 22 shows the impact direction distribution for all drops. It can be seen that the approximate proportions of flat drops, edge drops, and corner drops were 40%, 40%, and 20% respectively.

Table 22: Shock event impact direction distribution summary.

Flat Drops Direction	Frequency (%)		Edge Drops Direction	Frequency (%)		Corner Drops Direction	Frequency (%)	
	Unload	Load		Unload	Load		Unload	Load
Left	0.8	2.4	Le-Fr	1.0	3.2	Le-Fr-To	2.4	1.4
Right	1.8	10.8	Le-Ba	0	0	Le-Fr-Bo	2.6	2.0
Front	9.2	1.2	Le-To	0	4.6	Le-Ba-To	1.6	0
Back	6.4	2.8	Le-Bo	4.2	4.2	Le-Ba-Bo	2.2	3.8
Top	2.8	1.2	Ri-Fr	0.8	3.4	Ri-Fr-To	0.8	2.6
Bottom	20.4	21.0	Ri-Ba	0	5.8	Ri-Fr-Bo	10.2	2.8
			Ri-To	0	4.6	Ri-Ba-To	0	0.8
			Ri-Bo	5.6	12.2	Ri-Ba-Bo	1.4	0.6
			Fr-To	3.6	0			
			Fr-Bo	15.4	1.2			
			Ba-To	1.4	0			
			Ba-Bo	5.4	7.4			
Total	41.4	39.4	Total	37.4	46.6	Total	21.2	14.0

Note: Le = left, Ri = right, Fr = front, Ba = back, To = top, Bo = bottom.

Figure 31, Figure 32, and Figure 33 illustrate the impact direction distributions by drop type.

Figure 31: Shock event impact direction distribution: Face impacts.

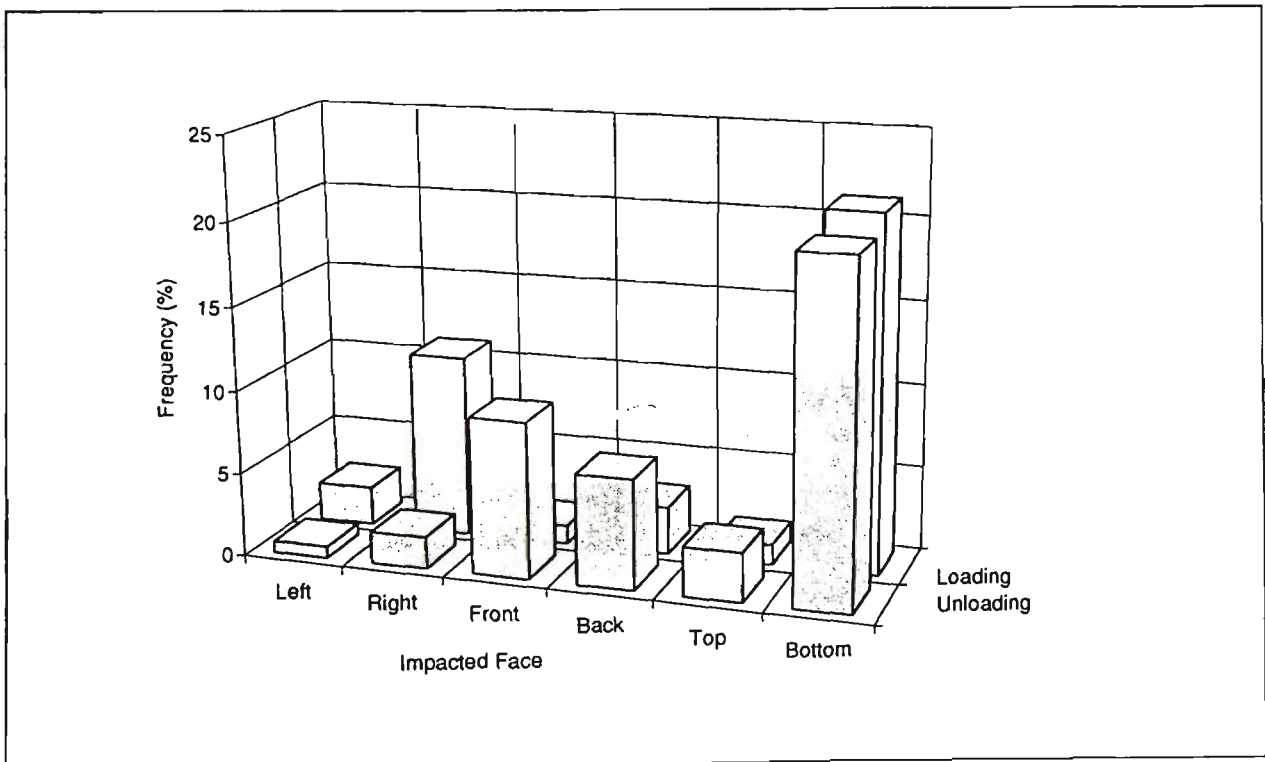
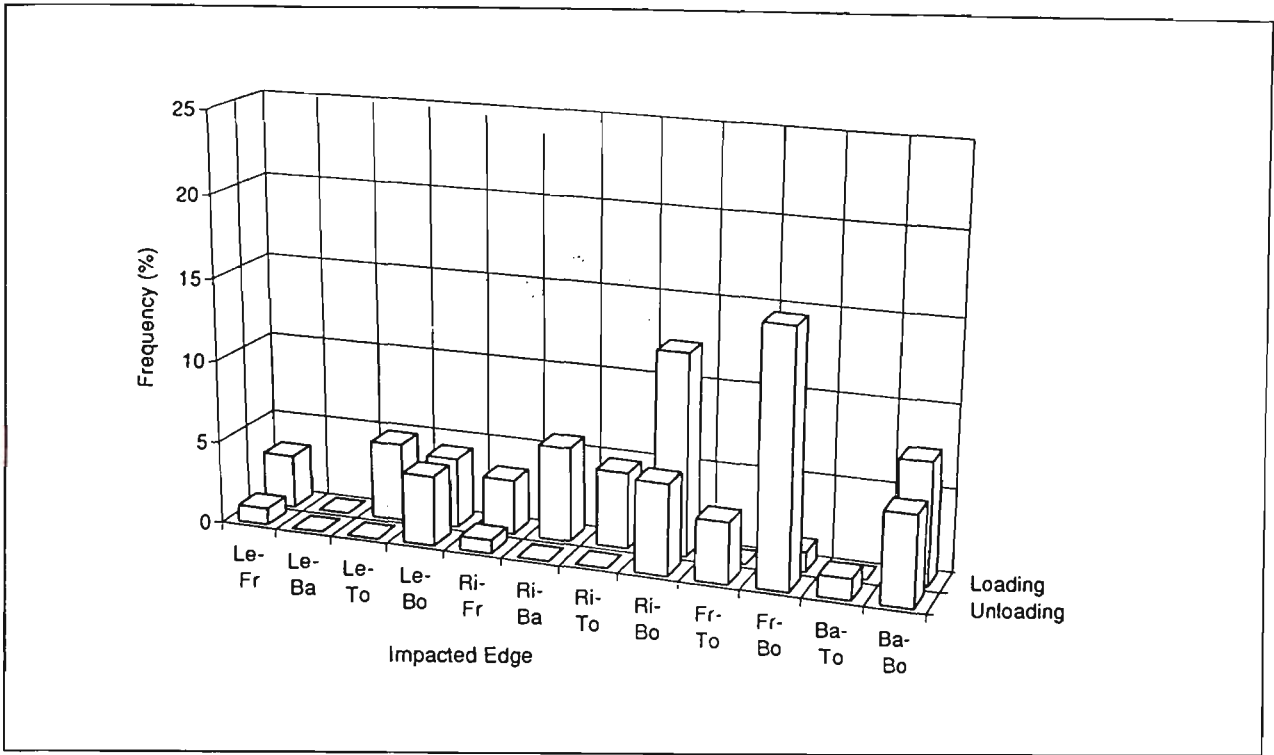
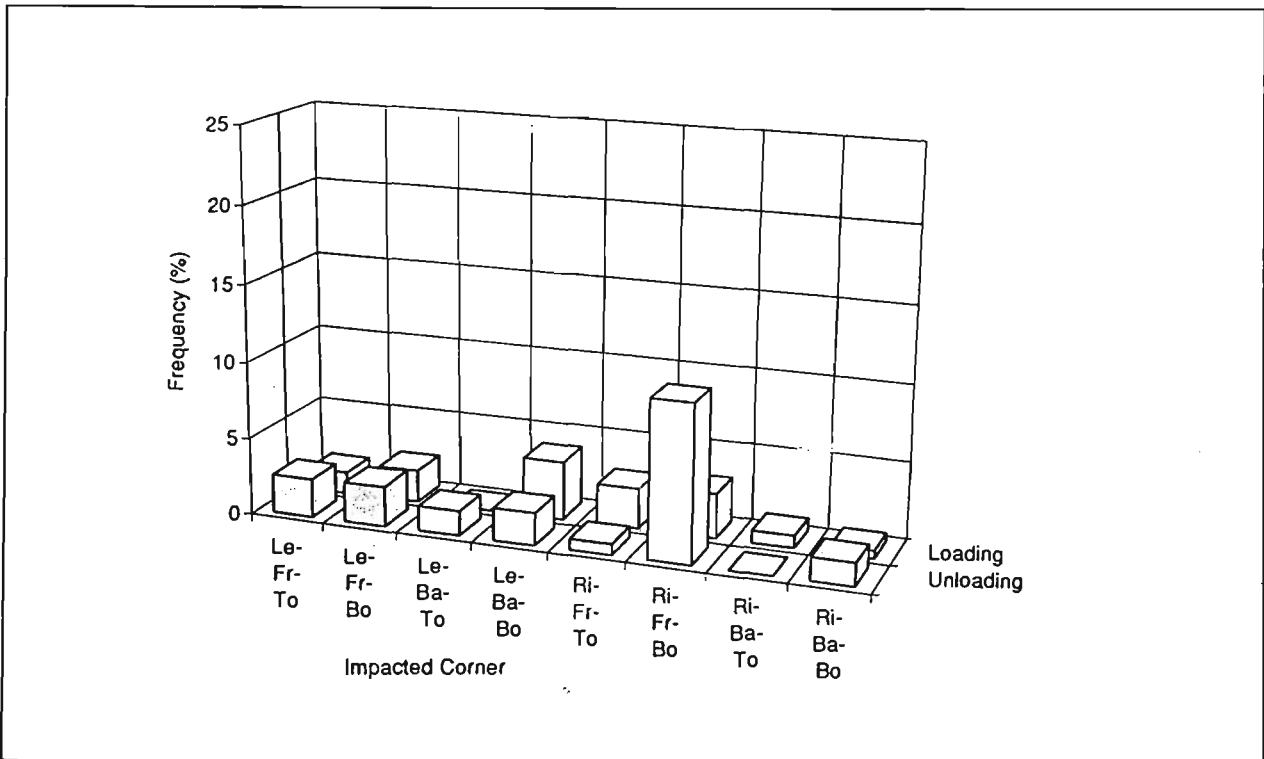


Figure 32: Shock event impact direction distribution: Edge impacts.



Note: Le = left, Ri = right, Fr = front, Ba = back, To = top, Bo = bottom.

Figure 33: Shock event impact direction distribution: Corner impacts.



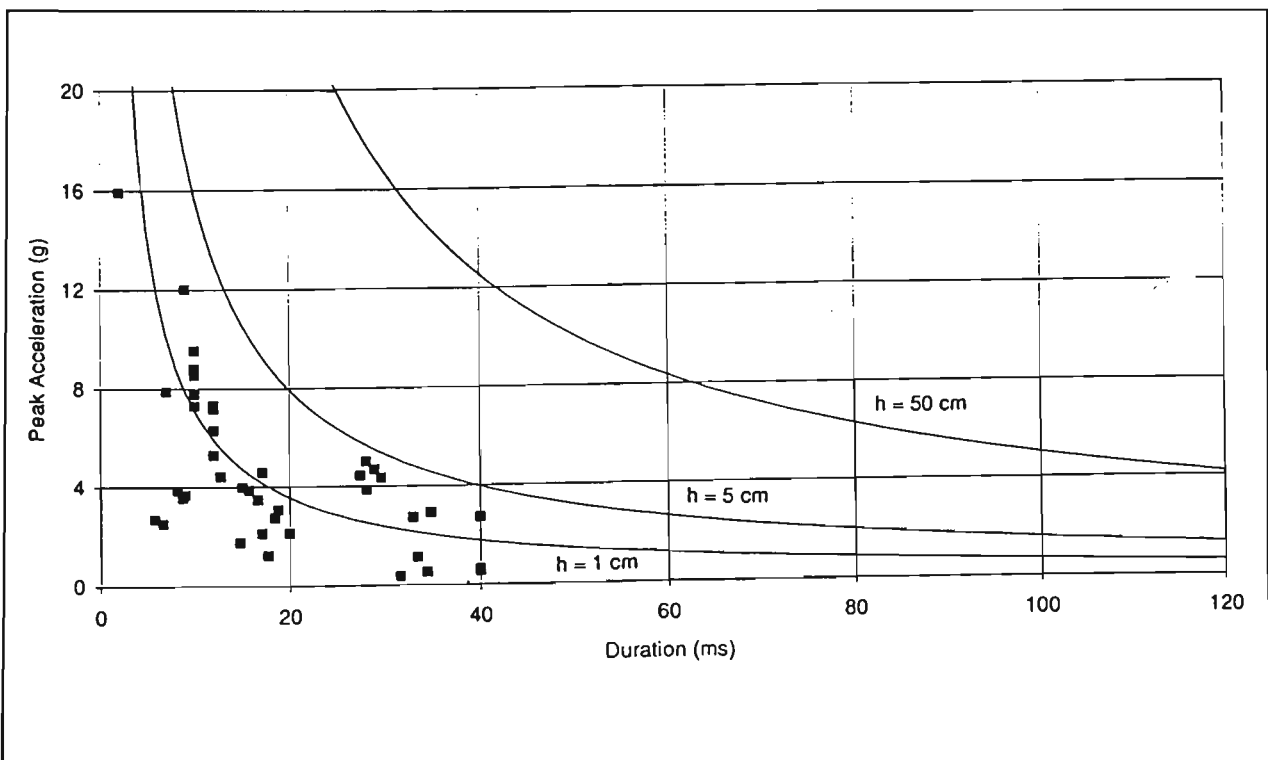
Note: Le = left, Ri = right, Fr = front, Ba = back, To = top, Bo = bottom.

It can be seen that the majority of handling impacts occurred to the bottom of the pallet, with the front and right sides also having large numbers of impacts. Impacts to the bottom of the pallet probably arose from the pallet being dropped or placed on the ground or shelf,

or from severe bumps, such as those recorded as the pallet was being loaded into the truck. Impacts to the front of the pallet would probably have resulted from the forklift contacting the pallet before lifting.

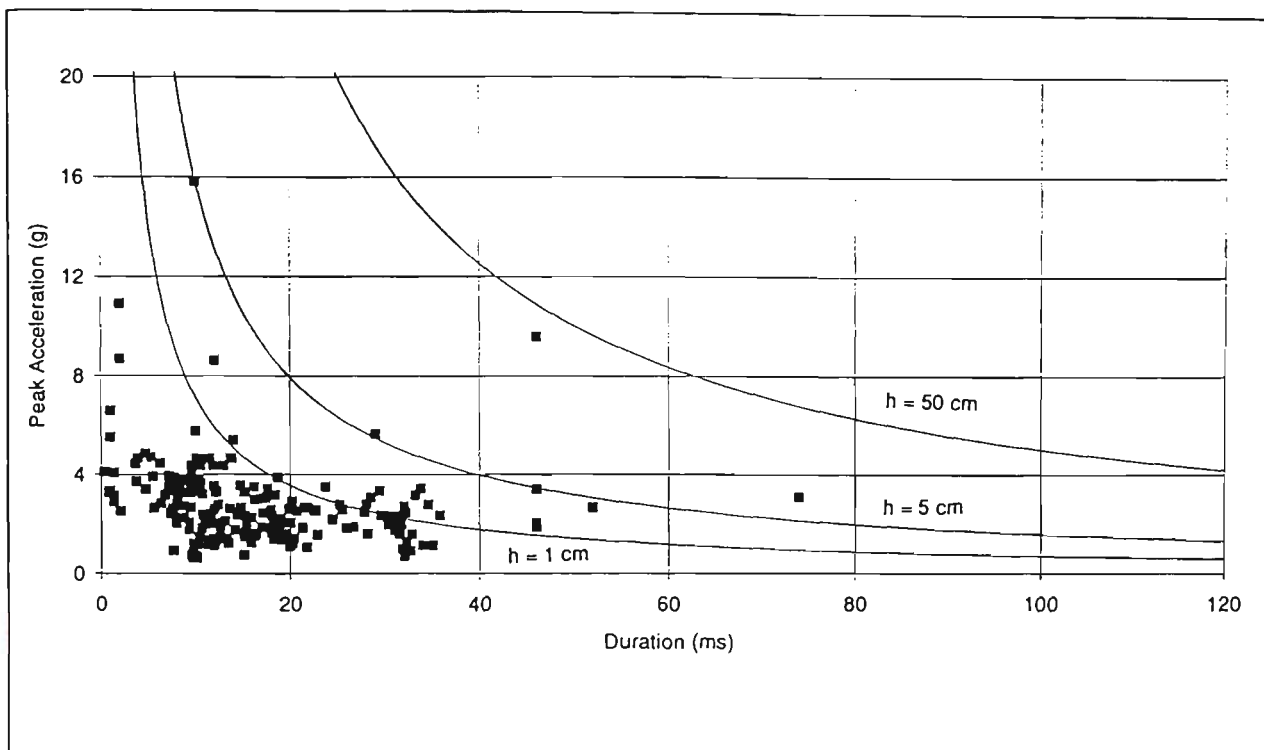
Figure 34 and Figure 35 show the calculation of EDHs for the unloading and loading operations respectively. These EDHs are calculated from the recorded peak acceleration and duration for each event, with the assumption that the waveform has a half-sine shape, as calculated from Equations (2.8) and (2.15). This method was found to be accurate when verifying the EDR set-up (as described in Appendix C). The curves in these Figures refer to the corresponding equivalent drops heights of 1, 5, and 50 cm. It can be seen that for the unloading operations, all of the events have EDHs less than 5 cm, with the maximum being 4 cm. The loading operations have several events with EDHs greater than 5 cm, with the maximum being 39 cm. More data points are plotted for the loading operations than for the unloading operations, as events with durations equal to the length of the event were not considered for analysis.

Figure 34: Calculation of equivalent drop height for half-sine waveform: Unloading operations.



Note: All data points are not shown as durations equal to the event length are omitted.

Figure 35: Calculation of equivalent drop height for half-sine waveform: Loading operations.



Note: All data points are not shown as durations equal to the event length are omitted.

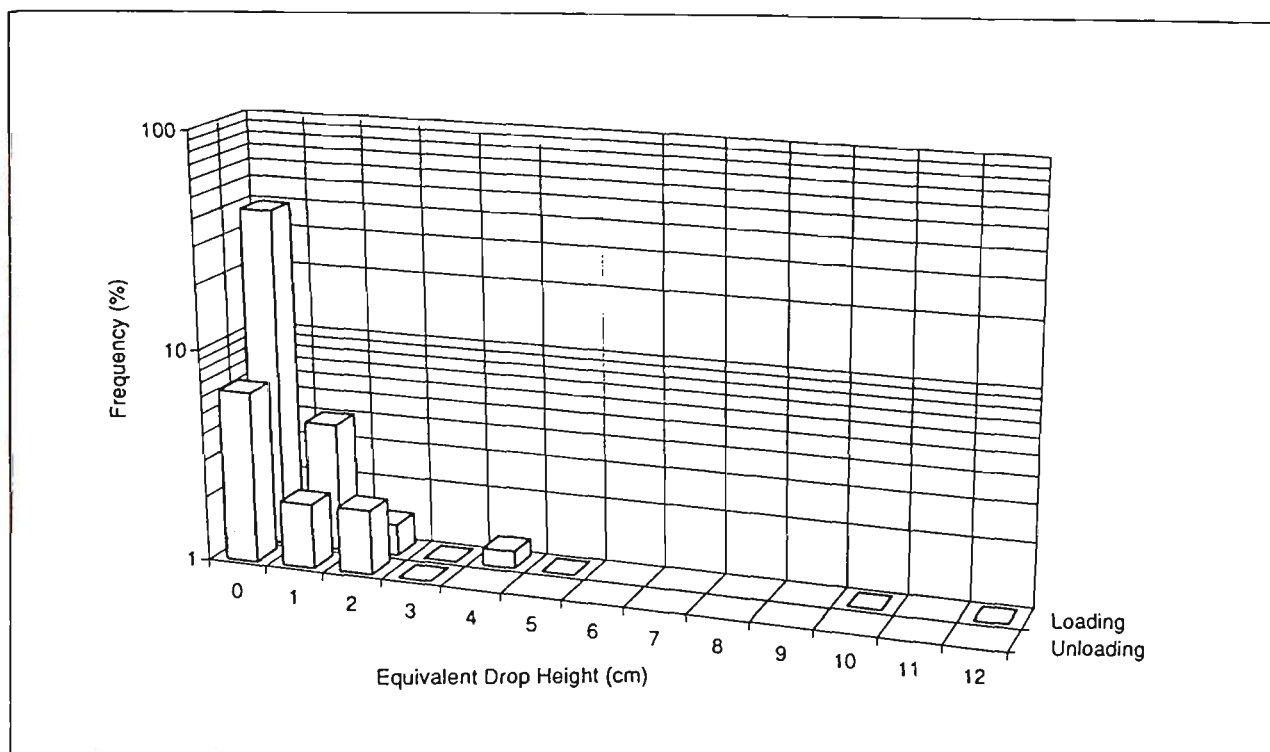
The distributions of the calculated equivalent drop heights are shown in Table 23 and Figure 36.

Table 23: Calculated equivalent drop height distribution for handling operations.

Handling Operation:	Unloading	Loading
Equivalent Drop Height (cm)	Frequency (%)	Frequency (%)
0	6	39
1	2	4
2	2	1.4
3	1	1
4	0	1.2
5	0	1
6	0	0
7	0	0
8	0	0
9	0	0
10	0	1
11	0	0
> 12	0	1
Maximum (cm):	4	39

Note: Percentages do not add up to 100% as durations equal to the event length are omitted.

Figure 36: Shock event equivalent drop height distribution assuming half-sine waveforms.



Note: Percentages do not add up to 100% as durations equal to the event length are omitted.

From these results it appears that the loading operations are more severe than the unloading operations, when considering the calculated equivalent drop heights from the handling impact study data.

4.4 SUMMARY OF RESULTS

This section lists summarised results from the measurement and analysis of shock, vibration, temperature, relative humidity, and handling impacts for the fresh produce distribution environment.

4.4.1 Vibration

1. The ASTM truck PSD profile is significantly different from the PSD profile found in these field experiments, and the suitability of the ASTM profile for laboratory simulation of this transport vibration environment is therefore questionable.

2. A more suitable PSD profile for laboratory vibration simulation would be based on the PSD profile obtained for trailer PT279 in Melbourne, and the appropriate RMS acceleration level would be 0.44 g-RMS.

4.4.2 Shock

1. The distributions of peak acceleration, velocity change, and crest factor can be used to confirm that any laboratory simulation of the transportation environment is providing shocks of the appropriate quantity and magnitude.
2. The environmental damage potential plots (i.e. plots of peak acceleration against velocity change for each shock event) can be used in conjunction with product damage boundary curves to quantify the occurrence of potentially damaging shocks in any transportation environment. However fresh horticultural produce generally cannot be modelled using DBCs, and hence this application is of limited use for these products.
3. The distributions of peak acceleration, velocity change, and crest factor can be successfully modelled using both the Weibull and gamma probability distributions. These would enable a quantitative comparison of two or more transportation environments.
4. From non-quantitative comparison of the Weibull and gamma distributions, it appears that the gamma distribution is better at modelling these shock distributions than the Weibull distribution.

4.4.3 Temperature

1. Large fluctuations were found to occur between different locations in the trailer, consecutive samples at the same location, and subsequent journeys at the same time and thermocouple location. The distribution of individual air temperature measurements appeared to fluctuate up to $\pm 5^{\circ}\text{C}$ about the hourly mean temperature.
2. There was little difference between the mean air temperatures at any location in the trailer. The mean air temperatures followed the general pattern of ambient air temperature.

3. The air temperature profiles were in excess of maximum recommendations for the shipment of non-tropical horticultural products. Other basic recommendations for the transport of horticultural products, such as precooling of the load, were not followed.

4.4.4 Relative Humidity

1. As for temperature, large fluctuations were found to occur between different locations in the trailer, consecutive samples at the same location, and subsequent journeys at the same time and location. The distribution of individual RH measurements appeared to fluctuate up to $\pm 15\%$ about the mean hourly RH.
2. There was little difference between the mean RH at any location in the trailer. The mean RH inside the trailer followed the general pattern of ambient RH.
3. The RH levels were below the minimum values recommended for the shipment of horticultural products.

4.4.5 Handling

1. In the verification of the EDR-3 set-up for handling recording, it was found that better estimates of equivalent drop height could be obtained by taking a half-sine approximation to the shock waveform, rather than by using the EDR's in-built drop height estimation.
2. In the typical handling environment studied, there appeared to be no difference between the majority of handling operations, with the exception that operations involving the loading of pallets into refrigerated trailers appeared more severe than operations involving the unloading of pallets.
3. The handling environment appears less severe than the transport shock environment, and the transport environment may therefore provide a better a worst-case scenario of package impacts than the handling environment.
4. The majority of handling impacts occurred to the bottom of the pallet, with the front and right sides also having large numbers of impacts. The proportions of flat, edge, and corner drops were approximately 40%, 40%, and 20% respectively.

5. LABORATORY EXPERIMENTS

These experiments describe an engineering-fatigue approach to the prediction of packaging performance. This approach was expected to have the advantage of simulating the forces most relevant to packaging for fresh horticultural produce. That is, these experiments simulated the road transport vibration environment for a short time at high humidity, rather than static loading conditions for an extended time at cycling humidity. From the distribution temperature and humidity measurements described in Chapter 4, it was concluded that cyclic conditions would not be appropriate for short-duration dynamic laboratory tests. In addition, the produce handling measurements described in Chapter 4 suggested that the handling environment was not as severe as the transport environment, and need not be considered in short-duration laboratory tests.

The main objective to these experiments was to determine whether measurements of box creep under short-duration dynamic loading and constant relative humidity can be reliably used to predict box performance, based on previously obtained data under static loading.

5.1 METHODOLOGY

These laboratory experiments were conducted using a servohydraulic vibration system with the box placed under a load of varying mass. The life of each loaded box under vibration was then measured. The box survival time was defined as the number of seconds to elapse under vibration until the average (i.e. static) deflection of the box was greater than the peak deflection of the box, as previously measured under quasi-static compression. The deflection was measured using three Baumer ultrasonic displacement transducers. The output from the transducers was then filtered using 1 Hz LPFs to remove the high frequency signal from the motion of the vibration table, leaving only the gradual creep of the box as it deflected under load. The experimental equipment is described in detail in Appendix B. The set-up and verification of the vibration system is described in Appendix C.

Four different corrugated fibreboard boxes for fresh horticultural produce were selected for these experiments, consisting of each combination of two variables (i.e. a full 2² factorial experiment). Two of the boxes had an internal width dimension of 350 mm, while the other two had an internal width dimension of 370 mm. Two of the boxes had a grade 140C medium, while the other two had a grade 180C medium. The combinations of each variable, and the box types, are shown in Table 24.

Table 24: Description of corrugated fibreboard boxes used for testing.

Box Type	144837	133101	116036	147145
Internal Dims (mm)	565 × 370 × 280	565 × 350 × 280	565 × 370 × 280	565 × 350 × 280
Board Grade	EW220/140C/K210	EW220/140C/K210	EW220/180C/K210	EW220/180C/K210

Each box type was waxed and had ventilation holes, as usual for produce boxes. The boxes were preconditioned to ISO standard conditions (23°C, 50% RH) for 24 hours. They were then conditioned at conditions consistent with those measured in the field study (12°C, 95% RH) for a further 72 hours.

The box under test was placed on the vibration table and blocked into place to prevent any horizontal movement across the table surface. The box was then covered with a plywood sheet (found to be suitable for the reflection for the ultrasonic sound) and loaded with weights. The cradle for the weights had a nominal mass of 65 kg and each lead ingot had a nominal mass of 25 kg. The weights used during testing consisted of the cradle plus either 3, 4, 5, or 6 ingots (nominal masses of 140, 165, 190, and 215 kg respectively).

The table was then set in its equilibrium position, and the distance between the plywood reflector and the ultrasonic sensors was set at 150 mm. The pens on the chart recorder were then zeroed to the centre of the page. The transducer calibration constants were 40 mm/V, and this gave a maximum pen deviation of ±2.5 V, corresponding to a box deflection of ±100 mm. To prevent the recorder pens from exceeding the limits of the recorder, a set of jacks were set at 50 mm below the equilibrium position of the plywood sheet. Hence the box would never be allowed to deflect more than 50 mm, which would correspond to a net movement of the pens of half of the page width. The LPFs effectively

removed the motion of the table from the signal, leaving a clear view of the net deflection of the box as it failed. It was assumed that the equilibrium position of the table would not drift over time as each test progressed. The equilibrium position was zeroed at the start of each new test.

5.2 RESULTS AND DISCUSSION

5.2.1 Quasi-Static Compression of Corrugated Fibreboard Boxes

The quasi-static compression strengths of each of the four box types was determined to allow a basis for comparison with dynamic performance. Rather than determine the compression strengths at ISO conditions (23°C, 50% RH), the compression strengths were determined at the same conditions as the dynamic tests were conducted, i.e. preconditioning at ISO standard conditions (23°C, 50% RH) for 12 hours, followed by conditioning at 12°C and 95% RH for a further 72 hours. Ten of each box type were tested, and the results are shown in Table 25. The deflections listed in Table 25 are the peak deflections, at which the compressive force is equal to the box compressive strength. The compression testing was performed in accordance with ASTM D 642.

Table 25: Box quasi-static compression strengths.

Box Type	144837	133101	116036	147145
Count	10	10	10	10
Mean Strength (N)	4790	4650	4810	5300
95% Bounds (N)	±200	±170	±200	±280
Bound Fraction	0.041	0.037	0.041	0.053
Mean Deflection (mm)	10.8	9.6	13.81	12.5
95% Bounds (mm)	±0.4	±0.5	±1.3	±0.5
Bound Fraction	0.037	0.052	0.094	0.040

The mean strengths were calculated, together with 95% confidence bounds for the mean. The confidence bounds were obtained by multiplication of the standard error of the mean by the appropriate t statistic. The bound fractions (the ratio of the confidence bounds to the mean) were also calculated. The differences between the mean strengths for each box type are shown in Table 26. It can be seen that the first three box types (144837, 133101,

and 116036) are not statistically different at the 95% level of confidence. However box type 147145 has a significantly higher quasi-static compression strength than each of the three other box types.

Table 26: Box quasi-static compression strength differences.

Box Type	133101	116036	147145
144837	-140 ±260	20 ±280	500 ±300*
133101		160 ±260	700 ±300*
116036			500 ±300*

Notes: (1) Units of compression strength: N.

(2) * indicates a significant difference at the 95% level of confidence.

From the load-displacement histories of each sample, the stiffness of each box during compression was determined. The stiffness of a box was taken as the gradient of the load-displacement curve at the point of inflection, i.e. where the second derivative of the load-displacement curve is equal to zero. At the onset of compression, each curve shows a positive second derivative (i.e. an increasing stiffness), followed by a near-linear section (containing the point of inflection), and ending with a negative double-derivative section (i.e. decreasing stiffness) before the maximum of the curve is reached. At this point the box was deemed to have failed. The calculated stiffness of each box is shown in Table 27.

Table 27: Stiffness of boxes during quasi-static compression.

Box Type	144837	133101	116036	147145
Mean (kN/m)	990	1420	1500	1090
95% Bounds (kN/m)	±120	±280	±900	±120
Bound Fraction	0.121	0.197	0.600	0.110

Calculation of the box stiffness in this way enabled the estimation of the box natural frequencies, using Equation (5.1), based on the assumption that a vibrating box under load acts as a simple spring-mass system. The estimated natural frequencies for each box type are tabulated in Table 28, and 95% confidence bounds for the mean natural frequency are shown in Figure 37.

$$f_n = \frac{1}{2\pi} \sqrt{\frac{k}{m}} \quad (5.1)$$

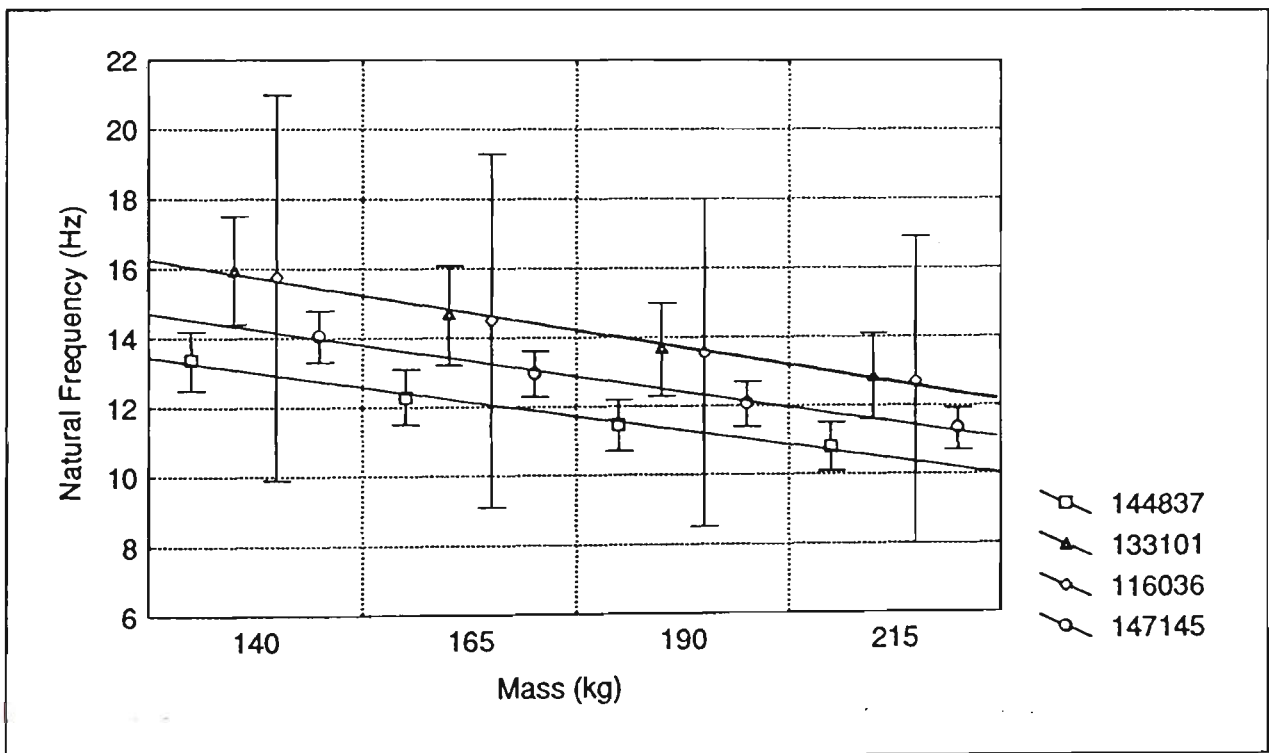
where f_n is the estimated natural frequency of the box (Hz), k is the calculated box stiffness (N/m), and m is the mass on the box (kg).

Table 28: Estimated box mean natural frequencies during vibration assuming a simple spring-mass system.

Box Type	144837	133101	116036	147145
140 kg	13.4 ±0.9	16.0 ±1.6	16 ±6	14.1 ±0.8
165 kg	12.3 ±0.8	14.8 ±1.5	15 ±5	13.0 ±0.7
190 kg	11.5 ±0.8	13.8 ±1.4	14 ±5	12.1 ±0.7
215 kg	10.8 ±0.7	12.9 ±1.3	13 ±4	11.4 ±0.6

Note: Units of natural frequency: Hz.

Figure 37: Estimated box natural frequencies (mean and 95% confidence bounds for mean).



It can be seen from Figure 37 that some box types could resonate if their natural frequencies coincide with demand frequencies of high PSD. The PSD profile used in the dynamic testing, shown in Figure 50, had high PSD values in the range 0.5 - 7 Hz, and lower PSD values above 7 Hz. Because the estimated box natural frequencies were generally greater than 10 Hz, box resonance was not expected to occur. If, however, sufficiently high PSD levels were present at the box natural frequencies, then resonance could be a problem, resulting in lower box survival times than otherwise expected.

5.2.2 Dynamic Creep Testing of Corrugated Fibreboard Boxes

In fatigue testing, the relationship between stress (S) and number of load applications (N) is commonly represented graphically by plotting the stress as ordinate and the cycles to failure on the abscissa. This results in the S/N diagram. This methodology was not entirely applicable to corrugated fibreboard boxes, and some modifications for these experiments was required. As the box was a structure rather than a material, mass (kg) rather than stress (kN/m^2) was used as the independent variable. And as the dynamic loading was applied through the use of a random vibration profile, the term 'cycles to failure' was also not applicable, as the concept of wave duration is not applicable to random vibration. Instead, the number of seconds to failure was used as the dependent variable. The use of time in this way is only valid for one random vibration PSD profile at one RMS level; the use of other PSD profiles or RMS levels cannot be correlated to these results.

Each box type was tested under four different masses: 140, 165, 190, and 215 kg. Each box type was replicated ten times, and hence 120 individual tests were required. Each test was run for a maximum of 1 hour, which resulted in a few non-failure results (i.e. censored data) being recorded, particularly for the smaller masses and the stronger boxes. These, however, were dealt with through the use of statistical regression techniques for censored data.

Brief observations of the behaviour of each box type during the duration of the test and while failing are tabulated in Table 29. Generally the boxes failed in one of four ways. Firstly, deformation of the box could begin (i) soon into the test and continue gradually over the duration, or (ii) deformation could occur late in the test. Secondly, the failure could be (i) sudden, occurring over the last few seconds, or (ii) failure could be more gradual, and take several minutes. The combination of these two modes was dependent on both the box type and mass.

Table 29: General observations of box deformation and failure during dynamic testing.

Mass (kg)	Box Type	Observations
140	144837	Non-manufacturers joint end deforms and fails over last 2 mins of test. Manufacturers joint end then fails immediately after.
	133101	Manufacturers joint end deforms over duration of test, then fails over last 2 mins of test. Non-manufacturers joint end did not fail.
	116036	Either end deforms over duration of test, then fails over last few seconds of test. The other end then fails immediately after.
	147145	No failures recorded.
165	144837	Both ends deform and fail together over last 15 secs of test.
	133101	Manufacturers joint end deforms and fails over last few seconds of test. Non-manufacturers joint end did not fail.
	116036	Manufacturers joint end deforms over duration of test, then fails over last 15 secs of test. Non-manufacturers joint end did not fail.
	147145	Manufacturers joint end deforms over duration of test, then fails over the last 2 mins of test. Non-manufacturers joint end did not fail.
190	144837	Both ends deform over duration of test, and fail together over last few secs of test.
	133101	Manufacturers joint end deforms over duration of test, then fails over last few secs of test. Non-manufacturers joint end then deforms and fails immediately after.
	116036	Both ends deform and fail together over last 30 secs of test.
	147145	Manufacturers joint end deforms over duration of test (characterised by tearing of joint glue). Non-manufacturers joint end deforms and fails immediately after.
215	144837	Both ends suddenly deform and fail together over last 2 secs of test.
	133101	Both ends suddenly deform and fail together over last 2 secs of test.
	116036	Both ends suddenly deform and fail together over last 2 secs of test.
	147145	Both ends suddenly deform and fail together over last 15 secs of test.

5.2.2.1 Raw Survival Time Data

The observed survival time results for the dynamic testing are detailed in Table 30, and summarised in Table 31. Censored (i.e. non-failure) data was recorded for box types 133101, 116036, and 147145 under a mass of 140 kg, and for box type 147145 under a mass of 165 kg.

Table 30: Observed box survival times.

Mass (kg)	Box Type	144837	133101	116036	147145
140	Count(censored)	10	10(2)	10(6)	10(10)
	Median (s)	2682	2679	3600*	3600*
	Mean (s)	2600	2700*	3400*	3600*
	95% Bounds (s)	±400	±500*	±300*	n/a*
	Bound Fraction	0.154	0.185*	0.088*	n/a*
165	Count(censored)	10	10	10	10(2)
	Median (s)	200	363	640	1810
	Mean (s)	300	310	690	1600*
	95% Bounds (s)	±150	±90	±140	±600*
	Bound Fraction	0.500	0.290	0.203	0.375*
190	Count(censored)	10	10	10	10
	Median (s)	105	206	209	563
	Mean (s)	115	190	220	530
	95% Bounds (s)	±20	±70	±80	±130
	Bound Fraction	0.174	0.368	0.364	0.245
215	Count(censored)	10	10	10	10
	Median (s)	50	60	79	82
	Mean (s)	51	62	80	98
	95% Bounds (s)	±2	±6	±8	±25
	Bound Fraction	0.039	0.097	0.100	0.255

Note: * indicates that the result is affected by the presence of censored data.

Table 31: Summary of observed box survival times.

Box Type	144837	133101	116036	147145
140 kg	2600 ±400	2700* ±500*	3400* ±300*	3600*
165 kg	300 ±150	310 ±90	690 ±140	1600* ±600*
190 kg	115 ±20	190 ±70	220 ±80	530 ±130
215 kg	51 ±2	62 ±6	80 ±8	98 ±25

Notes: (1) Units of survival time: s.

(2) * indicates that the result is affected by the presence of censored data.

Despite the presence of some censored data, the differences between each box type were calculated, and are shown in Table 32. These results are not necessarily statistically valid, except for those comparisons where censored data is not included, but do indicate the relative trends between each of the four box types.

Table 32: Differences between mean box survival times.

Mass (kg)	Box Type	133101	116036	147145
140	144837	100* ±600*	800* ±500* #	1000* ±400* #
	133101		700* ±600* #	900* ±500* #
	116036			200* ±280*
165	144837	10 ±180	390 ±210 #	1300* ±600* #
	133101		380 ±170 #	1300* ±600* #
	116036			900* ±600* #
190	144837	80 ±70 #	110 ±80 #	420 ±130 #
	133101		30 ±110	340 ±150 #
	116036			310 ±150 #
215	144837	11 ±6 #	29 ±8 #	47 ±25 #
	133101		18 ±10 #	36 ±26 #
	116036			18 ±26

- Note:
1. Units of survival time: s.
 2. * indicates that the result is affected by the presence of censored data.
 3. # indicates a significant difference at the 95% level of confidence.

Ignoring for the moment the presence of censored data, it appears that of the 24 comparisons in Table 32, all but 5 differences are significant. Based on these results, the boxes can be ranked on their relative performance under dynamic loading. From the strongest to the weakest box type: 147145 > 116036 > 133101 > 144837. The ranking is similar when comparing the relative quasi-static compression strengths of the boxes, implying that the greater the quasi-static compression strength, the greater the dynamic survival time.

Of the 4 box types, only box 147145 was found to have a significantly higher quasi-static compression strength than any other box type. In contrast, Table 32 indicates that in 19 out of 24 comparisons, the two box types are significantly different. This suggests that this dynamic testing is more sensitive in highlighting a difference between box types than quasi-static testing. Of course the comparisons in Table 32 are generally influenced by the censored data, and quantitative conclusions from this comparative method are therefore statistically invalid.

The relative performance of each box type can also be seen by indexing the performance against some basis, in this case the performance of the weakest box, type 144837. Table 33 shows the performance of each box type indexed for both quasi-static compression strength and dynamic survival time under each mass. The compression strength indices are simply the ratio of compression strengths (N), and the survival time indices are the ratio of

\log_{10} of survival time (s), as compared with box type 144837. These performance indices are also graphed in Figure 38.

Table 33: Box performance indices for raw survival time data.

Box Type	Static	Index	140 kg	Index	165 kg	Index	190 kg	Index	215 kg	Index
144837	4790 N	1.00	2613 s	1.00	295 s	1.00	115 s	1.00	51 s	1.00
133101	4650 N	0.97	2703 s*	1.00*	314 s	1.01	194 s	1.11	62 s	1.05
116036	4810 N	1.01	3398 s*	1.03*	689 s	1.15	220 s	1.14	80 s	1.11
147145	5300 N	1.11	3600 s*	1.04*	1610 s*	1.30*	530 s	1.32	98 s	1.17

Note: 1. * indicates that the result is affected by the presence of censored data.

Figure 38: Box performance indices for raw survival time data.

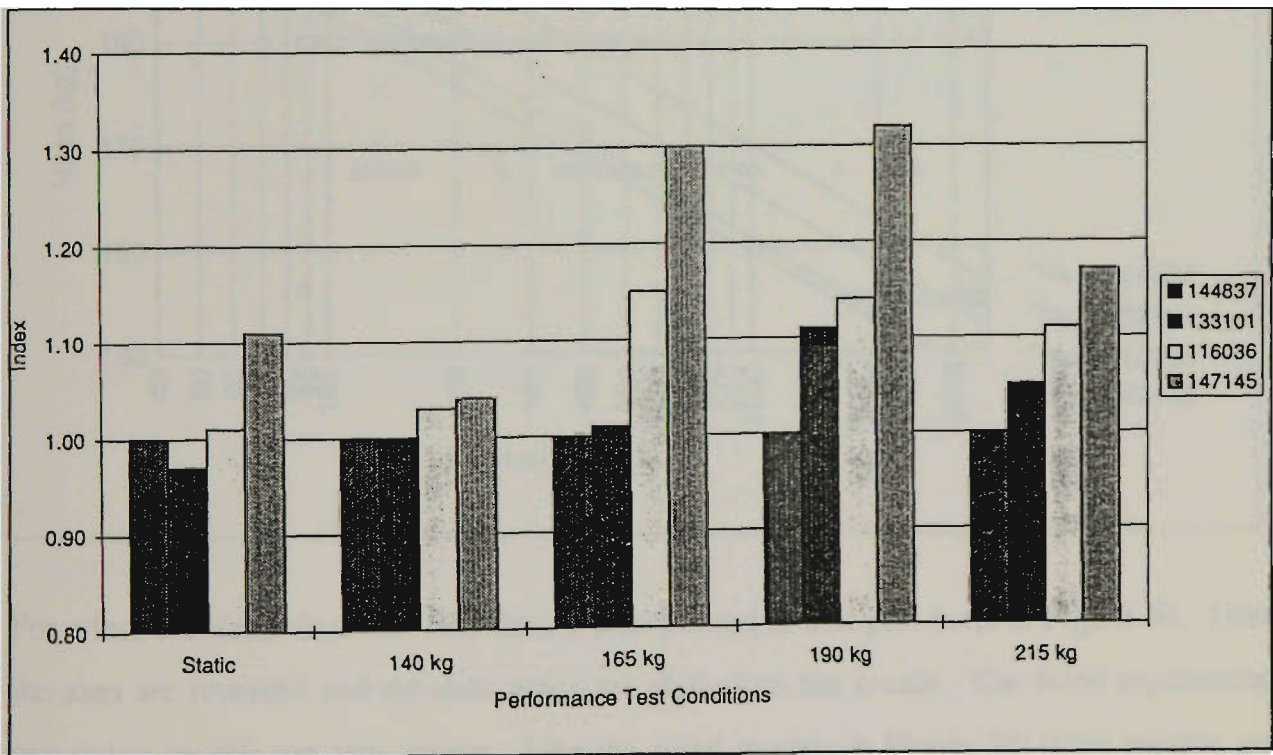


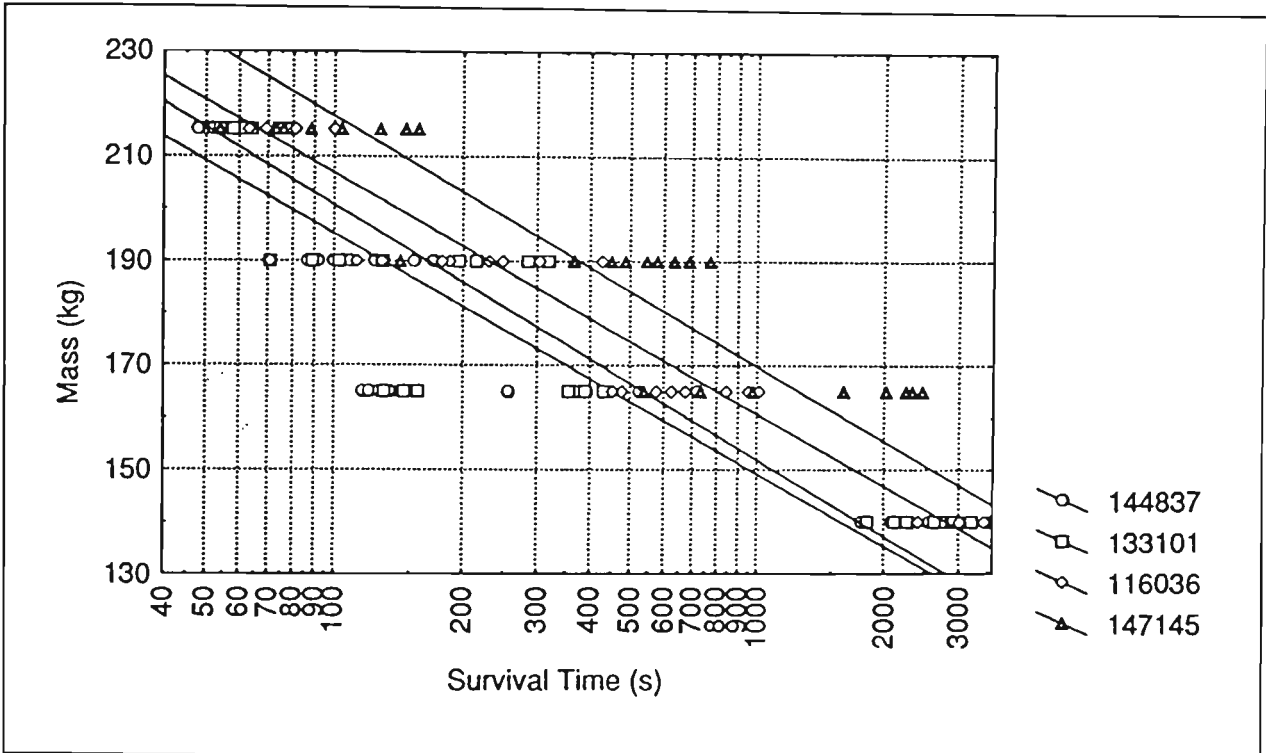
Table 33 and Figure 38 show the general trend in ranking each of the four box types. However this data is affected by the presence of censored data.

5.2.2.2 Regression Modelling of Survival Time Data

Plots of the observed box survival time (s) on a \log_{10} scale against the applied mass during vibration (kg) were found to give approximately a straight line. This was expected if the assumption of a typical S/N-type relationship was valid. The observed survival time data plotted on S/N-type axes can be seen in Figure 39. The mass (kg) on the box during

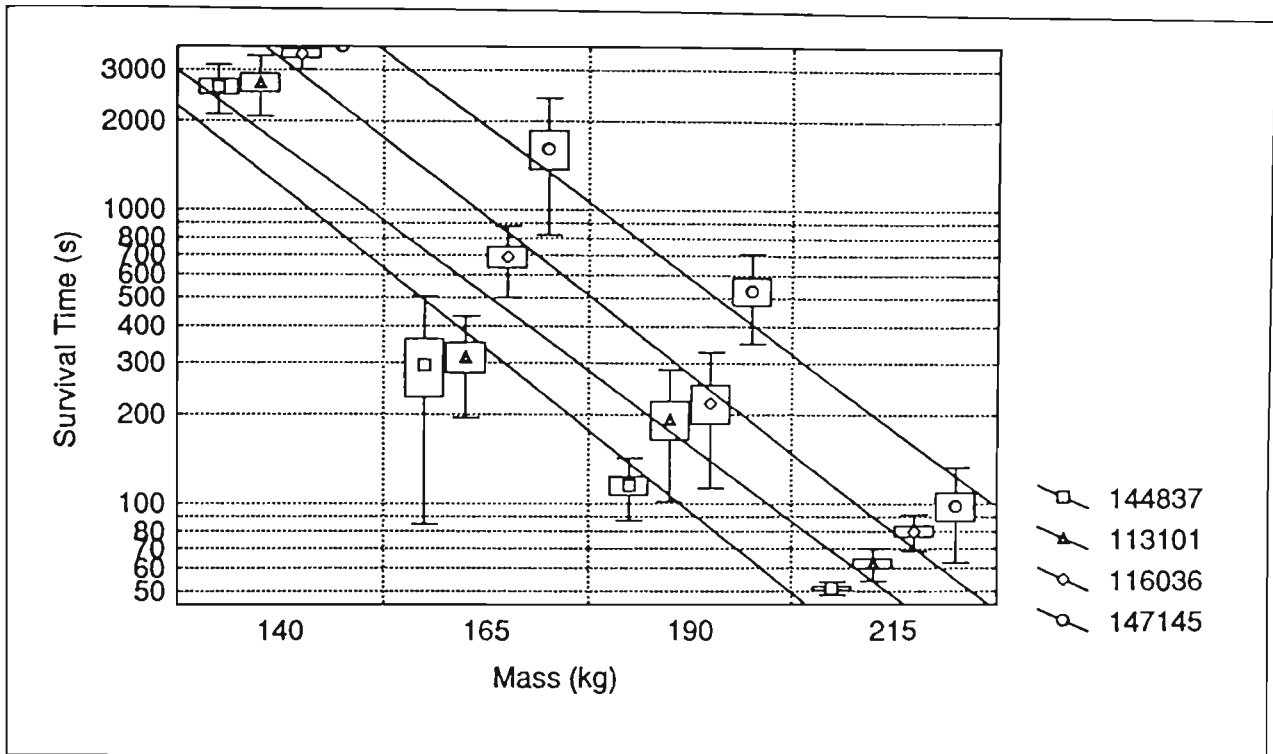
testing is on the y-axis, and the \log_{10} of the box survival time (s) is shown on the x-axis. It was found that an exponential regression model (i.e. a straight line on log-linear axes) provided the best least-squares fit. The STATISTICA software package was used to fit the regression models.

Figure 39: Applied mass during vibration vs box survival time (all raw data).



For a less cluttered view, the raw data is also plotted in box plot form in Figure 40. Here the axes are reversed and the data series are shifted on the x-axis. The fitted exponential regression models are also shown. Like the fitted models in Figure 39, these models are simple least-squares models and do not take the censored data into account.

Figure 40: Box survival time vs applied mass during vibration (mean, standard error of mean, standard deviation, and fitted exponential regression model).



Two exponential regression models were applied to the data; the first a general least-squares model, and the second a more specialised technique to account for the censored data. The simple least-squares model was fitted to determine whether it would approximate the more complex censored data model.

The exponential regression model applied to the raw survival time data was:

$$t_s = \exp(\beta_0 + \beta_1 m) \quad (5.2)$$

where t_s is the predicted survival time (s), m is the applied mass during vibration (kg), and β_0 and β_1 are the fitted regression parameters. The regression parameters for the non-censored data analysis are shown in Table 34. The regression parameters for the censored data analysis are shown in Table 35, together with the standard error of the mean and the corresponding t-value.

Table 34: Regression parameters for non-censored data analysis.

Box Type	β_0	β_1
144837	14.36	-0.050
133101	14.06	-0.047
116036	14.93	-0.050
147145	15.09	-0.048

Table 35: Regression parameters for censored data analysis.

Box Type	β_0	Std Err	t-Value	β_1	Std Err	t-Value
144837	14.79	0.9085	16.280	-0.0517	0.00504	-10.258
133101	14.83	0.9779	15.165	-0.0505	0.00537	-9.404
116036	16.49	1.1049	14.924	-0.0573	0.00593	-9.663
147145	19.82	1.5893	12.471	-0.0713	0.00823	-8.663

It can be seen that the use of simple least-squares regression analysis tends to underestimate the regression parameters for the exponential model. The difference is not large in the cases where censored data did not occur (e.g. for box type 144837) but is large in the cases where censored data did occur (e.g. for box type 147145).

The differences between the predicted survival times from each of the two regression models, and the observed survival times, can be seen in Figure 41, Figure 42, Figure 43, and Figure 44, for applied masses of 140, 165, 190, and 215 kg respectively. These Figures also show the measured static compression strengths of each box type, as a comparison between relative static and dynamic performance.

Figure 41: Comparison of observed and predicted box survival times (140 kg).

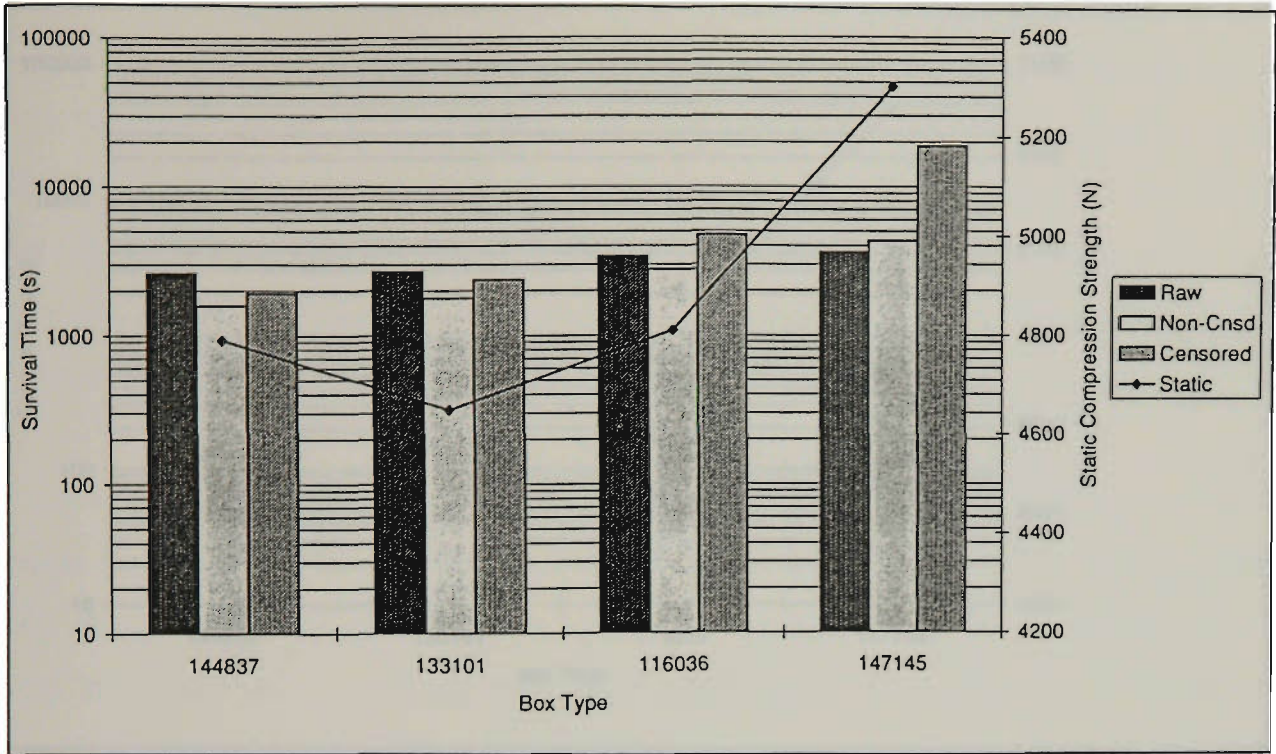


Figure 42: Comparison of observed and predicted box survival times (165 kg).

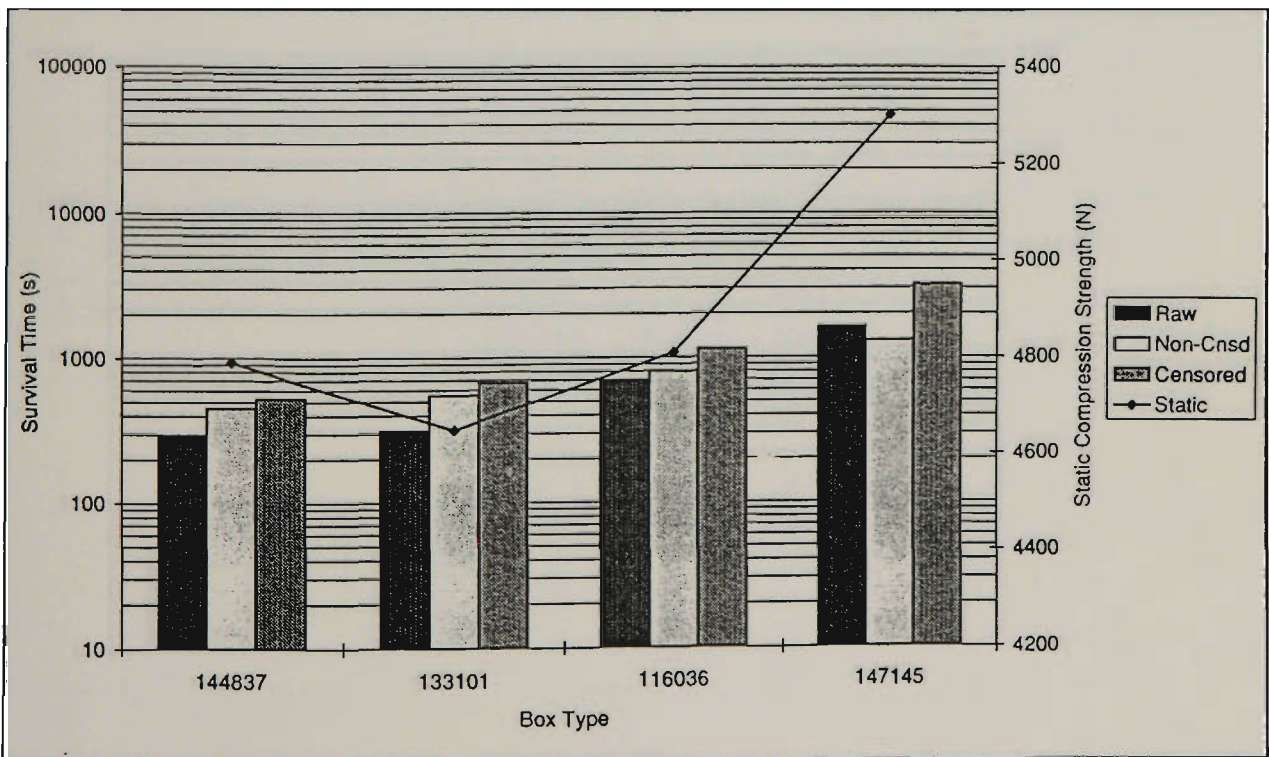


Figure 43: Comparison of observed and predicted box survival times (190 kg).

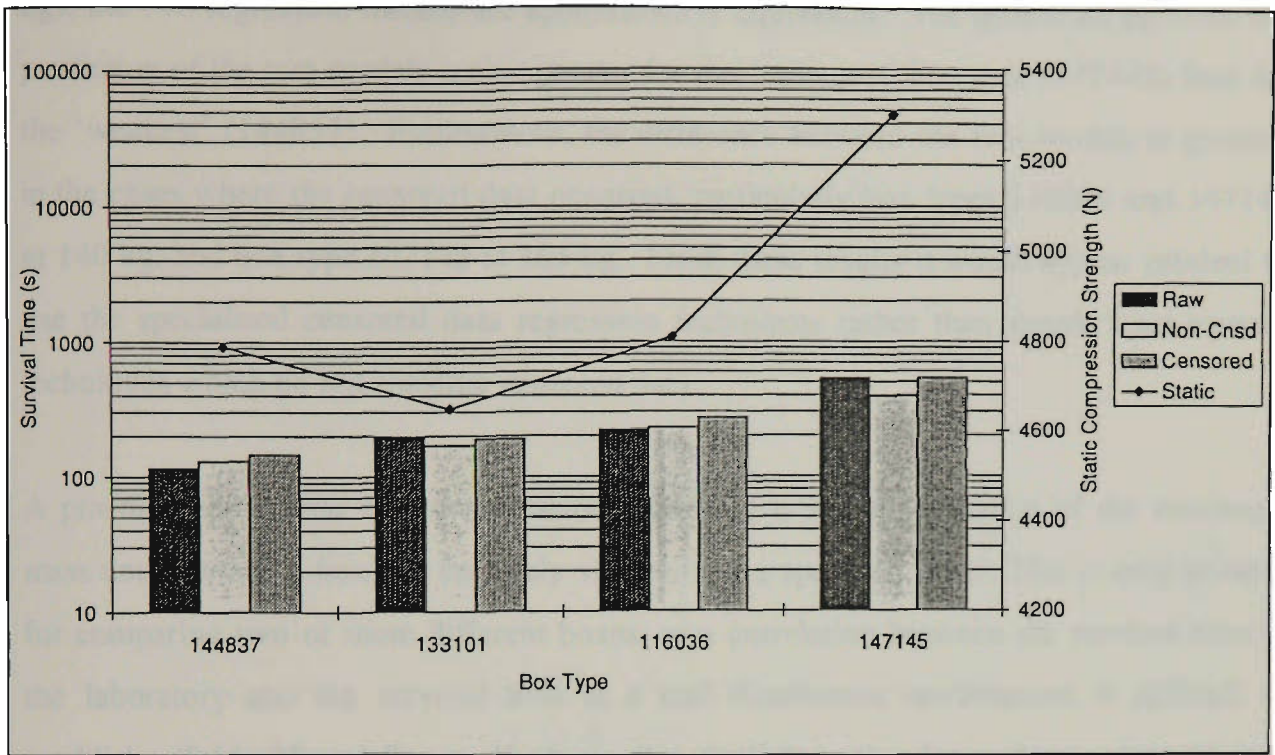
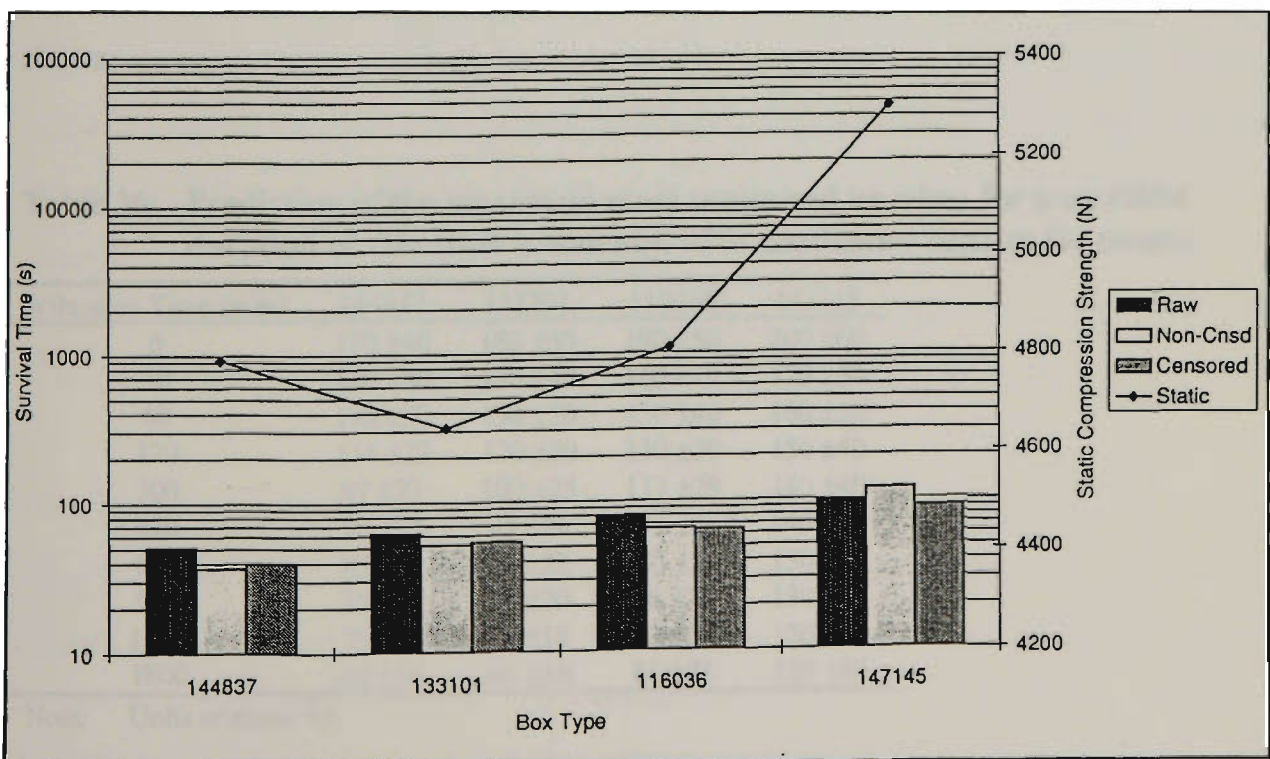


Figure 44: Comparison of observed and predicted box survival times (215 kg).



It can be seen from these Figures that both regression models correlate well with the observed values of survival time. At the lighter loads (masses of 140 and 165 kg), the censored data regression model generally predicts a higher survival time than the non-censored data regression model, as expected. At the higher loads (masses of 190 and 215

kg), the two regression models are approximately equivalent. The difference between the prediction of the two models is also greater for the 'strongest' box type (147145) than for the 'weakest' (144837). Furthermore, the difference between the two models is greatest in the cases where the censored data occurred, particularly box types 116036 and 147145 at 140 kg, and box type 147145 at 165 kg. From these results it would appear prudent to use the specialised censored data regression techniques rather than simple least-squares techniques which do not consider censored data.

A practical application of this regression modelling is in the estimation of the maximum mass under which a box can be safely vibrated for a specified time. This is only suitable for comparing two or more different boxes, as a correlation between the survival time in the laboratory and the survival time in a real distribution environment is difficult to establish. Table 36 and Figure 45 shows this predicted mass for various values of time extrapolated from the exponential regression model. The assumption is made that the exponential regression parameters given in Table 35 are also valid for the range of times shown.

Table 36: Prediction of the maximum mass supported by a box for a specified duration of vibration (mean and 95% confidence bounds for mean).

Vibration Time (min)	144837	133101	116036	147145
6	170 ±40	180 ±50	190 ±50	200 ±60
30	140 ±30	150 ±40	160 ±40	170 ±50
60	130 ±30	130 ±30	150 ±40	160 ±50
120	114 ±27	120 ±30	130 ±30	150 ±40
300	97 ±23	100 ±25	117 ±29	140 ±40
420	90 ±21	93 ±24	111 ±28	140 ±40
600	83 ±19	86 ±22	105 ±26	130 ±40
900	75 ±18	78 ±20	98 ±24	130 ±40
1200	70 ±16	72 ±18	92 ±23	120 ±30
1800	62 ±14	64 ±16	85 ±21	120 ±30

Note: Units of mass: kg.

Figure 45: Prediction of the maximum mass supported by a box for a specified duration of vibration (mean and 95% confidence bounds for mean).

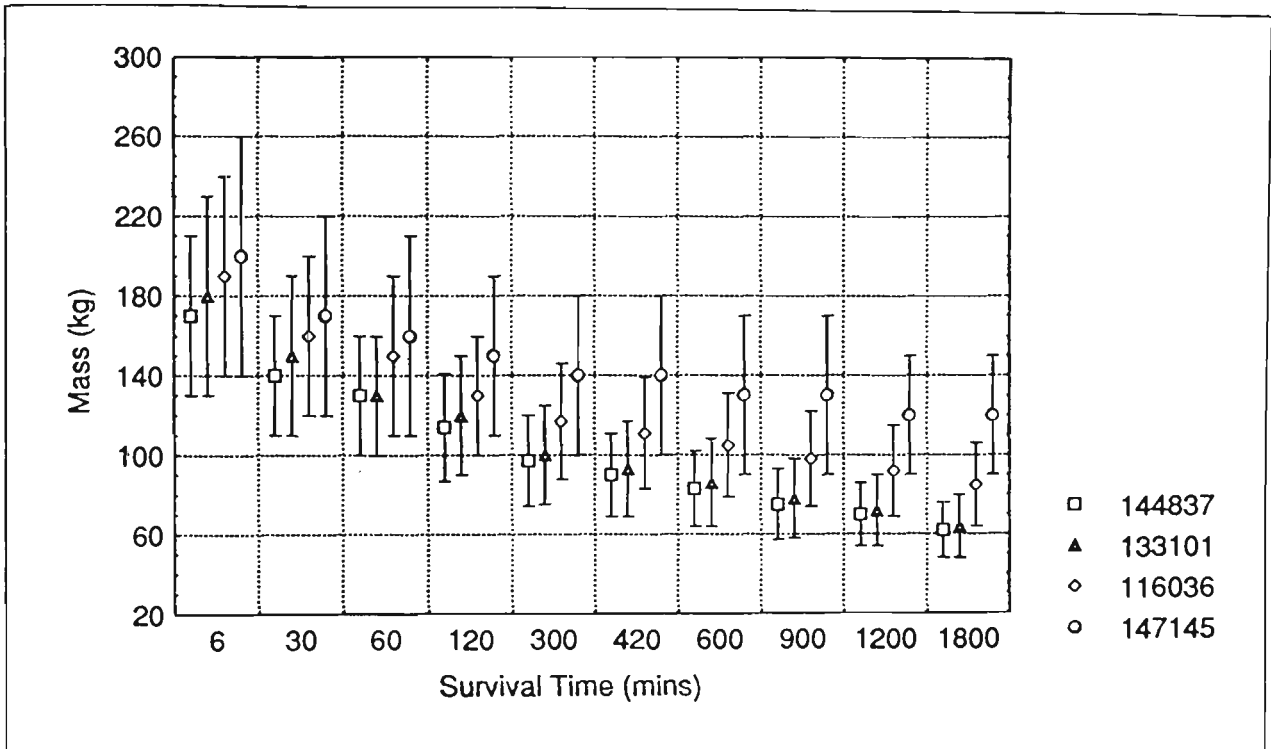


Figure 45 shows, for example, that box types 144837 and 133101 would be expected to support a mass of 100 kg (± 25 kg at the 95% level of confidence) for 300 min of vibration before failure, for the given PSD profile and RMS acceleration level. In contrast, box type 147145 would be expected to support 140kg (± 40 kg) before failing, for the same duration. However, due to the large variation in the observed survival time data, the difference between these two predictions is not statistically significant. For a vibration duration of 1800 min, however, there is a significant difference between these box types.

The predictive regression model obtained above does not take into account the physical structure of each box; the model only considers the applied mass, and uses a different set of regression parameters for each box type. A regression analysis was performed on all of the raw data, using the variables of box internal dimensions and board grade, in addition to applied mass. This resulted in a single equation to describe the survival time of any box based on its physical characteristics. The following exponential model was used, using censored data regression techniques:

$$t_s = \exp(\beta_0 + \beta_1 x_1 + \beta_2 x_2 + \beta_3 x_3) \quad (5.3)$$

where t_s is the predicted survival time (s), x_1 is the applied mass (kg), x_2 is the box internal width dimension (coded as -1 for 350 mm and +1 for 370 mm), and x_3 is the grade of the board medium (coded as -1 for 140C and +1 for 180C). The regression parameters for this model are shown in Table 37.

Table 37: Regression parameters for censored data analysis of physical structure of box.

Independent Variable	Parameter	Standard Error	t-Value
constant (β_0)	16.060	0.5382	29.840
mass (β_1)	-0.0555	0.002911	-19.064
internal dimensions (β_2)	-0.2314	0.08492	-2.725
board grade (β_3)	0.4402	0.08531	5.160

Note: $\chi^2 = 388.3$.

This model as a whole is significant, as indicated by the high χ^2 statistic. All of the regression parameters are significant at the 95% level of confidence, implying that each of the two physical characteristics of the box under study (internal width dimension and board medium grade), as well as the applied mass, influence the ultimate performance of the box. This model is not particularly complete, however, as the relatively large constant parameter suggests that other variables, not included in this analysis, also have an effect on box performance. No further attempt was made to predict box performance based on physical characteristics, as the relatively small sample sizes, few physical variables, and high variability between replicates introduced considerable uncertainty into the data.

5.3 SUMMARY OF RESULTS

The following general observations can be made following this section of the experimental work:

1. The use of recorded distributions of peak acceleration, velocity change, and crest factor to confirm that a laboratory vibration simulation is providing acceleration levels of the appropriate quantity and magnitude was found to be less pertinent than anticipated. This was due to a limitation of the particular random vibration controller in use, as it by

design produced instantaneous acceleration with a Gaussian distribution. This therefore produced a Rayleigh distribution of peak acceleration, rather than the Weibull or gamma distribution observed during the random vibration measurement. However it should be possible to produce acceleration values of any distribution by using a programmable RV controller and writing the appropriate code. This was not covered in these experiments.

2. The use of the ultrasonic displacement transducers, low pass filters, and a chart recorder in tracking the net displacement (or dynamic creep) of the boxes under loaded vibration provided better results than expected. It was estimated that the resolution of the displacement measurements was less than 3 mm. The static peak deflections of the boxes were found to be within the range of 9 - 15 mm, and the dynamic tests were conducted until the boxes had deflected 50 mm. This method could be used in other situations where non-contact measurement of the net creep of a vibrating surface is required.
3. The quantitative evaluation of the performance of corrugated fibreboard boxes was difficult due to the large variances within the experimental data. In evaluating the quasi-static compression strength of four box types, only one type was found to have a compression strength significantly (at the 95% level of confidence) different from any other box type, despite the fact that each box differed from all others in both size and material.
4. The dynamic testing of the same box types indicated that this method is more sensitive to differences between boxes than the quasi-static testing. In 24 comparisons of mean survival time (between 4 box types for 4 loadings), 19 comparisons were found to be different. However these results contained some censored data, and some of these comparisons are therefore statistically invalid.
5. In comparing the quasi-static and dynamic performance of each box type, it was generally found that as quasi-static compression strength increases, so does the dynamic survival time. More quantitative comparisons were not possible due to the large variances in the observed data, especially for the quasi-static results.
6. Plots of the \log_{10} of dynamic survival time against the mass under which the boxes were vibrated were found to experience an approximate straight line, in a manner analogous to S/N curves for fatigue testing. An exponential regression model was found to give

the best least-squares fit, however the simple least-squares model is inappropriate due to the presence of censored data.

7. A specialised regression technique to take censored data in account was also applied to the data, and appeared to model the experimental data more adequately than the simple least-squares model. Extrapolation of this model was used to predict the maximum mass under which each box type could be expected to survive vibration for a specified duration. This model is only appropriate for the particular PSD profile and RMS acceleration level used in the tests, and cannot be easily correlated to real distribution systems, but is useful as a comparison between different box types. While this method does appear to have the advantage of being more sensitive to differences than quasi-static testing, the tests take considerably more time to conduct and do not lend themselves well to automation.

6. CONCLUSIONS

Gunderson (1991) summarised corrugated box testing and corrugated box performance in the 'real world' and found that "today's tests for corrugated board do not adequately predict a container's performance in actual use", and that the "move toward performance based criteria for corrugated containers will better serve producers and users, and will encourage engineering and process innovations". He suggested that new methods must account for extended duration of load (progressive creep deformation) and humidity changes (hygroexpansion) that are part of the distribution environment.

The distribution environment for fresh horticultural produce, however, was found to involve relatively long transportation distances, relatively short storage times, and a reasonably constant humidity environment. For these reasons it was felt that the dynamic transportation phase of the total distribution environment would be more appropriate as a 'performance-based criteria' than either long-duration storage or cycling humidity.

The conclusions from this study of the fresh produce distribution environment include:

Transport vibration: The ASTM truck PSD profile is not suitable for the laboratory simulation of the fresh produce transport environment around the Melbourne and east Gippsland regions of Victoria. A more suitable PSD profile, and the appropriate RMS acceleration level, was developed based on recorded acceleration data.

Transport shock: The distributions of peak acceleration, velocity change, and crest factor could be used to confirm that any laboratory simulation of the transportation environment provides shocks of the appropriate quantity and magnitude, and to quantitatively compare two or more transportation environments. These distributions were found to approximate the Weibull and gamma distributions, suggesting that instantaneous acceleration levels in transportation do not follow the Gaussian distribution as often assumed.

Distribution temperature: Large fluctuations were found to exist between different locations in the refrigerated trailer, consecutive samples at the same location, and subsequent journeys at the same time and location. The air temperature profiles were in excess of maximum recommendations for the shipment of non-tropical horticultural products. Other basic recommendations for the transport of horticultural products, such as the precooling of the load, had not been followed.

Distribution relative humidity: As for temperature, large fluctuations were found to exist between different locations in the trailer, consecutive samples at the same location, and subsequent journeys at the same time and location. Generally, the RH profiles are all below minimum recommendations for the shipment of horticultural products.

Manual and mechanical handling: In the typical handling environment studied, there was no difference between the majority of handling operations, with the exception that operations involving the loading of pallets into refrigerated trailers were more severe than operations involving the unloading of pallets. The handling environment was less severe than the transport shock environment, and the transport environment may therefore provide a better a worst-case scenario of package impacts than the handling environment.

The laboratory experiments indicated that this method of dynamic box performance testing is more sensitive to differences between boxes than quasi-static testing. In comparing the quasi-static and dynamic performance of each box type, it was found that as quasi-static compression strength increases, so does the dynamic survival time. More quantitative comparisons were not possible due to the large variances in the observed data, especially for the quasi-static results. Plots of the \log_{10} of dynamic survival time against the mass under which the boxes were vibrated were found to give an approximate straight line, in a manner analogous to S/N curves for engineering fatigue testing.

A specialised regression technique to take censored data in account was found to model the experimental data adequately. Extrapolation of this model was used to predict the maximum mass under which each box type could be expected to survive vibration for a specified duration. This model cannot be easily correlated to real distribution systems, but

is useful as a comparison between different box types. While this method does have the advantage of being more sensitive to performance differences than quasi-static testing, the tests take considerably more time to conduct and do not lend themselves well to automation.

From the results obtained in these experiments, it is difficult to state with any certainty that the dynamic creep tests used here can be used to reliably predict box performance. In both the quasi-static compression tests, and the dynamic vibration tests, large variances within the experimental data were observed. The dynamic test method may have uses in developing a database for the comparison of different box types, however for routine performance testing quasi-static testing is more appropriate.

7. REFERENCES

- Adams, A., B. Harte, D. Young, & J. Lee (1992). The effect of simulated vibration on the compressive strength of unitised corrugated shipping containers. *Institute of Packaging Professionals Technical Journal*, **10**(2), 5-9.
- Antle, J.R. (1989). *Measurement of lateral and longitudinal vibration in commercial truck shipments*. School of Packaging, Michigan State University.
- Armstrong, L.D., & G.N. Christensen (1961). Influence of moisture changes on creep in wood. *Nature*, **191**, 869.
- Armstrong, L.D., & R.S.T. Kingston (1960). Effect of moisture changes on creep in wood. *Nature*, **185**, 862.
- Armstrong, L.D., & R.S.T. Kingston (1962). The effect of moisture content changes on the deformation of wood under stress. *Australian Journal of Applied Science*, **13**(4), 257-276.
- ASTM (1994). *Selected ASTM standards on packaging*. Philadelphia: American Society for Testing and Materials.
- Back, E.L. (1985). The relative moisture sensitivity of compression as compared to tensile strength. STFI-Paper Series A, No. 934, 1985.
- * Barca, F.D. (1975a). *Acquisition of drop height data during package handling operations*. United States Army Natick Development Centre Technical Report 75-108-AMEL, June 1975.
- Barca, F.D. (1975b). *Acquisition of climatic data during transportation on storage of containers*. United States Army Natick Development Centre Technical Report 75-78-AMEL, April 1975.
- Benson, R.E. (1971). The effects of relative humidity and temperature on tensile stress-strain properties of kraft linerboard. *TAPPI Journal*, **54**(5), 699-703.
- Bollen, A.F., & N.R. Cox (1991). A technique for predicting the probability of bruising for use with an instrumented sphere. American Society of Agricultural Engineers Paper No. 91-6595. St. Joseph, Michigan: American Society of Agricultural Engineers.

- Boonyasarn, A., B.R. Harte, D. Twede, & J.L. Lee (1992). The effect of cyclic environments on the compression strength of boxes made from high-performance (fibre-efficient) corrugated fibreboard. *TAPPI Journal*, October 1992, pp.79-85
- Brana, L. (1993). International test standards - test procedure equivalents. *International Safe Transit Association Newsletter*, **16**(6), 2.
- Brandenburg, R.K., & J.J.-L. Lee (1988). *Fundamentals of packaging dynamics*. Michigan: MTS Systems Corporation.
- Bull, K.W., & C.F. Kossack (1960). *Measuring field handling and transportation conditions*. WADD Technical Report 60-4 AD 240 777, February 1960.
- Burgess, G.J. (1988). Product fragility and damage boundary theory. *Packaging Technology and Science*, **1**(1), 5-10.
- Byrd, V.L. (1972a). Effect of relative humidity changes during creep on handsheet paper properties. *TAPPI Journal*, **55**(2), 247-252.
- Byrd, V.L. (1972b). Effect of relative humidity changes on compressive creep response of paper. *TAPPI Journal*, **55**(11).
- Byrd, V.L. (1984a). Edgewise compression creep of fibreboard components in a cyclic relative humidity environment. *TAPPI Journal*, **67**(7), 86-90.
- Byrd, V.L. (1984b). A proposed mechanism of creep acceleration in a cyclic RH environment based on sorption behaviour. In *Progress in Paper Physics: A seminar on design criteria for paper performance*, pp.73-78. Stockholm, Sweden: STFI.
- Byrd, V.L. (1986). Adhesive's influence on edgewise compression creep in a cyclic relative humidity environment. *TAPPI Journal*, **60**(4), 70-82.
- Byrd, V.L., & J.W. Koning (1978). Edgewise compression creep in cyclic relative humidity environments. *TAPPI Journal*, **61**(6), 35-37.
- Cairns, J.A., C.R. Elson, G.A. Gordon, & E.H. Steiner (1971). Research Report 174. Leatherhead, England: British Food Manufacturing Industry Research Association.
- Considine, J.M., & T.L. Laufenburg (1992). Literature review of cyclic humidity effects on paperboard packaging. In *Proceedings of the Symposium on Cyclic Humidity Effects on Paperboard Packaging*, 14 - 15 September 1992, Forest Products Laboratory, Madison, Wisconsin.

- Considine, J.M., D.E Gunderson, P. Thelin, & C. Fellers (1989). Compressive creep behaviour of paperboard in a cyclic humidity environment: Exploratory experiment. *TAPPI Journal*, **72**(11), 131-136.
- Considine, J.M., D.L. Stoker, T.L. Laufenburg, & J.W. Evans (1994). Compressive creep behaviour of corrugating components affected by humid environment. *TAPPI Journal*, **77**(1), 87-95.
- * Crofts, B.W. (1989). The effect of simulated handling on the compression performance of corrugated fibreboard containers. M.S. Thesis, School of Packaging, Michigan State University, East Lansing, MI.
- Data Electronics (1985). *Datataker user's manual and operator's guide*. Data Electronics (Aust.) Pty Ltd.
- De Ruvo, A., R. Lundberg, S. Martin-Lof, & C. Soremark (1976). Influence of temperature and humidity on elastic and expansional properties of paper and the constituent fibre. In Transactions of BPBIF Symposium on Fundamental Properties of Paper Related to Uses, pp.785-806, 1976.
- DPI&E/AQIS (1990). *Code of practice for handling fresh fruit and vegetables in refrigerated shipping containers*. Department of Primary Industries and Energy/Australian Quarantine and Inspection Service.
- Eagleton, D.G., & J.A. Marcondes (1994). Moisture sorption isotherms for paper-based components of transport packaging for fresh produce. *TAPPI Journal*, **77**(7), 75-81.
- Fiedler, R.M. (1993). Using ASTM D 4169 test plans to comply with ISO 4180 performance testing requirements. In Proceedings of the 8th IAPRI World Conference on Packaging, Brazil, 1993.
- * Foley, J.T. (1972). *Transportation shock and vibration descriptions for package designers*. Sandia Laboratories Report SC-M-72 0076, July 1972.
- Foley, J.T., M.B. Gens, & C.F. Magnuson (1972). Current predictive models of the dynamic environment of transportation. Proceedings of the Institute for Environmental Sciences, pp.35-44.
- Fox, T.S. (1978). Shipping containers and cartons shown to fail only in compression when loaded internally. *Paperboard Packaging*, **62**(3), 23.

- Fox, T.S., W.J. Whitsitt, R.W. Nelson, & J.A. Watt (1978). *Determination of the fundamental combined board and component properties which govern corrugated container performance*. Progress Report One, Project 3272. Appleton, WI: The Institute of Paper Chemistry.
- Goff, J.W., J. Grebe, D. Twede, & T. Townsend (1984). *You'll never see it from the road*. Technical Report No. 26. Michigan: School of Packaging, Michigan State University.
- Gordon, J.E. (1978). *Structures*. Middlesex, England: Penguin Books Ltd.
- * Graesser, L.K., S.P. Singh, & G. Burgess (1992). A performance study for two portable data recorders used to measure package drop heights. *Packaging Technology and Science*, **5**, 57-61.
- Gunderson, D.E. (1981). A method for compressive creep testing of paperboard. *TAPPI Journal*, **64**(11), 67-71.
- Gunderson, D.E. (1991). Box performance in the real world. *MARI/Board Converting News*, Jan/Feb 1991.
- Gunderson, D.E., & W.E. Tobey (1990). Tensile creep of paperboard: Effect of humidity change rates. In *Materials Interactions Relevant to the Pulp, Paper, and Wood Industries*, pp.213-226. Pittsburg, PA: Materials Research Society.
- Gunderson, D.E., J.M. Considine, & C.T. Scott (1988). The compressive load-strain curve of paperboard: Rate of load and humidity effects. *JPPS*, **14**(2), J37-J41.
- Hanlon, J.F. (1984). *Handbook of package engineering*. New York: McGraw-Hill.
- Harris, C.M. (Ed.) (1988). *Shock and vibration handbook*. New York: McGraw-Hill Book Company.
- * Hasegawa, K. (1989). Analysis of vibration and shock occurring in transport systems. *Packaging Technology and Science*, **2**, 69-74.
- Haslach, H.W., M.G. Pecht, & X. Wu (1990). Viscoelastic model for variable humidity loading in creep. Presented at the Winter Annual Meeting of the American Society of Mechanical Engineers, 25-30 November 1990, Dallas, Texas.
- Haslach, H.W., M.G. Pecht, & X. Wu (1991). Variable humidity and load interaction in tensile creep of paper. In *Proceedings of the 1991 International Paper Physics Conference*, pp.219-224, TAPPI, Atlanta, Georgia, 1991.

- Haslach, H.W., S. Khan, S. Mohammad, & M.G. Pecht (1989). Behaviour of Virginia fibre paper as influenced by relative humidity. In *Mechanics of Cellulosic and Polymeric Materials*, pp.167-172. New York, NY: American Society of Mechanical Engineers.
- Evans, U.I. (1977). The effect of ambient relative humidity on the moisture content of palletised corrugated boxes. *TAPPI Journal*, **60**(4), 79-82.
- IST (1993a). *Environmental data recorder with EDRIS software program: User operating manual*. Lansing, Michigan: Instrumented Sensor Technology, Inc.
- IST (1993b). *EDR2S software user operating manual*. Lansing, Michigan: Instrumented Sensor Technology, Inc.
- Johnson, E.E. (1971). The shock and vibration environment of packages carried on a 3-ton general purpose truck. In *Shock Environment of Packages in Transport*, p.27. London: Society of Environmental Engineers.
- Johnson, M.W., & T.J. Urbanik (1984). A nonlinear theory for elastic plates with applications to characterising paper properties. *Journal of Applied Mechanics*, **51**(March), 146-152.
- Johnson, M.W., & T.J. Urbanik (1989). Analysis of the localised buckling in composite plate structures with applications to determining the strength of corrugated fibreboard. *Journal of Composite Technology and Research*, **11**(4), 121-127.
- Johnson, M.W., T.J. Urbanik, & W.E. Denniston (1979). Optimum fibre distribution in singlewall corrugated fibreboard. FPL Research Paper 348, United States Department of Agriculture, Forest Service, Forest Products Laboratory, Madison, Wisconsin.
- Jones, C.S., J.E. Holt, & D. Schoorl (1991). A model to predict damage to horticultural produce during transport. *Journal of Agricultural Engineering Research*, **50**, 259-272.
- Kawanishi, K. (1989). Estimation of the compression strength of corrugated fibreboard boxes and its application to box design using a personal computer. *Packaging Technology and Science*, **2**, 29-39.
- Kellicutt, K.Q., & E.F. Landt (1951). Safe stacking life of corrugated boxes. *Fibre Containers*, September 1951, pp.1-5.

- Kirkpatrick, J. (1989). Bureau of meteorology data - Australian cities. Note No. RTC89/460. Alphington, Victoria: Amcor Research and Technology Centre.
- Koning, J.W., & R.K. Stern (1977). Long term creep in corrugated fibreboard containers. *TAPPI Journal*, **60**(12), 129-130.
- Kutt, H., & B.B. Mithel (1968). Studies on compressive strength of corrugated containers. *TAPPI Journal* **51**(4), 79A.
- Labuza, T.P. (1985). An integrated approach to food chemistry: Illustrative cases. In O.R. Fennema (Ed.), *Food Chemistry*. New York: Marcel Dekker.
- Langbridge, D.M. (1983). *Corrugated fibre boxes: Their use in packaging fresh fruit and vegetables*. Melbourne, Victoria: Australian Paper Manufacturers.
- Lansmont (19??). Miscellaneous seminar notes. Monterey, California: Lansmont Corporation
- Lansmont (1990). *Test Partner user guide*. Monterey, California: Lansmont Corporation.
- Laufenburg, T.L. (1991). Characterisation of paperboard, combined board, and container performance in the service moisture environment. *TAPPI International Physics Conference Proceedings*, July 1991, pp.299-304.
- Leake, C.H. (1987). Measuring corrugated box performance. *TAPPI Journal*, **71**(10), 75.
- Leake, C.H., & R. Wojcik (1988). Influence of the combining adhesive on box performance. Presented to the TAPPI Corrugated Containers Conference, October 1988, Orlando, Florida.
- Leake, C.H., & R. Wojcik (1993). Humidity cycling rates: how they influence container life spans. *TAPPI Journal*, **71**(10), 26-30.
- Leng, M. (1994). Personal communication.
- Luo, S., J.C. Suhling, & J.M. Considine (1992). Analytical and experimental investigation on corrugated board. Proceedings of the VII International Congress on Experimental Mechanics, 1992.
- Maltenfort, G.G. (1988). *Corrugated shipping containers: An engineering approach*. Plainview, New York: Jelmar Publishing Company.
- Maltenfort, G.G. (Ed.) (1989). *Performance and evaluation of shipping containers*. Plainview, New York: Jelmar Publishing Company.

- Mansour, A. (1972). Methods of computing and probability of failure under extreme values of bending moment. *Journal of Ship Research*, **16**, 113-123.
- Marcondes, J.A. (1992a). Cushioning properties of corrugated fibreboard and the effects of moisture content. *Transactions of the American Society of Agricultural Engineers*, **35**(6), 1949-1953.
- Marcondes, J.A. (1992b). Effect of load history on the performance of corrugated fibreboard boxes. *Packaging Technology and Science*, **5**, 179-187.
- Marcondes, J.A. (1993). *Packaging for transport*. Presented to the Food Packaging Seminar, 20 - 21 May 1993, Food Research Institute, Werribee, Victoria.
- Marcondes, J.A. (1994). *An introduction to fibreboard packaging*. Melbourne: Victoria University of Technology.
- Marcondes, J.A., & W. Feather (1992). Assessment of vibration levels on truck shipments. Presented at IPENZ conference, December 1992, Auckland, New Zealand.
- Marcondes, J.A., S.P. Singh, & M.B. Snyder (1990). A method to predict vertical acceleration in truck shipments using road roughness information. *Institute of Packaging Professionals Technical Journal*, Fall 1990, 26-31.
- McDougall, A. (1992). Laboratory testing of packaging systems. *Food Technology in New Zealand*, August 1992.
- McKee, R.C., J.W. Gander, & J.R. Wachuta (1961). Edgewise compression strength of corrugated board. *Paperboard Packaging*, **46**(11), 70-76.
- McKee, R.C., J.W. Gander, & J.R. Wachuta (1962). Flexural stiffness of corrugated board. *Paperboard Packaging*, **47**(12), 111-118.
- McKee, R.C., J.W. Gander, & J.R. Wachuta (1963). Compression strength formula for corrugated boxes. *Paperboard packaging*, **48**(8), 149-159.
- Melbourne, W.H. (1977). Probability distributions associated with the wind loading of structures. *Civil Engineering Transactions, Institution of Engineers Australia*. **19**, 58-67.
- Mohsenin, N.N. (1970). *Physical properties of plant and animal materials*. New York: Gordon and Breach Science Publishers.

- Monaghan, J.D., & J.A. Marcondes (1992). Overhang and pallet gap effects on the performance of corrugated fibreboard boxes. *Transactions of the American Society of Agricultural Engineers*, **35**(6), 1945-1947.
- Montgomery, D.C. (1991). *Introduction to statistical quality control*. New York: Wiley.
- Moody, R.C., & K.E. Skidmore (1966). How dead load downward creep influence corrugated box design. *Package Engineering*, August 1966.
- Newland, D.E. (1984). *An introduction to random vibrations and spectral analysis*. New York: Wiley.
- Newton, R.E. (1976). *Fragility assessment: Theory and test procedure*, Report 160.06. Michigan: MTS Systems Corporation.
- Okushima, S., & A.A. Robertson (1979). Humidity and tensile behaviour of paper. In Proceeding of 1979 International Paper Physics Conference, pp.83-88, TAPPI, Atlanta, California, 1979.
- Ostrem, F.E., & W.D. Godshall (1979). *An assessment of the common carrier shipping environment*. General Technical Report FPL 22. Forest Products Laboratory, Forest Service, United States Department of Agriculture.
- PCB (1993a). *Vibration and shock sensor selection guide: Piezoelectric accelerometers*. Depew, New York: PCB Piezotronics, Inc.
- PCB (1993b). *Quartz compression model 308M310 operator's manual*. Depew, New York: PCB Piezotronics, Inc.
- Peleg, K. (1985). *Produce handling, packaging, and distribution*. Westport, Connecticut: AVI Publishing Company.
- Peleg, K., & S. Hinga (1986). Simulation of vibration damage in produce transportation. *Transactions of the American Society of Agricultural Engineers*, **29**(2), 633-641.
- Peterson, W.S., & T.S. Fox (1980). Workable theory proves how boxes fail in compression. *Paperboard Packaging*, **61**(10).
- Pierce, C.D., S.P. Singh, & G. Burgess (1992). A comparison of leaf-spring with air-cushion trailer suspensions in the transport environment. *Packaging Technology and Science*, **5**(1), 11-15.
- Pommier, J.C., J. Poustis, E. Fourcade, & P. Morlier (1991). Determination of the critical load of a corrugated cardboard box submitted to vertical compression by finite

- element methods. In Proceedings of the 1991 International Paper Physics Conference, pp.437-445, TAPPI, Atlanta, Georgia, 1991.
- Robertson, G.L. (1993). *Food packaging: Principles and practice*. New York: Marcel Dekker.
- Rodriguez, H., S.P. Singh, & G. Burgess (1994). Study of lateral shocks observed during fork truck and pallet jack operations for the handling of palletized loads. *Packaging Technology and Science*, **7**, 205-211.
- Schlue, J.W. (1966). *The dynamic environment of spacecraft surface transportation*. Jet Propulsion Laboratory Technical Report 32-876, March 1966.
- Schoorl, D., & J.E. Holt (1983). Mechanical damage in agricultural products: A basis for management. *Agricultural Systems*, **11**, 143-157.
- Sek, M.A., & V. Rouillard (1992). Application of frequency domain analysis in testing of packages. Presented at the 21st IAPRI Symposium, 20-24 September 1992, Gregersensvej, Denmark.
- Sharp, A. (1993). Personal communication.
- Sharpe, W.N., & T.J. Kusza (1973). *Preliminary measurement and analysis of the vibration environment of common carrier motor carriers*. Michigan State University, School of Packaging, Technical Report 22, September 1973.
- Silvers, W., & H. Caruso (1976). Advances in shipping damage prevention. *Shock and Vibration Bulletin*, **46**(4), 41-48.
- Singh, S.P., G.J. Burgess, J.A. Marcondes, & J.R. Antle (1993). Measuring the package shipping environment in refrigerated ocean vessels. *Packaging Technology and Science*, **6**(4), 175-181.
- Singh, S.P., J.R. Antle, & G.J. Burgess (1992). Comparison between lateral, longitudinal, and vertical vibration levels in commercial truck shipments. *Packaging Technology and Science*, **5**(2), 71-75.
- Siyami, S., G.K. Brown, G.J. Burgess, J.B. Gerrish, B.R. Tennes, C.L. Burton, & R.H. Zapp (1988). Apple impact bruise prediction models. *Transactions of the American Society of Agricultural Engineers*, **31**, 1038-1046.
- Sobczak, R.F. (1977). Clamp handling without case damage: A study of the lateral forces. *Package Development and Systems*, Nov/Dec, p.22.

- Soremark, C., & C. Fellers (1991). Mechanosorptive creep and hygroexpansion of corrugated board in bending. In Proceedings of the 1991 International Paper Physics Conference, pp.549-550, TAPPI, Atlanta, Georgia, 1991.
- SPI (1980). *Stacking performance of plastic bottles in corrugated boxes*. New York: The Society of Plastics Industry, Inc.
- Stevenson, B. (1994). Personal communication.
- Story, A. (1994). *The nature of fresh produce*. Presented at the workshop on Transportation of Fresh Horticultural Perishables, 25 March 1994, Melbourne, Victoria.
- Stott, R.A. (1991). Containment capability of corrugated boxes. *APPITA*, **44**(1).
- Swec, L.F. (1986). Boxes, corrugated. In M. Bakker (Ed.), *The Wiley Encyclopaedia of Packaging Technology*, pp.66 - 76. New York: Wiley.
- TAPPI (1991a). *TAPPI useful methods 1991*. Atlanta, Georgia: TAPPI Press.
- TAPPI (1991b). *TAPPI test methods 1992 - 1993*. Atlanta, Georgia: TAPPI Press.
- Tevelow, F.L. (1983). *The military logistical transportation vibration environment: It's characterisation and relevance to MIL-STD vibration testing*. United States Army Electronics Research and Development Command, Harry Dimond Laboratories.
- Thermo King (1992). Thermo King SB-III TF promotional material TK30172-2 (10/92).
- Thompson, W.T. (1993). *Theory of vibration with applications*. London: Chapman & Hall.
- Urbanik, T.J. (1981). *Effect of paperboard stress-strain characteristics on strength of singlewall corrugated fibreboard: A theoretical approach*. Madison, Wisconsin: United States Department of Agriculture, Forest Service, Forest Products Laboratory.
- USDoD (19??). *MIL-HDBK-304: Military standardisation handbook, package cushioning design*. United States Department of Defence.
- Vaisala Sensor Systems (1985). Benchtop indicator and probes for relative humidity and temperature: Technical data sheet A0485. Helsinki, Finland: Vaisala Sensor Systems.
- Vergano, P.J., R.F. Testin, A.C. Choudhari, & W.C. Newall (1992). Peach vibration bruising: The effect of paper and plastic films between peaches. *Journal of Food Quality*, **15**, 183-197.

- White, M.S. (1992). Starting with the foundation: The impact of pallet design on the performance of unit loads. *Institute of Packaging Professionals Technical Journal*, **10**(2), 44-50.
- Whitsitt, W.J., & R.C. McKee (1975). Effect of relative humidity on the stacking performance of boxes made with water-resistant adhesive and with regular and wet-strength components. Report One, Project 2695-16, IPC (A Summary Report to the Technical Division, Fourdrinier Kraft Board Institute).
- Wink, W.A. (1961). The effect of relative humidity and temperature on paper properties. *TAPPI Journal*, **44**(6), 171A-180A.
- Wright, P.G., P.R. McKinlay, & E.Y.N. Shaw (1992). *Corrugated fibreboard boxes: Their design, use, quality control, and testing*. Camberwell, Victoria: Amcor Fibre Packaging.
- Zhao, L. (1994). *Evaluation of the performance of corrugated shipping containers: Virgin versus recycled boards*. Master of Engineering thesis, Victoria University of Technology, Melbourne, Victoria.

APPENDIX A: PACKAGING PERFORMANCE TEST STANDARDS

This Appendix lists the documents referenced in each of the standards for the compilation of performance test schedules (ISO 4180, ASTM D 4169, and AS 2584). It also lists relevant documents which are referenced in this thesis but which are not necessarily referred to in these standards.

The following table shows some common international (ISO) transport packaging test standards and their equivalents in other systems.

Table 38: International (ISO) transport packaging test standards and test procedure equivalents.

Packaging Standards for Testing	ISO (Int'l)	ASTM (USA)	ISTA (USA)	BSI (UK)	EN (EC-Unified)	JSI (Japan)	DIN (Germany)
Identification of parts when testing	2206	D 996			JIS 0201		
Conditioning for testing	2233	D 4332	Project 1, 1A, 2, 2A	4826-2	EN 22233 (06/93)	JIS 0203	DIN ISO 2233 DIN 55438
Stacking test	2234	D 4577	Project 1, 1A, 2, 2A	4826-3	EN 22234 (06/93)		DIN ISO 2234
Horizontal impact test (inclined plane)	2244	D 4003	Project 1, 1A, 2, 2A	4826-5	EN 22244 (06/93)	JIS 0205	DIN ISO 2244
Vibration testing (low frequency)	2247	D 999	Project 1, 1A, 2, 2A	4826-6	EN 22247 (12/93)	JIS 0232 B-1	DIN ISO 2247
Vibration testing (variable frequency)	8318	D 3580 D 4728		4826-12	EN 28318 (12/93)	JIS 0232 A-1	DIN ISO 8318
Drop (vertical impact) testing	2248	D 5276	Project 1, 1A, 2, 2A	4826-4		JIS 0202 0217 (bag)	DIN ISO 2248
Compression test	2872	D 642	Project 1, 1A, 2, 2A	4826-9		JIS 0212B	
Low pressure test	2873						
Stacking test (using a compression tester)	2874	D 642	Project 1, 1A, 2, 2A	4826-9	EN 22874 (12/93)	JIS 0212A	DIN ISO 2875
Water spray test (climatic test)	2875	D 951		4826-10	EN 22875 (12/93)		
Rolling test	2876			4826-2			
General rules/test for distribution cycle	4180/2	D 4169	Project 1, 1A, 2, 2A			JIS 0200	

Source: Brana (1993), ASTM (1994).

A.1 INTERNATIONAL (ISO) STANDARDS

- ISO 2206: Packaging - Complete, filled transport packages - Part 1: Identification of parts when testing.
- ISO 2233: Packaging - Complete, filled transport packages - Part 2: Conditioning for testing.
- ISO 2234: Packaging - Complete, filled transport packages - Part 3: Stacking test.
- ISO 2244: Packaging - Complete, filled transport packages - Part 5: Horizontal impact tests (including plane test; pendulum test).
- ISO 2247: Packaging - Complete, filled transport packages - Part 6: Vibration test.
- ISO 2248: Packaging - Complete, filled transport packages - Part 4: Vertical impact test by dropping.
- ISO 2872: Packaging - Complete, filled transport packages - Part 7: Compression test.
- ISO 2873: Packaging - Complete, filled transport packages - Part 8: Low pressure test.
- ISO 2874: Packaging - Complete, filled transport packages - Part 9: Stacking test using compression tester.
- ISO 2875: Packaging - Complete, filled transport packages - Part 10: Water spray test.
- ISO 2876: Packaging - Complete, filled transport packages - Part 11: Rolling test.
- ISO 4180/1: Complete, filled transport packages - General rules for the compilation of performance test schedules - Part 1: General principles.
- ISO 4180/1: Complete, filled transport packages - General rules for the compilation of performance test schedules - Part 2: Quantitative data.

A.2 ASTM STANDARDS

- ASTM D 642: Method of compression test for shipping containers.
- ASTM D 951: Test method for water resistance of shipping containers by spray method.
- ASTM D 996: Terminology of packaging and distribution environments.
- ASTM D 999: Methods of vibration testing of shipping containers.
- ASTM D 1083: Test methods for mechanical handling of unitised loads and large shipping cases and crates.
- ASTM D 3332: Standard test methods for mechanical-shock fragility of products, using shock machines.
- ASTM D 4003: Methods of controlled horizontal impact test for shipping containers.
- ASTM D 4169: Practice for performance testing of shipping containers and systems.
- ASTM D 4332: Practice for conditioning containers, packages, for packaging components for testing.

- ASTM D 4577: Test method for compression resistance for a container under constant load.
- ASTM D 4728: Test method for random vibration testing of shipping containers.
- ASTM D 5276: Test method for drop test of loaded containers by free fall.
- ASTM D 5277: Test method for performing programmed horizontal impacts using an inclined tester.

A.3 AUSTRALIAN (AS) STANDARDS

- AS 1301: Endorsed APPITA test standards.
- AS 2400: SAA packaging code - Part 1: Glossary of packaging terms.
- AS 2582.1: Complete, filled transport packages - Methods of test - Identification of parts when testing.
- AS 2582.2: Complete, filled transport packages - Methods of test - Conditioning for testing.
- AS 2582.3: Complete, filled transport packages - Methods of test - Stacking, compression test.
- AS 2582.4: Complete, filled transport packages - Methods of test - Vertical impact test by dropping.
- AS 2582.5: Complete, filled transport packages - Methods of test - Horizontal impact test (modified plane test, pendulum test).
- AS 2582.6: Complete, filled transport packages - Methods of test - Vibration test.
- AS 2582.7: Complete, filled transport packages - Methods of test - Low pressure test.
- AS 2583: Complete, filled transport packages - Distribution trials - Information to be recorded.
- AS 2584.1: Complete, filled transport packages - General rules for the compilation of performance schedules - Part 1: General principles.
- AS 2584.2: Complete, filled transport packages - General rules for the compilation of performance schedules - Part 2: Quantitative data.

A.4 TAPPI STANDARDS

- UM 800: Performance testing of corrugated fibreboard shipping containers.
- T 801 om: Impact resistance of fibreboard shipping containers.
- T 802 om: Drop test for fibreboard shipping containers.
- T 817 om: Vibration test for fibreboard shipping containers.

A.5 APPITA STANDARDS

These test standards are endorsed by SAA as part of AS 1301.

- APPITA P414m: Conditioning of paper for testing.
- APPITA P415m: Standard atmosphere for paper testing.
- APPITA P416s: Determination of temperature and relative humidity of atmosphere for paper and paperboard testing.
- APPITA 800s: Compression resistance of fibreboard boxes (cases).

A.6 UNITED STATES MILITARY STANDARDS

- MIL-P-116: Methods of preservation.
- MIL-STD-2073-1: Department of Defence material, procedures for the development and application of packaging requirements.

APPENDIX B: DESCRIPTION OF EXPERIMENTAL EQUIPMENT

B.1 IST EDR-1 ENVIRONMENTAL DATA RECORDER

The IST Environmental Data Recorder model EDR-1, and EDR1S and EDR2S operating software packages, are designed for recording, reporting, and graphically analysing large amounts of transient or continuous acceleration data, measured over three independent sensing axes (IST, 1993a; IST 1993b). The EDR contains a built-in triaxial 100 g accelerometer, a rechargeable battery power supply, an RS-232 computer interface port, and 4 MB of solid state memory, and functions as a portable, self-contained digital sensor and recorder. The EDR also contains four external channel inputs for using up to three external accelerometers and a temperature sensor, and hence may be used as an acceleration recorder for remotely mounted accelerometers. The three external accelerometer channels record simultaneously and may therefore be used to measure acceleration at different locations on a structure, or acceleration in three directions at a single location.

The EDR records and stores acceleration waveform data only when certain pre-set waveform criteria are met. The actual recording operates in an event-triggered fashion, and the EDR only records an acceleration event when any one or more of the three selected accelerometer input channels (internal or external) exceed a pre-set trigger level (in g). In addition, a minimum trigger duration threshold (TDT) may be specified for which an acceleration event must continuously be above the specified trigger level before the event will be recorded. Pre- and post-trigger measurement sample lengths may also be specified to ensure that the complete leading and trailing edges of the acceleration waveforms are captured. These parameters are set using the EDR1S or EDR2S software.

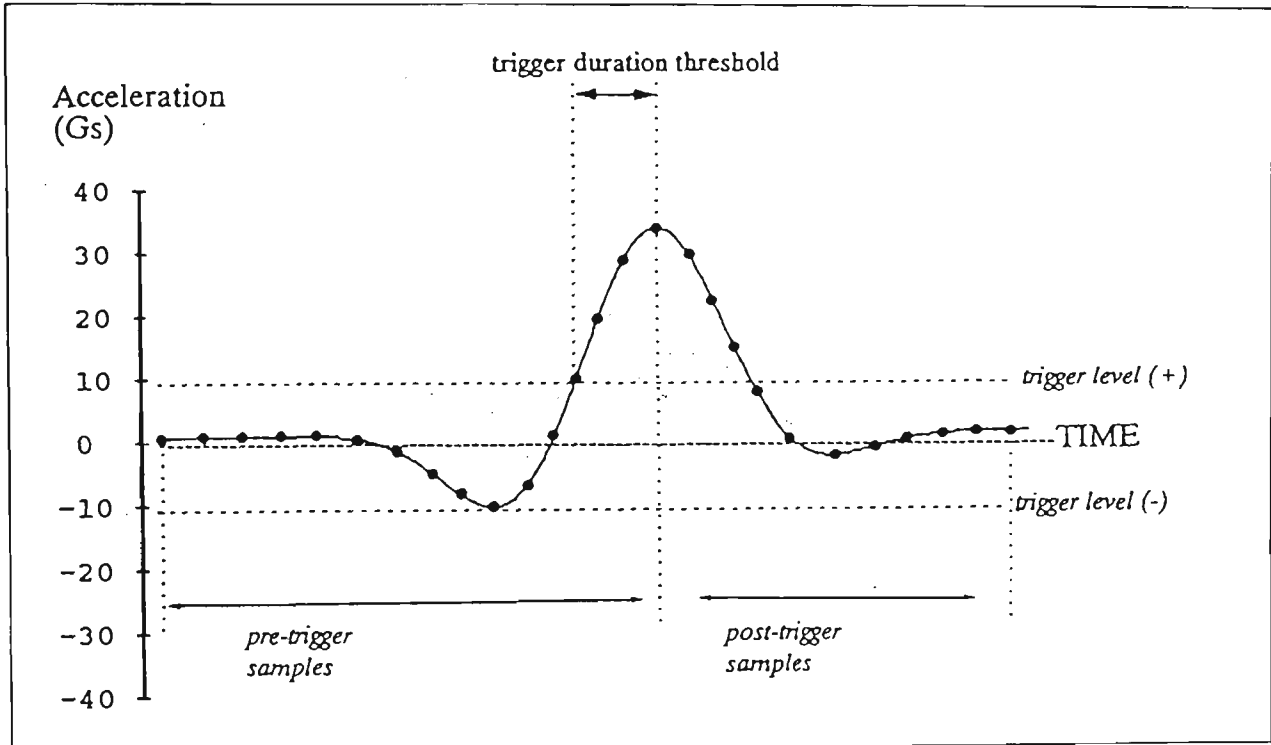
When recording is triggered by threshold excursions on any one or more of the three accelerometer channels, the acceleration waveforms on each channel are recorded simultaneously and stored independently in the EDR data memory. The EDR unit uses a

10-bit analogue-to-digital converter (ADC) to sample the continuous waveform data. The EDR has continuous timekeeping ability and stores the date and time of occurrence along with each recorded event. The EDR also measures and records environment temperature using either a solid state temperature sensor built into the unit, or an external temperature sensor. The temperature sampling period is specified independent of the acceleration event recording.

Configuration information from EDR1S or EDR2S is downloaded to the EDR using the RS-232 link between the PC and the EDR. The selections for the recording control parameters (RCPs) directly affect the recording function of the EDR. User documentation can also be downloaded to the EDR with the RCPs and retained along with the recorded data for future retrieval.

Once the EDR has recorded the maximum number of events specified, subsequent events will only be recorded if the total velocity change of their waveform exceeds that of any one or more of previously recorded events. The previously recorded event having the smallest total velocity change will then be overwritten by the current event. The total event length in this overwrite mode is fixed at pre-trigger plus post-trigger samples as shown in Figure 46.

Figure 46: Example of EDR event-triggered acceleration waveform recording in overwrite memory mode.



Source: IST (1993a).

B.2 PCB ICP ACCELEROMETERS

The three accelerometers used in this study were integrated circuit piezoelectric (ICP) accelerometers of an upright compression design, manufactured by PCB Piezotronics, Inc., as detailed in Table 39.

Table 39: PCB ICP accelerometers for transport shock and vibration recording.

	Channel 1	Channel 2	Channel 3
Accelerometer model	308M347	303M173	308M310
Voltage sensitivity (mV/g)	2.03	4.95	50.6
Range ($\pm g$)	237.56	98.36	9.65
Resolution ($\pm g$)	0.46	0.19	0.02

These accelerometers are modified versions of standard PCB accelerometers, and are specifically designed to operate in conjunction with the EDR. The accelerometer ranges and resolutions given in Table 39 are the effective ranges and resolutions when the accelerometer are used with the EDR. The accelerometers were linked to the EDR with

general purpose coaxial cables, approximately 50 cm in length, which terminated with 10-32 coaxial ('microdot') plugs.

These three accelerometers were chosen to obtain a variety of acceleration ranges and resolutions. The large range of the channel 1 accelerometer was suitable for recording high-amplitude shocks, and the high resolution of the channel 3 accelerometer was suitable for recording low-amplitude vibration. The channel 2 accelerometer was selected to provide an intermediate range and resolution.

B.3 IST EDR1S AND EDR2S SOFTWARE PACKAGES

The EDR1S program is used for communicating set-up information and recorded data to and from the EDR via a PC. EDR1S also contains several features for analysing transient (shock) acceleration events, including graphical waveform display and hardcopy generation, EDH determination from triaxial acceleration waveforms, and statistical data reduction.

The EDR2S program also allows communication for set-up and data retrieval, graphical waveform display, and hardcopy generation. EDR2S is designed primarily for application to random vibration data, but it can also be used for transient data analysis. It provides some statistical data reduction, but its main strength is its PSD generation and graphical analysis.

The major difference between these two programs is that EDR1S returns the results in terms of shock event amplitude, velocity change, duration, and EDH, with the assumption that a triaxial arrangement of accelerometers is used. In contrast, EDR2S makes no assumptions about the direction or location of the accelerometers, and the results are returned independently as acceleration characteristics for each channel.

Shock and vibration data from the EDR1S and EDR2S software were exported in ASCII files, and imported into the Microsoft Excel for Windows spreadsheet for further analysis and presentation.

B.4 DT100F DATATAKER DATA LOGGER

The model DT100F Datataker data logger is a microprocessor-based data acquisition unit able to monitor, record, and control a wide variety of physical parameters such as temperature, pressure, flow rates, counts, and events (Data Electronics, 1985). The Datataker can be operated using any computer or terminal host with a RS-232C, RS-422, or RS-423 serial interface. Data may either be received by the host as the input channels are scanned by the Datataker, or stored in the Datataker's memory for later upload. All communications to and from the Datataker are in standard ASCII format and may be made via any serial communications program.

The Datataker has 23 differential analogue input channels, which may also be used as 46 single-ended channels or any mix of differential and single ended channels. The only information required by the Datataker is a specification of the type of analogue input in use (e.g. voltage, current, frequency, resistance, thermocouple type, etc.) on each channel. The Datataker also has 8 digital input channels, 1 or 2 analogue output channels, and 8 digital output channels.

The Datataker incorporates a real-time clock which keeps the current time to the nearest second and the current day in a serial number format. The Datataker has 24 kB of battery-backed data-storage memory, which is sufficient for storage of approximately 10700 readings. Programming of the Datataker is accomplished using a simple set of commands which provide for scanning input channels, storing or returning recorded data, and setting output channels, alarms, and control loops.

The Datataker fully supports the ANSI thermocouple types J, K, N, T, R, and S, and automatically provides reference junction temperature compensation, zero voltage

compensation, and linearisation calculations over the useful temperature range for each thermocouple type. Readings are returned directly in various degree scales with a resolution of 0.1°C and an accuracy better than $\pm 0.5^{\circ}\text{C}$ (maximum error when used with an isothermal block).

For these experiments the Datataker data logger was hard-wired to provide 23 differential analogue input channels for use with the thermocouples and the RH probe. Twelve ANSI Type T thermocouples were used for all temperature measurements. Two Vaisala HMP 35 humidity and temperature probes were used for all RH measurements.

B.5 ANSI TYPE T THERMOCOUPLES

The reference junctions of thermocouples are traditionally maintained at 0°C , as assumed in standard thermocouple calibration tables. However, this is impractical for portable or remote applications, and a more practical approach is to maintain the thermocouple reference junctions at ambient temperature, and to allow them to drift with the ambient temperature. In this approach, the thermocouple reference junctions are maintained at equal temperatures by placing them in close thermal proximity to a good heat conductor, or isothermal block, usually a block of copper, aluminium, or similar material with a high thermal conductivity. If the temperature of the thermocouple reference junctions is known, then the temperature measured by the thermocouple measurement junction can be corrected. This correction overcomes errors produced by a non-zero thermocouple reference junction temperature, and is referred to as reference junction temperature compensation.

A working alternative to using a separate isothermal block is to connect the thermocouples directly to the rear panel connector of the Datataker (which therefore becomes the reference junctions), and to use the case temperature as the reference junction temperature. The case temperature of the Datataker is measured by an LM335 temperature sensor internally connected to analogue input channel 25. Using the case temperature of the Datataker as the reference temperature can lead to temperature

measurement errors, particularly if there is a temperature gradient across the Datalogger. However these errors can be minimised by maintaining the Datalogger in a reasonably isothermal environment, and in such cases an accuracy of $\pm 1^\circ\text{C}$ has been reported (Stevenson, 1994).

A potential source of error in measurement of thermocouple inputs are the various thermoelectric voltages produced by the effects of temperature gradients on the mixtures of metals in the thermocouple circuit and the measuring instrument. These voltages must be measured and then used to correct the signal voltage read from the thermocouple measurement junction. This is referred to as zero voltage compensation, and is usually achieved using a thermocouple mounted in thermal contact with both the thermocouple reference junctions. As with the reference junction temperature compensation, the zero voltage compensation can also be achieved using a thermocouple measurement junction in thermal contact with the Datalogger case. The internal zero reference is measured on analogue input channel 24.

Another potential source of error arises from the fact that the relationship between temperature and voltage for a thermocouple is not linear. The temperature-voltage relationship of commonly used thermocouples have been accurately measured and published, and are used to calculate the thermocouple temperature from measured voltage in a technique called linearisation.

To calculate the temperature sensed by the thermocouples, the zero reference voltage is subtracted from the voltage measured for the true thermocouple junctions, The resultant voltage is then linearised to calculate the junction temperature of the thermocouples, which is then corrected for the reference junction temperature measured by the LM335 sensor. Linearisation of the thermocouple voltage is carried out by applying two third-order polynomials. The reported linearisation error for a type T thermocouple is less than 1°C for the range -100 - 450°C (Data Electronics, 1985).

B.6 VAISALA HMP 35 HUMIDITY AND TEMPERATURE PROBES

The Vaisala model HMP 35 humidity and temperature probe is a calibrated probe designed for general temperature and relative humidity measurement (Vaisala, 1985). The probe measures approximately 235 mm in length by 25 mm in diameter. The RH measurement range is 0 - 100%, with an accuracy (at 20°C and 90% RH) of $\pm 3\%$. The temperature measurement range is -40 to 60°C.

B.7 IST EDR-3 ENVIRONMENTAL DATA RECORDER

The IST model EDR-3 Environmental Data Recorder is similar to the model EDR-1 used in the transport shock and vibration studies. Its major differences are:

1. The EDR-3's smaller dimensions of $110 \times 105 \times 55$ mm and weight of 1 kg make it more suitable for attaching to a pallet or bulk bin, especially as the unit casing already has holes for screw mountings, and for placing inside a packed box of produce.
2. The EDR-3 is powered by eight 9 V batteries, and has only 1 MB of RAM, which are disadvantageous where extended recording times or data quantities are required, but acceptable for the purposes of this study.
3. The EDR-3 data recorder has an internal 930 Hz anti-aliasing LPF, making it more appropriate for recording short duration handling shocks.
4. The EDR-3 internal accelerometers are detailed in Table 40. The accelerometer ranges and resolutions given in Table 40 are for the accelerometers when used in conjunction with the EDR-3.

Table 40: EDR-3 internal accelerometers used for handling recording.

	Channel 1	Channel 2	Channel 3
Voltage sensitivity (mV/g)	0.2102	0.2063	0.2086
Range ($\pm g$)	78.41	79.89	79.01
Resolution ($\pm g$)	0.15	0.16	0.15

B.8 SERVOHYDRAULIC VIBRATION SYSTEM

The vibration table used was a Lansmont 6000-15 servohydraulic vibration system together with a Schlumberger random vibration (RV) controller providing electrohydraulic closed-loop control. The table itself measured 1520×1520 mm and could accommodate a maximum payload of 1000 kg. The stroke of the table was ± 76 mm, and it had a frequency range of 1 - 300 Hz and an maximum acceleration of 10 g peak.

B.9 BAUMER ULTRASONIC DISPLACEMENT TRANSDUCERS

The deflection of the boxes as the tests progressed was measured using three Baumer Electric UNAM30U9101 ultrasonic sensors. These transducers returned a voltage proportional to the distance from the sensor. The three transducers were calibrated to return the voltage values shown in Table 41. The maximum range of the ultrasonic sensors was 10 V, but the maximum expected displacement was of 250 mm was arbitrarily set to 5.0 V. It can be seen from Table 41 that the calibration constant of each transducer was 40 mm/V, as the sensors had a blind zone at less than 100 mm.

Table 41: Calibration of ultrasonic displacement transducers.

Distance (mm)	Output Sensor 1 (V)	Output Sensor 2 (V)	Output Sensor 3 (V)
100	0.04	0.04	0.04
150	1.68	1.63	1.66
200	3.34	3.30	3.31
250	5.01	5.00	5.00
300	6.68	6.75	6.55

After filtering, the signals were displayed on a chart recorder with a full scale deflection of 5 V (hence the requirement to utilise no more than half of the available sensor output range) and a paper speed of 2 cm/min.

APPENDIX C: SET-UP OF EXPERIMENTAL EQUIPMENT

C.1 IST EDR-1 ENVIRONMENTAL DATA RECORDER

The EDR2S software program was used to set the major RCPs for the EDR, as shown in Table 42.

Table 42: EDR2S RCPs for EDR for transport shock and vibration recording.

Recording Control Parameter	RCP Value
Sample frequency (SF)	500 Hz
Trigger level	0.5 g
Trigger duration threshold (TDT)	4 samples (8 ms)
Pre-trigger samples	250 samples (500 ms)
Post-trigger samples	250 samples (500 ms)
Maximum number of events	1000
Dead-time period (DTP)	500 ms

The definitions of these RCPs are as follows (IST, 1993b):

1. *Sample frequency*: The SF determines the digitisation rate for each accelerometer channel in the instrument. This is the rate at which the analogue input signals are sampled by the ADC and converted to discrete digital numbers for storage in memory.
2. *Trigger level*: The trigger level setting specifies the minimum g-level required on any one or more of the three accelerometer channels before recording will occur. Acceleration levels which do not exceed the trigger level on any of the three channels will not be recorded. A trigger level of 0.5 g means that an acceleration of at least $(0.5 \times 9.81) \text{ m/s}^2$ is required to trigger recording.
3. *Trigger duration threshold*: The TDT specifies the minimum time period for which any one or more of the accelerometer channels must be continuously above trigger level before recording occurs. The TDT is used to control the time duration as well as the amplitude of events to be recorded. The TDT is used primarily for transient shock recording since 'duration' is meaningless when applied to random vibration. A TDT of 4 samples means that event recording will occur only when any of the accelerometer channels is continuously above the trigger level for at least 8 ms. The TDT was used

in this study to conserve battery power by not recording high frequency vibration arising from, for example, the compressor in the trailer refrigeration unit.

4. *Pre-trigger samples*: This specifies the number of data samples that will be recorded before the trigger point on any one or more of the three accelerometer channels. Pre-trigger samples are used to capture the leading edges of acceleration event waveforms. A pre-trigger samples setting of 250 samples means that 500 ms of the event prior to triggering will be recorded.
5. *Post-trigger samples*: The post-trigger samples setting specifies the number of data samples that will be recorded for each event immediately after the trigger. Post-trigger samples are used to capture the trailing edges of acceleration event waveforms. A post-trigger samples setting of 250 samples means that 500 ms of the event waveform after triggering will be recorded. The total length of each recorded event will therefore be 500 samples, or 1000 ms at a SF of 500 Hz.
6. *Maximum number of events*: This RCP specifies the maximum number of events to be recorded before event overwriting will begin. Selecting a maximum of 1000 events means that up to 1000 events can be recorded before the event waveform with the lowest velocity change is overwritten by a more recent event waveform with a higher velocity change. A maximum of 1000 events was chosen as it was slightly below the maximum number possible for the instrument based on the available memory (4 MB).
7. *Dead-time period*: The dead-time period (DTP) specifies a minimum time period between successive event recordings. During this time period the instrument will not trigger. A DTP of 500 ms means that at least 0.5 s will pass after the instrument records one event before it will record the next. A DTP was used in this study to conserve battery power, as the instrument would only be recording for a maximum of 1000 ms per 1500 ms, instead of continuously as it would if subjected to a long period of vibration. While it was possible that some interesting shock events could be missed, the presence of a DTP would have had little effect on vibration recording.

For this study, the frequency range of interest was from 1 - 100 Hz. The EDR contained a 110 Hz anti-aliasing low-pass filter (LPF) with a 3 dB per octave drop-off. The 500 Hz SF gave a Nyquist frequency of $SF / 2 = 250$ Hz, which is at least twice the maximum frequency present and the maximum frequency of interest. A 3 dB software 2nd order

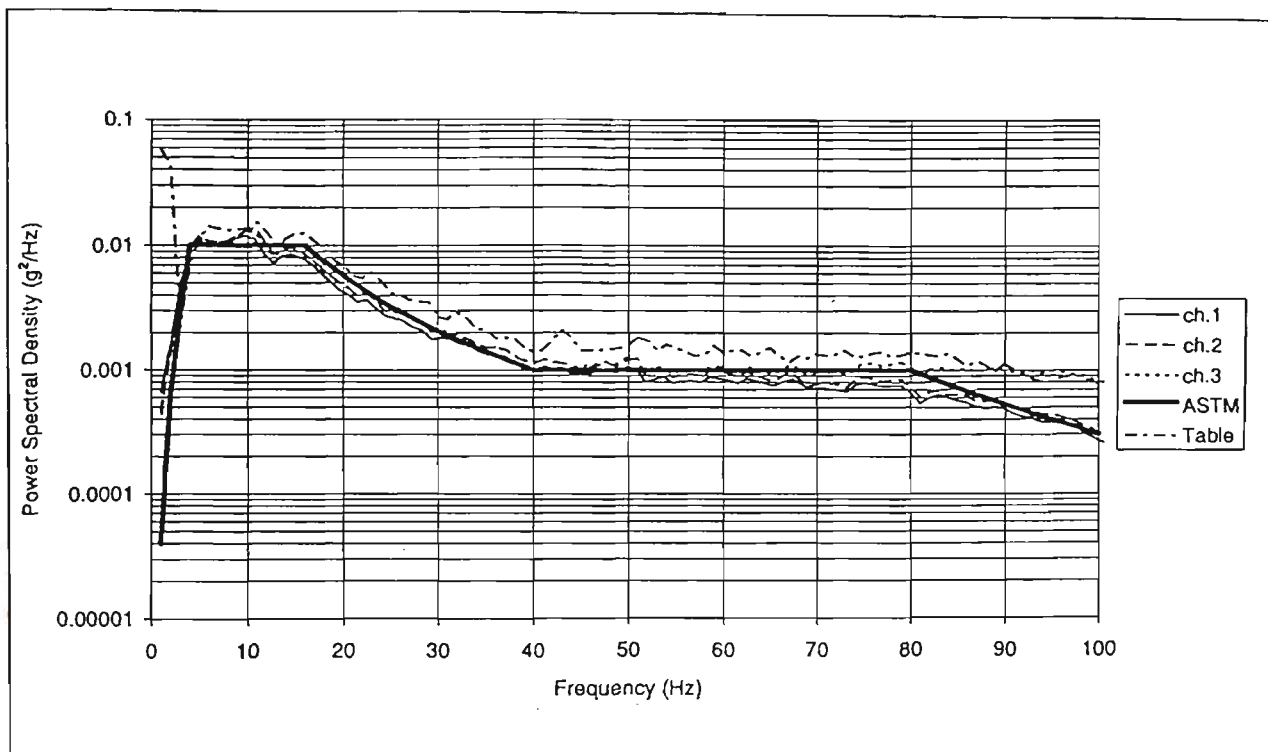
LPF was also used to digitally filter the data during raw data processing. The software LPF cut-off frequency was 100 Hz, which did not alter the data in the frequency range of interest, but it had the effect of smoothing frequencies above 80 Hz. The apparent need for smoothing at these frequencies arose from gain effects of the hardware 110 Hz LPF.

As the SF was 500 Hz and the frame length (FL) of each event was 500 samples, the actual real time frame length was $FL / SF = 1000$ ms with a time resolution of $1 / SF = 2$ ms. The effective digital bandwidth (DBW) of the recorded vibration data was $SF / 2 = 250$ Hz, and the frequency resolution was $SF / FL = 1$ Hz. However, during spectral analysis the frame length was zero-padded to 512 samples, as the discrete Fourier transform (DFT) algorithm used required the length of each sequence of data points to be a power of two. Hence the actual frequency resolution was $SF / 512 \approx 0.977$ Hz. The selection of the SF required a trade-off between time-domain resolution (for shock analysis) and frequency-domain resolution (for vibration analysis), and this SF was regarded as adequate for both purposes.

The spectral analysis was conducted using a Hamming windowing function in order to minimise the problem of side-lobe leakage in the spectral estimates. No overlap between successive records was used, due the discontinuous nature of the EDR recording.

Before the recording of shock and vibration on the trucks could begin, the EDR rig was tested by securing it to a vibration table and subjecting it to a standard acceleration PSD profile. The profile chosen was the ASTM truck random vibration spectrum found in ASTM D 4728 (ASTM, 1994). The test level selected was 0.5 g-RMS, and the test was conducted for about 20 min; sufficient time for 500 events to be recorded. Once the test was completed, the EDR rig was removed from the vibration table, and the recorded data was uploaded to a PC where it was analysed using the EDR2S software and exported in ASCII format to Excel for presentation. It can be seen from Figure 47 that the response of each channel closely follows the vibration table demand, and the EDR rig was deemed to be suitable for the recording of transport shock and vibration.

Figure 47: Verification of EDR test rig using ASTM D 4728 truck spectrum on vibration table.



C.2 DT100F DATATAKER DATA LOGGER

As the Datalogger accepts and uses standard ASCII characters, it may be programmed and interrogated using any serial communications package. For these experiments, the shareware communications package Telix v3.22, from deltaComm Development, was used. The communication between the PC and the Datalogger used the following serial communication parameters: 4800 baud, no parity, 1 stop bit, 8 data bits, and XON/XOFF communication protocol enabled.

When the Datalogger was installed in the refrigerated trailer, the data acquisition could be started in one of two ways. Firstly, the data acquisition functions could be initially software disabled and then software enabled; or secondly, the data acquisition functions could be initially software enabled but hardware. This second approach was used for these experiments. Digital input channel 1 was hard-wired with a small switch. When the switch was closed so that digital input channel 1 was high, analogue input channel scanning was enabled, and when the switch was opened so that digital input channel 1 was low, analogue input channel scanning was disabled. This eliminated the need to use a

portable PC to start and stop the data acquisition when installing and removing the unit at the beginning and end of each week. However a portable PC did have to be used to upload the data each day and to reset the logger without removing the unit from the trailer during the week.

The Datataker contained sufficient memory for approximately 10700 data points. Each scan used 15 data points (1 for the day, 2 for the time, and 12 for each of the 12 analogue input channels) for temperature recording, or 5 data points (only two analogue input channels) for the RH recording. The data logger could therefore record approximately 700 scans for temperature. As the Datataker was checked daily, the maximum rate of temperature scanning was therefore one scan per 2.1 min. For these experiments a scan interval of 3 min was selected, which allows for possible inaccuracies in the logger internal clock, failure of one or more memory chips, and variations in the truck schedule. Approximately 36 hr would therefore have elapsed before memory overwrite occurred. This 3 min interval was chosen for the RH recording, both for simplicity and to allow for response time from the RH probe.

Upload of the acquired data from the Datataker simply required the serial connection of the PC, and the issue of an unload command from Telix. The Telix input buffer could then be saved to disk and loaded into Excel as an ASCII file with space column-delimiting. Resetting the Datataker required resending the program, which was saved as a Telix macro.

Verification of the experimental set-up using a calibrated glass thermometer and a water bath established the maximum measurement error to be $\pm 2^{\circ}\text{C}$ at the 95% level of confidence. The temperature range temperature examined was from 0°C to 30°C with a reference junction temperature of 15°C . This is the range of temperatures likely to be present in a refrigerated trailer, and the accuracy and precision of the experimental set-up was regarded as adequate for the purposes of these experiments.

The accuracy of the RH probes was not verified, as they had been recently calibrated. Their accuracy is reported to be better than 3% RH (20°C , 90 - 100% RH) with a

temperature dependence of 0.04% RH/°C (assuming the probe and electronics are at the same temperature). The long term stability of the probes is reported to be better than 1% RH under normal conditions (Vaisala, 1985).

C.3 IST EDR-3 ENVIRONMENTAL DATA RECORDER

The EDR1S software program was used for the handling study. The EDR1S RCPs used for programming the EDR-3 are detailed in Table 43.

Table 43: EDR1S RCPs for EDR-3 for handling recording.

Recording Control Parameter	Value
Sample frequency (SF)	2000 Hz
Trigger level	0.5 g
Trigger duration threshold (TDT)	4 samples (2 ms)
Pre-trigger samples	400 samples (200 ms)
Post-trigger samples	400 samples (200 ms)
Maximum number of events	100
Dead-time period (DTP)	0 ms

The SF of 2000 Hz, the trigger level of 0.5 g, and the TDT of 2 ms were chosen to ensure sampling of all handling shocks and impacts, even if they were for durations as short as 2 ms. The pre- and post-trigger sample settings were set to adequately sample events up to 400 ms in duration. The maximum number of events to be recorded was set at 100 as the memory of the EDR was only 1 MB, and the handling studies were conducted and analysed continuously and a short processing time was desirable. The DTP was set at 0 ms to sample continuously, if necessary, so that significant handling events could not occur during the dead time period.

Before the study of handling operation was conducted, the EDR and the RCPs were tested by placing the unit inside a typical produce box, packing the box with appropriate ballast, and dropping the box from a series of known heights onto a steel plate on a concrete floor. This was to ascertain whether the EDR's calculation of drop heights based on the recorded shock waveform was accurate and repeatable. A total of 20 flat

drops were made, using drop heights from 5-20 cm at intervals of 5 cm, and five replicates for each drop height.

The EDR calculates drop height from the velocity change in each direction. The individual velocity changes from each internal triaxial accelerometer are used to determine the resultant velocity change according to:

$$\Delta V_R = \sqrt{\Delta V_x^2 + \Delta V_y^2 + \Delta V_z^2} \quad (C.1)$$

where the individual velocity changes are the sum of the impact and rebound velocities. The coefficient of restitution, e , is the ratio of the rebound and impact velocities. The EDR has an acceptable range for e of between 0.3 and 0.75. If the calculated value is outside this range, the EDR uses a default value of 0.5. The drop height is then calculated using the resultant velocity change and Equation (2.15). The results from the test drops are shown in Table 44.

Table 44: Drop test verification of EDR-3 for handling study.

Drop Height (cm)	5	10	15	20
Rep 1	5.1	5.1	7.6	7.6
Rep 2	2.5	7.6	5.1	12.7
Rep 3	5.1	7.6	2.5	2.5
Rep 4	0.0	7.6	7.6	15.2
Rep 5	2.5	5.1	7.6	15.2
Average	3.0	6.6	6.1	10.6
Percent difference (%)	-40%	-34%	-59%	-47%

It can be seen from Table 44 that the accuracy and repeatability of the EDR-3 for drop height measuring is not particularly good. This could be due to:

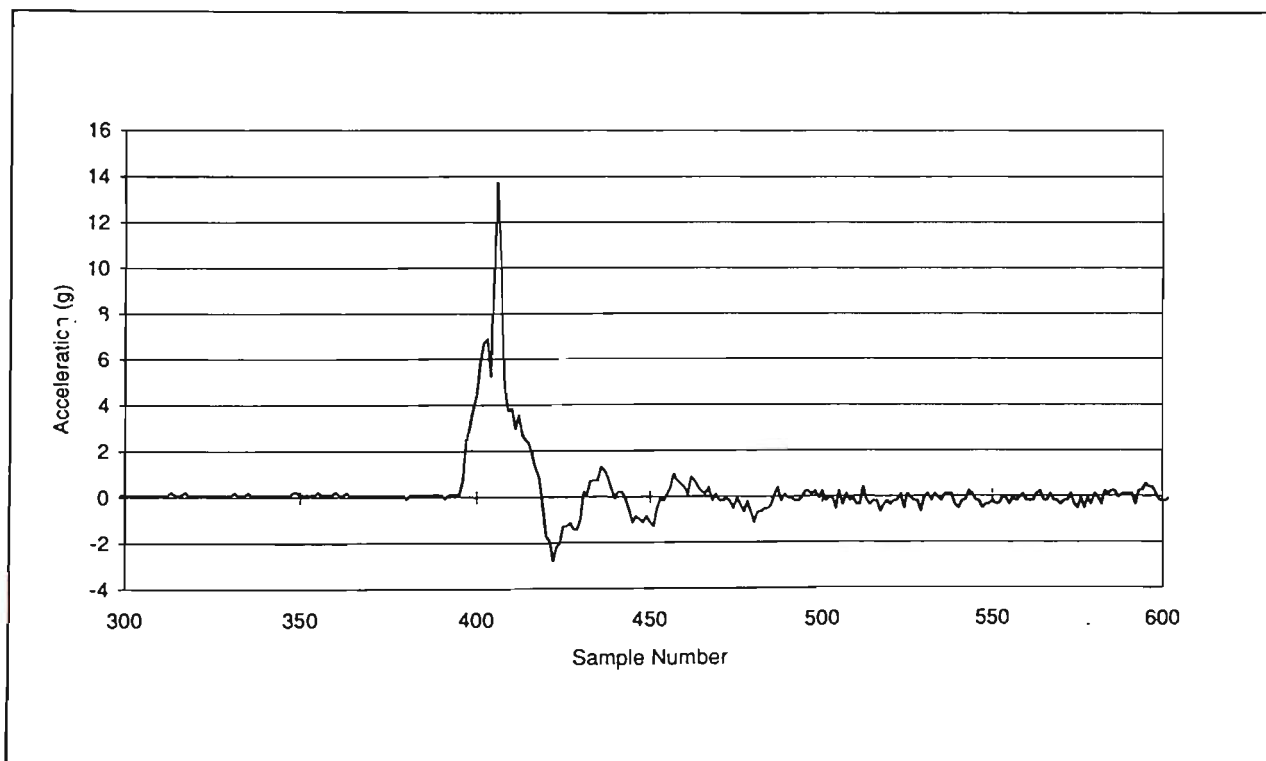
1. The relatively low drop heights involved. Graesser et al. (1992) found errors between 5 and 25% for flat drops between 18 and 36 in (46 and 91 cm). In addition, the drop heights calculated have a resolution of 1 in (2.54 cm) due to limitations of the EDR.
2. The method the EDR uses to calculate e . The assumption that the instant of peak acceleration corresponds to the point of zero velocity is not always true, and the instant of peak acceleration may not be correctly located for uneven or relatively flat waveforms.

3. Dissipation of some free-fall energy. If the falling package rotates on impact, then some free-fall energy is dissipated without being detected by the accelerometers. Equation (2.15) assumes that e is calculated from a flat drop, and the effect of any energy dissipation is that the package appears to have fallen from a lower height.

The EDR also is unable to distinguish between events caused by drops and events caused by impacts. For impacts, the calculated EDH is the ideal free-fall drop height required to produce the same total velocity change as measured on the recorded impact waveform.

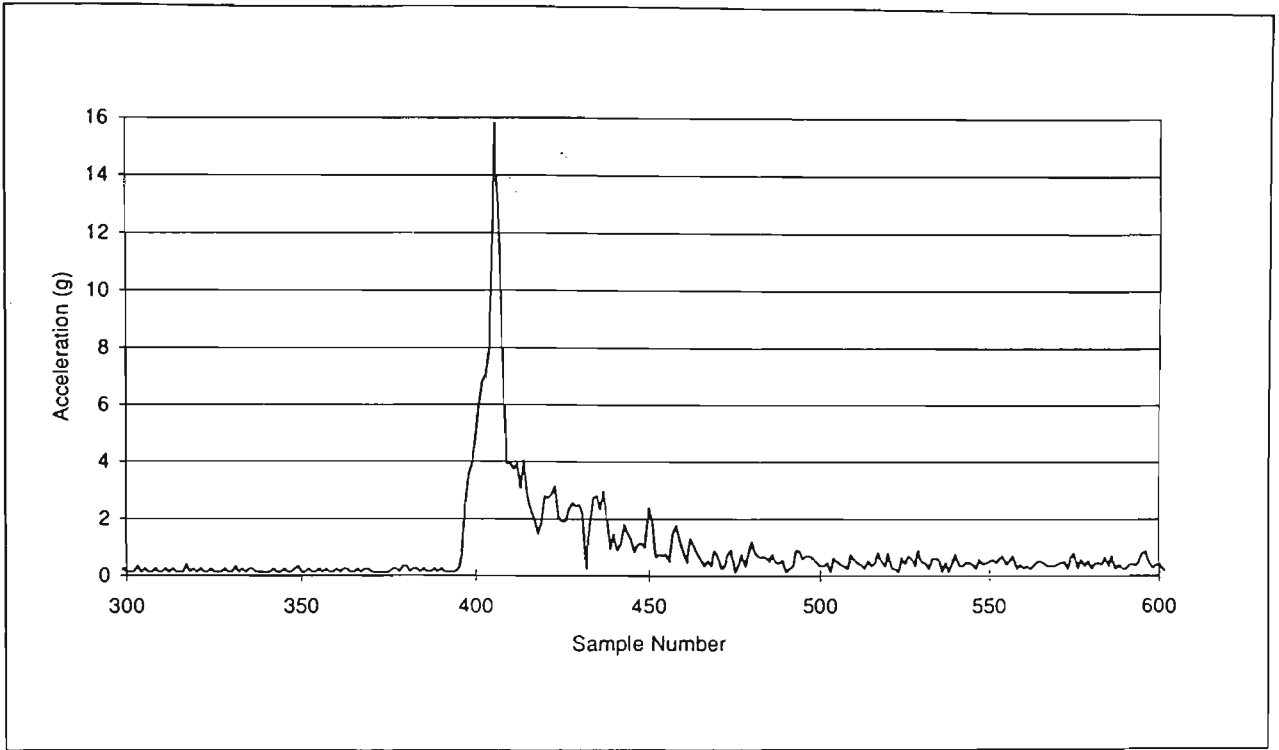
Figure 48 and Figure 49 show a typical package drop shock pulse. This shock pulse is the fourth replicate drop from 5 cm. From the EDR1S software, the statistics for this event are: duration $\tau = 10$ ms, velocity changes $\Delta V_x = 51$ cm/s, $\Delta V_y = 8$ cm/s, $\Delta V_z = 5$ cm/s, $\Delta V_R = 51$ cm/s, $G_m = 15.7$ g, drop height $h = 0.0$ cm, and $e = 0$. Figure 48 shows the vertical component of the waveform and Figure 49 shows the resultant waveform.

Figure 48: Typical package drop shock pulse (vertical axis).



Note: 1 sample taken per 0.5 ms.

Figure 49: Typical package drop shock pulse (triaxial resultant).



Note: 1 sample taken per 0.5 ms.

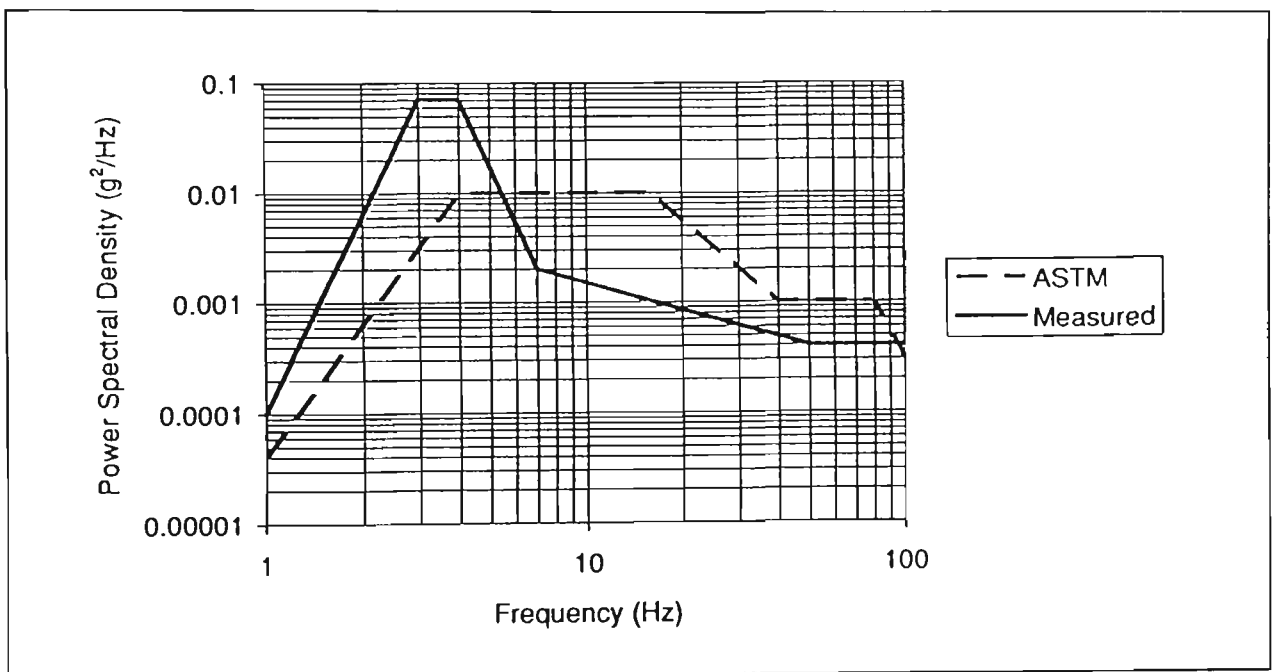
Because the EDR tended to underestimate the calculated drop height, it was decided to obtain only the distributions of peak acceleration, duration, and velocity change for each event. The drop height distribution was then calculated from the velocity change distribution in the same manner as for the transport shock recording shown in Table 14.

For example, for the resultant waveform in Figure 49, the EDH calculated by the EDR is 0.0 cm, and the EDH calculated by Equation (2.15) with $\Delta V_R = 51$ cm/s and $e = 0$ (i.e. worst case) is 1.3 cm. This is more precise than the EDR calculation, but still inaccurate. If the resultant waveform is assumed to be a half-sine in shape, then the velocity change calculated from Equation (2.8), with $G_m = 15.7$ g and $\tau = 10$ ms, is 98 cm/s. When this velocity change is used in Equation (2.15), the calculated EDH is 4.9 cm. Although several assumptions are made in this calculation, the result is close to the true drop height. When this calculation was repeated for the other drops in Table 44, the results were largely within 20%. Hence the waveform peak acceleration and duration, together with the assumptions that the waveform is half-sine in shape and that the coefficient of restitution is zero, appears to give a better estimate of the true drop height, and this approach is used in this study.

C.4 IST EDR-3 ENVIRONMENTAL DATA RECORDER

The demand PSD profile used on the RV controller was that collected during the field shock and vibration recording, as shown in Figure 6. The breakpoints for the average envelope of these recorded PSD profiles were then set in the RV controller. The measured experimental PSD profile and the recommended ASTM truck PSD profile are shown together in Figure 50 for comparison.

Figure 50: Comparison of experimental and standard ASTM truck PSD profiles.



It can be seen from the experimental curve in Figure 50 that frequencies in the range of 0.5 - 7 Hz are the most significant.

The values of the breakpoints used to program the RV controller with this PSD profile are listed in Table 45. Frequencies above 100 Hz were not included in the profile.

Table 45: Breakpoints used for programming the experimental PSD profile on the random vibration controller.

Frequency (Hz)	1	3	4	7	50	100
Power Spectral Density (g²/Hz)	0.0001	0.07	0.07	0.002	0.0004	0.0004

The PSD profile was run to produce a response RMS level of 0.44 g, which was found in the field study to be the appropriate RMS level for this profile. The RMS acceleration level of 0.44 g was stepped up to in a sequence. Firstly the controller ran the table at high acceleration in an analysis phase for several seconds in order to determine the necessary frequency response function used to compensate for the dynamic characteristics of the vibration system. This function depends on several mechanical characteristics of the vibration system, including the mass on the table. Following the analysis phase, the demand PSD profile was stepped up from 0.1 g to 0.44 g over a period of 30 s. At this point the timing of the tests began.

C.5 SERVO-HYDRAULIC VIBRATION SYSTEM

As noted in Chapter 4, the distributions of peak acceleration, velocity change, and crest factor could be used to confirm that any laboratory simulation of the transportation environment provides shocks of the appropriate quantity and magnitude. The verification of the set-up for these experiments consisted of running the table at the required PSD profile and RMS level for 1 hour, and recording the acceleration of the table using an EDR-3 Environmental Data Recorder, with the same EDR set-up as used in Chapter 4. The distributions of these parameters were then obtained in the same way as described in Chapter 4. The displacement of the table during this hour was also recorded using the ultrasonic sensors, LPFs, and chart recorder.

The acceleration distribution results from the EDR indicated that the response PSD was similar to the demand PSD and the acceleration levels were in the expected range. However the distribution of peak acceleration closely followed a Rayleigh distribution, rather than the Weibull or gamma distributions observed in Chapter 4. This difference was attributed to the fact that the RV controller produces instantaneous acceleration which follows a Gaussian distribution, which is a limitation of a typical FFT controller. The differences between the peak acceleration distributions was not great, and was deemed acceptable for these purposes.

The results from the chart recorder indicated that all three ultrasonic displacement transducers behaved with acceptable accuracy and precision. A LPF frequency of 1 Hz was found to be effective in filtering out high frequency vibration from the table motion, and provided the optimal tradeoff between signal noise and pen response time. At higher cut-off frequencies, more noise from the table movement was introduced into the signal, and at lower cut-off frequencies the movement of the recorder pens lagged noticeably behind the displacement of the table. After allowing for the effect of the low-frequency table movement on the pens, it was determined that the net displacement of the box could be estimated to within ± 3 mm, i.e. the resolution of the displacement recording is less than 3 mm.